
Iterative Methods for Linear Systems

6.1. Introduction

Iterative algorithms for solving $Ax = b$ are used when methods such as Gaussian elimination require too much time or too much space. Methods such as Gaussian elimination, which compute the exact answers after a finite number of steps (in the absence of roundoff!), are called *direct methods*. In contrast to direct methods, iterative methods generally do not produce the exact answer after a finite number of steps but decrease the error by some fraction after each step. Iteration ceases when the error is less than a user-supplied threshold. The final error depends on how many iterations one does as well as on properties of the method and the linear system. Our overall goal is to develop methods which decrease the error by a large amount at each iteration and do as little work per iteration as possible.

Much of the activity in this field involves exploiting the underlying mathematical or physical problem that gives rise to the linear system in order to design better iterative methods. The underlying problems are often finite difference or finite element models of physical systems, usually involving a differential equation. There are many kinds of physical systems, differential equations, and finite difference and finite element models, and so many methods. We cannot hope to cover all or even most interesting situations, so we will limit ourselves to a *model problem*, the standard finite difference approximation to Poisson's equation on a square. Poisson's equation and its close relation, Laplace's equation, arise in many applications, including electromagnetics, fluid mechanics, heat flow, diffusion, and quantum mechanics, to name a few. In addition to describing how each method works on Poisson's equation, we will indicate how generally applicable it is, and describe common variations.

The rest of this chapter is organized as follows. Section 6.2 describes on-line help and software for iterative methods discussed in this chapter. Section 6.3 describes the formulation of the model problem in detail. Section 6.4 summarizes and compares the performance of (nearly) all the iterative methods in this chapter for solving the model problem.

The next five sections describe methods in roughly increasing order of their effectiveness on the model problem. Section 6.5 describes the most basic iterative methods: Jacobi, Gauss–Seidel, successive overrelaxation, and their variations. Section 6.6 describes Krylov subspace methods, concentrating on the conjugate gradient method. Section 6.7 describes the fast Fourier transform and how to use it to solve the model problem. Section 6.8 describes block cyclic reduction. Finally, section 6.9 discusses multigrid, our fastest algorithm for the model problem. Multigrid requires only $O(1)$ work per unknown, which is optimal.

Section 6.10 describes domain decomposition, a family of techniques for combining the simpler methods described in earlier sections to solve more complicated problems than the model problem.

6.2. On-line Help for Iterative Methods

For Poisson’s equation, there will be a short list of numerical methods that are clearly superior to all the others we discuss. But for other linear systems it is not always clear which method is best (which is why we talk about so many!). To help users select the best method for solving their linear systems among the many available, on-line help is available at NETLIB/templates. This directory contains a short book [24] and software for most of the iterative methods discussed in this chapter. The book is available in both PostScript (NETLIB/templates/templates.ps) and Hypertext Markup Language (NETLIB/templates/template.html). The software is available in Matlab, Fortran, and C++.

The word *template* is used to describe this book and the software, because the implementations separate the details of matrix representations from the algorithm itself. In particular, the *Krylov subspace methods* (see section 6.6) require only the ability to multiply the matrix A by an arbitrary vector z . The best way to do this depends on how A is represented but does not otherwise affect the organization of the algorithm. In other words, matrix-vector multiplication is a “black-box” called by the template. It is the user’s responsibility to supply an implementation of this black-box.

An analogous templates project for eigenvalue problems is underway. Other recent textbooks on iterative methods are [15, 134, 212].

For the most challenging practical problems arising from differential equations more challenging than our model problem, the linear system $Ax = b$ must be “preconditioned,” or replaced with the equivalent systems $M^{-1}Ax = M^{-1}b$, which is somehow easier to solve. This is discussed at length in sections 6.6.5 and 6.10. Implementations, including parallel ones, of many of these techniques are available on-line in the package PETSc, or Portable Extensible Toolkit for Scientific computing, at <http://www.mcs.anl.gov/petsc/petsc.html> [230].

6.3. Poisson's Equation

6.3.1. Poisson's Equation in One Dimension

We begin with a one-dimensional version of Poisson's equation,

$$-\frac{d^2v(x)}{dx^2} = f(x), \quad 0 < x < 1, \quad (6.1)$$

where $f(x)$ is a given function and $v(x)$ is the unknown function that we want to compute. $v(x)$ must also satisfy the boundary conditions²³ $v(0) = v(1) = 0$. We *discretize* the problem by trying to compute an approximate solution at $N + 2$ evenly spaced points x_i between 0 and 1: $x_i = ih$, where $h = \frac{1}{N+1}$ and $0 \leq i \leq N + 1$. We abbreviate $v_i = v(x_i)$ and $f_i = f(x_i)$. To convert differential equation (6.1) into a linear equation for the unknowns v_1, \dots, v_N , we use *finite differences* to approximate

$$\begin{aligned} \left. \frac{dv(x)}{dx} \right|_{x=(i-.5)h} &\approx \frac{v_i - v_{i-1}}{h}, \\ \left. \frac{dv(x)}{dx} \right|_{x=(i+.5)h} &\approx \frac{v_{i+1} - v_i}{h}. \end{aligned}$$

Subtracting these approximations and dividing by h yield the *centered difference approximation*

$$-\left. \frac{d^2v(x)}{dx^2} \right|_{x=x_i} = \frac{2v_i - v_{i-1} - v_{i+1}}{h^2} - \tau_i, \quad (6.2)$$

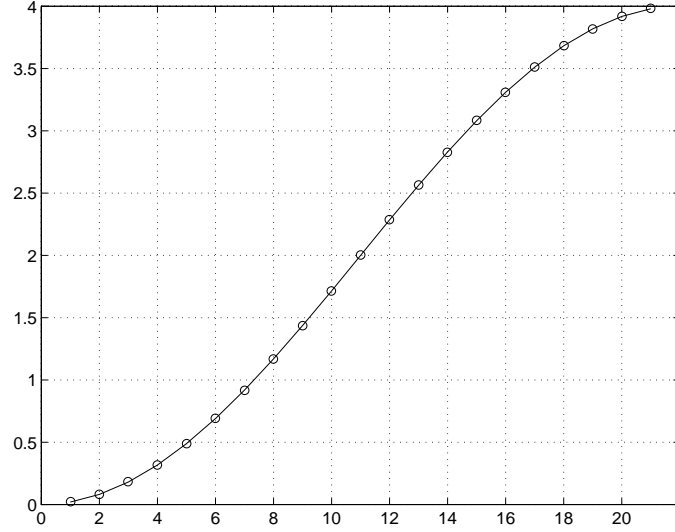
where τ_i , the so-called *truncation error*, can be shown to be $O(h^2 \cdot \|\frac{d^4v}{dx^4}\|_\infty)$. We may now rewrite equation (6.1) at $x = x_i$ as

$$-v_{i-1} + 2v_i - v_{i+1} = h^2 f_i + h^2 \tau_i,$$

where $0 < i < N + 1$. Since the boundary conditions imply that $v_0 = v_{N+1} = 0$, we have N equations in N unknowns v_1, \dots, v_N :

$$\begin{aligned} T_N \cdot \begin{bmatrix} v_1 \\ \vdots \\ \vdots \\ v_N \end{bmatrix} &\equiv \begin{bmatrix} 2 & -1 & & 0 \\ -1 & \ddots & \ddots & \\ & \ddots & \ddots & -1 \\ 0 & & -1 & 2 \end{bmatrix} \cdot \begin{bmatrix} v_1 \\ \vdots \\ \vdots \\ v_N \end{bmatrix} \\ &= h^2 \begin{bmatrix} f_1 \\ \vdots \\ \vdots \\ f_N \end{bmatrix} + h^2 \begin{bmatrix} \tau_1 \\ \vdots \\ \vdots \\ \tau_N \end{bmatrix} \end{aligned} \quad (6.3)$$

²³These are called *Dirichlet boundary conditions*. Other kinds of boundary conditions are also possible.

Fig. 6.1. *Eigenvalues of T_{21} .*

or

$$T_N v = h^2 f + h^2 \bar{\tau}. \quad (6.4)$$

To solve this equation, we will ignore $\bar{\tau}$, since it is small compared to f , to get

$$T_N \hat{v} = h^2 f. \quad (6.5)$$

(We bound the error $v - \hat{v}$ later.)

The coefficient matrix T_N plays a central role in all that follows, so we will examine it in some detail. First, we will compute its eigenvalues and eigenvectors. One can easily use trigonometric identities to confirm the following lemma (see Question 6.1).

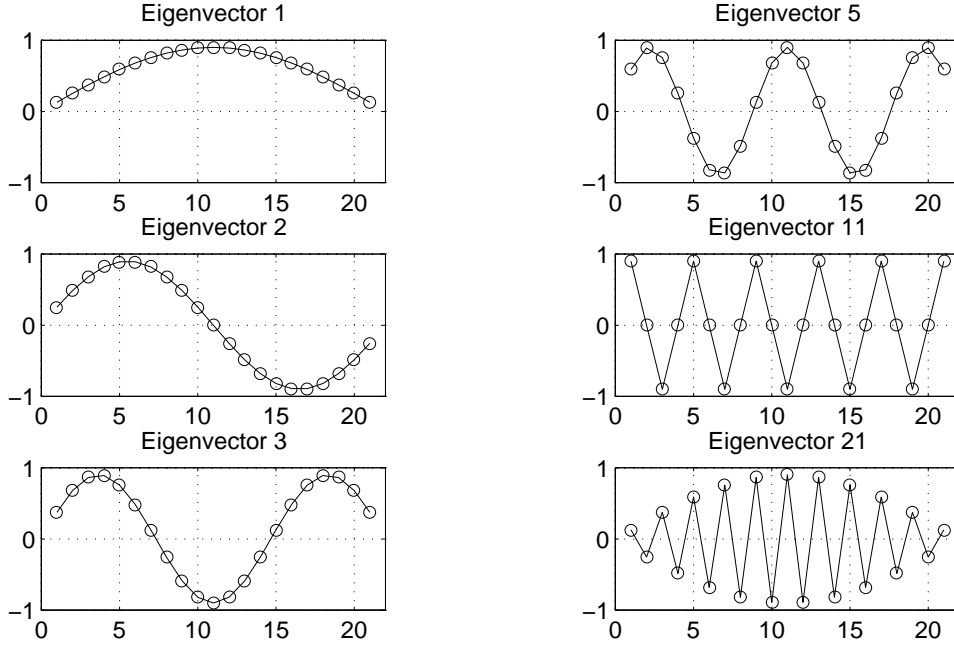
LEMMA 6.1. *The eigenvalues of T_N are $\lambda_j = 2(1 - \cos \frac{\pi j}{N+1})$. The eigenvectors are z_j , where $z_j(k) = \sqrt{\frac{2}{N+1}} \sin(jk\pi/(N+1))$. z_j has unit two-norm. Let $Z = [z_1, \dots, z_n]$ be the orthogonal matrix whose columns are the eigenvectors, and $\Lambda = \text{diag}(\lambda_1, \dots, \lambda_n)$, so we can write $T_N = Z\Lambda Z^T$.*

Figure 6.1 is a plot of the eigenvalues of T_N for $N = 21$.

The largest eigenvalue is $\lambda_N = 2(1 - \cos \pi \frac{N}{N+1}) \approx 4$. The smallest eigenvalue²⁴ is λ_1 , where for small i

$$\lambda_i = 2 \left(1 - \cos \frac{i\pi}{N+1} \right) \approx 2 \left(1 - \left(1 - \frac{i^2 \pi^2}{2(N+1)^2} \right) \right) = \left(\frac{i\pi}{N+1} \right)^2.$$

²⁴Note that λ_N is the largest eigenvalue and λ_1 is the smallest eigenvalue, the opposite of the convention of Chapter 5.

Fig. 6.2. Eigenvectors of T_{21} .

Thus T_N is positive definite with condition number $\lambda_N/\lambda_1 \approx 4(N+1)^2/\pi^2$ for large N . The eigenvectors are sinusoids with lowest frequency at $j = 1$ and highest at $j = N$, shown in Figure 6.2 for $N = 21$.

Now we know enough to bound the error, i.e., the difference between the solution of $T_N \hat{v} = h^2 f$ and the true solution v of the differential equation: Subtract equation (6.5) from equation (6.4) to get $v - \hat{v} = h^2 T_N^{-1} \bar{\tau}$. Taking norms yields

$$\|v - \hat{v}\|_2 \leq h^2 \|T_N^{-1}\|_2 \|\bar{\tau}\|_2 \approx h^2 \frac{(N+1)^2}{\pi^2} \|\bar{\tau}\|_2 = O(\|\bar{\tau}\|_2) = O\left(h^2 \left\| \frac{d^4 v}{dx^4} \right\|_\infty\right),$$

so the error $v - \hat{v}$ goes to zero proportionally to h^2 , provided that the solution is smooth enough. ($\| \frac{d^4 v}{dx^4} \|_\infty$ is bounded.)

From now on we will not distinguish between v and its approximation \hat{v} , and so will simplify notation by letting $T_N v = h^2 f$.

In addition to the solution of the linear system $h^{-2} T_N v = f$ approximating the solution of the differential equation (6.1), it turns out that the eigenvalues and eigenvectors of $h^{-2} T_N$ also approximate the eigenvalues and *eigenfunctions* of the differential equation: We say that $\hat{\lambda}_i$ is an eigenvalue and $\hat{z}_i(x)$ is an eigenfunction of the differential equation if

$$-\frac{d^2 \hat{z}_i(x)}{dx^2} = \hat{\lambda}_i \hat{z}_i(x) \quad \text{with} \quad \hat{z}_i(0) = \hat{z}_i(1) = 0.$$

Let us solve for $\hat{\lambda}_i$ and $\hat{z}_i(x)$: It is easy to see that $\hat{z}_i(x)$ must equal $\alpha \sin(\sqrt{\hat{\lambda}_i}x) + \beta \cos(\sqrt{\hat{\lambda}_i}x)$ for some constants α and β . The boundary condition $\hat{z}_i(0) = 0$ implies $\beta = 0$, and the boundary condition $\hat{z}_i(1) = 0$ implies that $\sqrt{\hat{\lambda}_i}$ is an integer multiple of π , which we can take to be $i\pi$. Thus $\hat{\lambda}_i = i^2\pi^2$ and $\hat{z}_i(x) = \alpha \sin(i\pi x)$ for any nonzero constant α (which we can set to 1). Thus the eigenvector z_i is *precisely* equal to the eigenfunction $\hat{z}_i(x)$ evaluated at the sample points $x_j = jh$ (when scaled by $\sqrt{\frac{2}{N+1}}$). And when i is small, $\hat{\lambda}_i = i^2\pi^2$ is well approximated by $h^{-2} \cdot \lambda_i = (N+1)^2 \cdot 2(1 - \cos \frac{i\pi}{N+1}) = i^2\pi^2 + O((N+1)^{-2})$.

Thus we see there is a close correspondence between T_N (or $h^{-2}T_N$) and the second derivative operator $-\frac{d^2}{dx^2}$. This correspondence will be the motivation for the design and analysis of later algorithms.

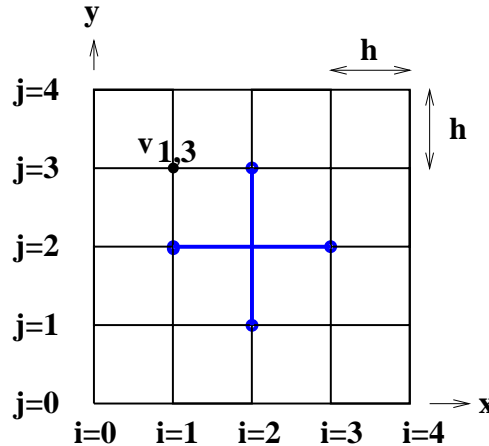
It is also possible to write down simple formulas for the Cholesky and LU factors of T_N ; see Question 6.2 for details.

6.3.2. Poisson's Equation in Two Dimensions

Now we turn to Poisson's equation in two dimensions:

$$-\frac{\partial^2 v(x, y)}{\partial x^2} - \frac{\partial^2 v(x, y)}{\partial y^2} = f(x, y) \quad (6.6)$$

on the unit square $\{(x, y) : 0 < x, y < 1\}$, with boundary condition $v = 0$ on the boundary of the square. We discretize at the grid points in the square which are at (x_i, y_j) with $x_i = ih$ and $y_j = jh$, with $h = \frac{1}{N+1}$. We abbreviate $v_{ij} = v(ih, jh)$ and $f_{ij} = f(ih, jh)$, as shown below for $N = 3$:



From equation (6.2), we know that we can approximate

$$-\frac{\partial^2 v(x, y)}{\partial x^2} \Big|_{x=x_i, y=y_j} \approx \frac{2v_{i,j} - v_{i-1,j} - v_{i+1,j}}{h^2} \quad \text{and} \quad (6.7)$$

$$-\frac{\partial^2 v(x, y)}{\partial y^2} \Big|_{x=x_i, y=y_j} \approx \frac{2v_{i,j} - v_{i,j-1} - v_{i,j+1}}{h^2}. \quad (6.8)$$

Adding these approximations lets us write

$$\begin{aligned} & -\frac{\partial^2 v(x, y)}{\partial x^2} - \frac{\partial^2 v(x, y)}{\partial y^2} \Big|_{x=x_i, y=y_j} \\ & = \frac{4v_{ij} - v_{i-1,j} - v_{i+1,j} - v_{i,j-1} - v_{i,j+1}}{h^2} - \tau_{ij}, \end{aligned} \quad (6.9)$$

where τ_{ij} is again a truncation error bounded by $O(h^2)$. The heavy (blue) cross in the middle of the above figure is called the (5-point) *stencil* of this equation, because it connects all (5) values of v present in equation (6.9). From the boundary conditions we know $v_{0j} = v_{N+1,j} = v_{i,0} = v_{i,N+1} = 0$ so that equation (6.9) defines a set of $n = N^2$ linear equations in the n unknowns v_{ij} for $1 \leq i, j \leq N$:

$$4v_{ij} - v_{i-1,j} - v_{i+1,j} - v_{i,j-1} - v_{i,j+1} = h^2 f_{ij}. \quad (6.10)$$

There are two ways to rewrite the n equations represented by (6.10) as a single matrix equation, both of which we will use later.

The first way is to think of the unknowns v_{ij} as occupying an N -by- N matrix V with entries v_{ij} and the right-hand sides $h^2 f_{ij}$ as similarly occupying an N -by- N matrix $h^2 F$. The trick is to write the matrix with i, j entry $4v_{ij} - v_{i-1,j} - v_{i+1,j} - v_{i,j-1} - v_{i,j+1}$ in a simple way in terms of V and T_N : Simply note that

$$\begin{aligned} 2v_{ij} - v_{i-1,j} - v_{i+1,j} &= (T_N \cdot V)_{ij}, \\ 2v_{ij} - v_{i,j-1} - v_{i,j+1} &= (V \cdot T_N)_{ij}, \end{aligned}$$

so adding these two equations yields

$$(T_N \cdot V + V \cdot T_N)_{ij} = 4v_{ij} - v_{i-1,j} - v_{i+1,j} - v_{i,j-1} - v_{i,j+1} = h^2 f_{ij} = (h^2 F)_{ij}$$

or

$$T_N \cdot V + V \cdot T_N = h^2 F. \quad (6.11)$$

This is a linear system of equations for the unknown entries of the matrix V , even though it is not written in the usual “ $Ax = b$ ” format, with the unknowns forming a vector x . (We will write the “ $Ax = b$ ” format below.) Still, it is enough to tell us what the eigenvalues and eigenvectors of the underlying matrix A are, because “ $Ax = \lambda x$ ” is the same as “ $T_N V + V T_N = \lambda V$.” Now suppose that $T_N z_i = \lambda_i z_i$ and $T_N z_j = \lambda_j z_j$ are any two eigenpairs of T_N , and let $V = z_i z_j^T$. Then

$$\begin{aligned} T_N V + V T_N &= (T_N z_i) z_j^T + z_i (z_j^T T_N) \\ &= (\lambda_i z_i) z_j^T + z_i (z_j^T \lambda_j) \\ &= (\lambda_i + \lambda_j) z_i z_j^T \\ &= (\lambda_i + \lambda_j) V, \end{aligned} \quad (6.12)$$

so $V = z_i z_j^T$ is an “eigenvector” and $\lambda_i + \lambda_j$ is an eigenvalue. Since V has N^2 entries, we expect N^2 eigenvalues and eigenvectors, one for each pair of eigenvalues λ_i and λ_j of T_N . In particular, the smallest eigenvalue is $2\lambda_1$ and the largest eigenvalue is $2\lambda_N$, so the condition number is the same as in the one-dimensional case. We rederive this result below using the “ $Ax = b$ ” format. See Figure 6.3 for plots of some eigenvectors, represented as surfaces defined by the matrix entries of $z_i z_j^T$.

Just as the eigenvalues and eigenvectors of $h^{-2}T_N$ were good approximations to the eigenvalues and eigenfunctions of one-dimensional Poisson’s equation, the same is true of two-dimensional Poisson’s equation, whose eigenvalues and eigenfunctions are as follows (see Question 6.3):

$$\begin{aligned} \left(-\frac{\partial^2}{\partial x^2} - \frac{\partial^2}{\partial y^2} \right) \sin(i\pi x) \sin(j\pi y) \\ = (i^2\pi^2 + j^2\pi^2) \sin(i\pi x) \sin(j\pi y). \end{aligned} \quad (6.13)$$

The second way to write the n equations represented by equation (6.10) as a single matrix equation is to write the unknowns v_{ij} in a single long N^2 -by-1 vector. This requires us to choose an order for them, and we (somewhat arbitrarily) choose to number them as shown in Figure 6.4, columnwise from the upper left to the lower right.

For example, when $N = 3$ one gets a column vector $v \equiv [v_1, \dots, v_9]^T$. If we number f accordingly, we can transform equation (6.10) to get

$$\begin{aligned} T_{3 \times 3} \cdot \begin{bmatrix} v_1 \\ v_2 \\ \vdots \\ \vdots \\ \vdots \\ v_9 \end{bmatrix} &\equiv \left[\begin{array}{cc|cc|cc} 4 & -1 & -1 & & & \\ -1 & 4 & -1 & & & \\ & -1 & 4 & & & \\ \hline -1 & & & 4 & -1 & -1 \\ & -1 & & -1 & 4 & -1 \\ & & -1 & & -1 & 4 \\ \hline & & & -1 & & \\ & & & & -1 & \\ & & & & & -1 \end{array} \right] \begin{bmatrix} v_1 \\ v_2 \\ \vdots \\ \vdots \\ \vdots \\ v_9 \end{bmatrix} \\ &= h^2 \begin{bmatrix} f_1 \\ f_2 \\ \vdots \\ \vdots \\ \vdots \\ f_9 \end{bmatrix}. \end{aligned} \quad (6.14)$$

The -1 ’s immediately next to the diagonal correspond to subtracting the top and bottom neighbors $-v_{i-1,j} - v_{i+1,j}$. The -1 ’s farther away from the diagonal correspond to subtracting the left and right neighbors $-v_{i,j-1} - v_{i,j+1}$. For general N , we confirm in the next section that we get an N^2 -by- N^2 linear system

$$T_{N \times N} \cdot v = h^2 f, \quad (6.15)$$

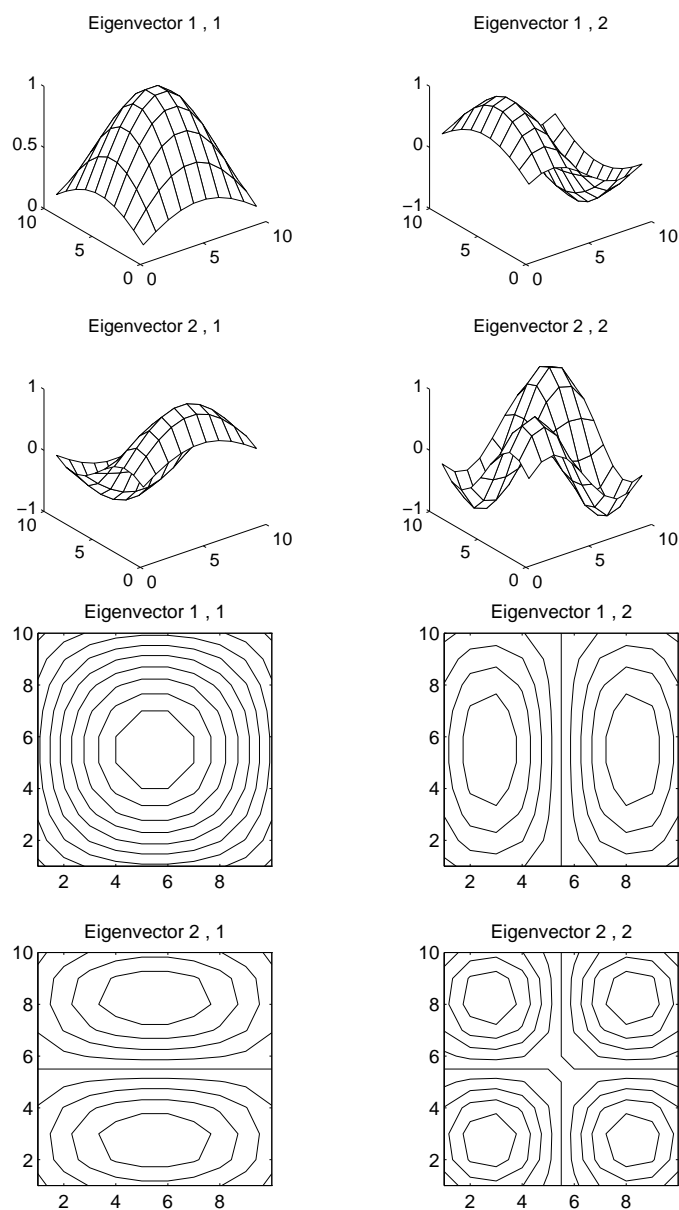
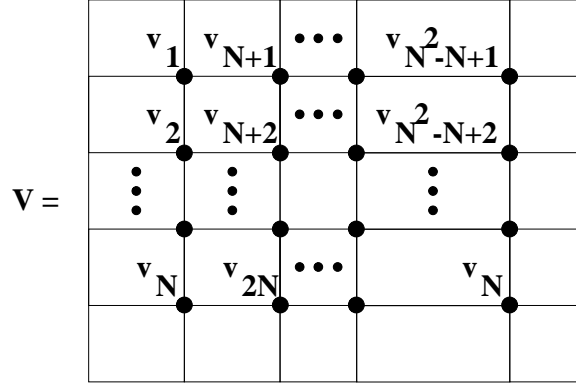


Fig. 6.3. Three-dimensional and contour plots of first four eigenvectors of the 10-by-10 Poisson equation.

Fig. 6.4. *Numbering the unknowns in Poisson's equation.*

where $T_{N \times N}$ has N N -by- N blocks of the form $T_N + 2I_N$ on its diagonal and $-I_N$ blocks on its offdiagonals:

$$T_{N \times N} = \begin{bmatrix} T_N + 2I_N & -I_N & & & \\ -I_N & \ddots & \ddots & & \\ & \ddots & \ddots & -I_N & \\ & & -I_N & T_N + 2I_N & \end{bmatrix}. \quad (6.16)$$

6.3.3. Expressing Poisson's Equation with Kronecker Products

Here is a systematic way to derive equations (6.15) and (6.16) as well as to compute the eigenvalues and eigenvectors of $T_{N \times N}$. The method works equally well for Poisson's equation in three or more dimensions.

DEFINITION 6.1. *Let X be m -by- n . Then $\text{vec}(X)$ is defined to be a column vector of size $m \cdot n$ made of the columns of X stacked atop one another from left to right.*

Note that N^2 -by-1 vector v defined in Figure 6.4 can also be written $v = \text{vec}(V)$.

To express $T_{N \times N}$ as well as compute its eigenvalues and eigenvectors, we need to introduce *Kronecker products*.

DEFINITION 6.2. *Let A be an m -by- n matrix and B be a p -by- q matrix. Then $A \otimes B$, the Kronecker product of A and B , is the $(m \cdot p)$ -by- $(n \cdot q)$ matrix*

$$\begin{bmatrix} a_{1,1} \cdot B & \dots & a_{1,n} \cdot B \\ \vdots & & \vdots \\ a_{m,1} \cdot B & \dots & a_{m,n} \cdot B \end{bmatrix}.$$

The following lemma tells us how to rewrite the Poisson equation in terms of Kronecker products and the $\text{vec}(\cdot)$ operator.

LEMMA 6.2. *Let A be m -by- m , B be n -by- n , and X and C be m -by- n . Then the following properties hold:*

1. $\text{vec}(AX) = (I_n \otimes A) \cdot \text{vec}(X)$.
2. $\text{vec}(XB) = (B^T \otimes I_m) \cdot \text{vec}(X)$.
3. *The Poisson equation $T_N V + VT_N = h^2 F$ is equivalent to*

$$T_{N \times N} \cdot \text{vec}(V) \equiv (I_N \otimes T_N + T_N \otimes I_N) \cdot \text{vec}(V) = h^2 \text{vec}(F). \quad (6.17)$$

Proof. We prove only part 3, leaving the other parts to Question 6.4. We start with the Poisson equation $T_N V + VT_N = h^2 F$ as expressed in equation (6.11), which is clearly equivalent to

$$\text{vec}(T_N V + VT_N) = \text{vec}(T_N V) + \text{vec}(VT_N) = \text{vec}(h^2 F).$$

By part 1 of the lemma

$$\text{vec}(T_N V) = (I_N \otimes T_N) \text{vec}(V).$$

By part 2 of the lemma and the symmetry of T_N ,

$$\text{vec}(VT_N) = (T_N^T \otimes I_N) \text{vec}(V) = (T_N \otimes I_N) \text{vec}(V).$$

Adding the last two expressions completes the proof of part 3. \square

The reader can confirm that the expression

$$\begin{aligned} T_{N \times N} &= I_N \otimes T_N + T_N \otimes I_N \\ &= \begin{bmatrix} T_N & & & \\ & \ddots & & \\ & & \ddots & \\ & & & T_N \end{bmatrix} + \begin{bmatrix} 2I_N & -I_N & & \\ -I_N & \ddots & \ddots & \\ & \ddots & \ddots & -I_N \\ & & -I_N & 2I_N \end{bmatrix} \end{aligned}$$

from equation (6.17) agrees with equation (6.16).²⁵

To compute the eigenvalues of matrices defined by Kronecker products, like $T_{N \times N}$, we need the following lemma, whose proof is also part of Question 6.4.

LEMMA 6.3. *The following facts about Kronecker products hold:*

1. *Assume that the products $A \cdot C$ and $B \cdot D$ are well defined. Then $(A \otimes B) \cdot (C \otimes D) = (A \cdot C) \otimes (B \cdot D)$.*

²⁵We can use this formula to compute $T_{N \times N}$ in two lines of Matlab:

```
TN = 2*eye(N) - diag(ones(N-1,1),1) - diag(ones(N-1,1),-1);
TNxN = kron(eye(N),TN) + kron(TN,eye(N));
```

2. If A and B are invertible, then $(A \otimes B)^{-1} = A^{-1} \otimes B^{-1}$.

3. $(A \otimes B)^T = A^T \otimes B^T$.

PROPOSITION 6.1. Let $T_N = Z\Lambda Z^T$ be the eigendecomposition of T_N , with $Z = [z_1, \dots, z_N]$ the orthogonal matrix whose columns are eigenvectors, and $\Lambda = \text{diag}(\lambda_1, \dots, \lambda_N)$. Then the eigendecomposition of $T_{N \times N} = I \otimes T_N + T_N \otimes I$ is

$$I \otimes T_N + T_N \otimes I = (Z \otimes Z) \cdot (I \otimes \Lambda + \Lambda \otimes I) \cdot (Z \otimes Z)^T. \quad (6.18)$$

$I \otimes \Lambda + \Lambda \otimes I$ is a diagonal matrix whose $(iN + j)$ th diagonal entry, the (i, j) th eigenvalue of $T_{N \times N}$, is $\lambda_{i,j} = \lambda_i + \lambda_j$. $Z \otimes Z$ is an orthogonal matrix whose $(iN + j)$ th column, the corresponding eigenvector, is $z_i \otimes z_j$.

Proof. From parts 1 and 3 of Lemma 6.3, it is easy to verify that $Z \otimes Z$ is orthogonal, since $(Z \otimes Z)(Z \otimes Z)^T = (Z \otimes Z)(Z^T \otimes Z^T) = (Z \cdot Z^T) \otimes (Z \cdot Z^T) = I \otimes I = I$. We can now verify equation (6.18):

$$\begin{aligned} & (Z \otimes Z) \cdot (I \otimes \Lambda + \Lambda \otimes I) \cdot (Z \otimes Z)^T \\ &= (Z \otimes Z) \cdot (I \otimes \Lambda + \Lambda \otimes I) \cdot (Z^T \otimes Z^T) \\ & \quad \text{by part 3 of Lemma 6.3} \\ &= (Z \cdot I \cdot Z^T) \otimes (Z \cdot \Lambda \cdot Z^T) + (Z \cdot \Lambda \cdot Z^T) \otimes (Z \cdot I \cdot Z^T) \\ & \quad \text{by part 1 of Lemma 6.3} \\ &= (I) \otimes (T_N) + (T_N) \otimes (I) \\ &= T_{N \times N}. \end{aligned}$$

Also, it is easy to verify that $I \otimes \Lambda + \Lambda \otimes I$ is diagonal, with diagonal entry $(iN + j)$ given by $\lambda_j + \lambda_i$, so that equation (6.18) really is the eigendecomposition of $T_{N \times N}$. Finally, from the definition of Kronecker product, one can see that column $iN + j$ of $Z \otimes Z$ is $z_i \otimes z_j$. \square

The reader can confirm that the eigenvector $z_i \otimes z_j = \text{vec}(z_j z_i^T)$, thus matching the expression for an eigenvector in equation (6.12).

For a generalization of Proposition 6.1 to the matrix $A \otimes I + B^T \otimes I$, which arises when solving the Sylvester equation $AX - XB = C$, see Question 6.5 (and Question 4.6).

Similarly, Poisson's equation in three dimensions leads to

$$T_{N \times N \times N} \equiv T_N \otimes I_N \otimes I_N + I_N \otimes T_N \otimes I_N + I_N \otimes I_N \otimes T_N,$$

with eigenvalues all possible triple sums of eigenvalues of T_N , and eigenvector matrix $Z \otimes Z \otimes Z$. Poisson's equation in higher dimensions is represented analogously.

Method	Serial Time	Space	Direct or Iterative	Section
Dense Cholesky	n^3	n^2	D	2.7.1
Explicit inverse	n^2	n^2	D	
Band Cholesky	n^2	$n^{3/2}$	D	2.7.3
Jacobi	n^2	n	I	6.5
Gauss–Seidel	n^2	n	I	6.5
Sparse Cholesky	$n^{3/2}$	$n \cdot \log n$	D	2.7.4
Conjugate gradients	$n^{3/2}$	n	I	6.6
Successive overrelaxation	$n^{3/2}$	n	I	6.5
SSOR with Chebyshev accel.	$n^{5/4}$	n	I	6.5
Fast Fourier transform	$n \cdot \log n$	n	D	6.7
Block cyclic reduction	$n \cdot \log n$	n	D	6.8
Multigrid	n	n	I	6.9
Lower bound	n	n		

Table 6.1. *Order of complexity of solving Poisson’s equation on an N -by- N grid ($n = N^2$).*

6.4. Summary of Methods for Solving Poisson’s Equation

Table 6.1 lists the costs of various direct and iterative methods for solving the model problem on an N -by- N grid. The variable $n = N^2$, the number of unknowns. Since direct methods provide the exact answer (in the absence of roundoff), whereas iterative methods provide only approximate answers, we must be careful when comparing their costs, since a low-accuracy answer can be computed more cheaply by an iterative method than a high-accuracy answer. Therefore, we compare costs, assuming that the iterative methods iterate often enough to make the error at most some fixed small value²⁶ (say, 10^{-6}).

The second and third columns of Table 6.1 give the number of arithmetic operations (or time) and space required on a serial machine. Column 4 indicates whether the method is direct (D) or iterative (I). All entries are meant in the $O(\cdot)$ sense; the constants depend on implementation details and the stopping criterion for the iterative methods (say, 10^{-6}). For example, the entry for Cholesky also applies to Gaussian elimination, since this changes the constant only by a factor of two. The last column indicates where the algorithm is discussed in the text.

The methods are listed in increasing order of speed, from slowest (dense

²⁶Alternatively, we could iterate until the error is $O(h^2) = O((N+1)^{-2})$, the size of the truncation error. One can show that this would increase the costs of the iterative methods in Table 6.1 by a factor of $O(\log n)$.

Cholesky) to fastest (multigrid), ending with a lower bound applying to any method. The lower bound is n because at least one operation is required per solution component, since otherwise they could not all be different and also depend on the input. The methods are also, roughly speaking, in order of decreasing generality, with dense Cholesky applicable to any symmetric positive definite matrix and later algorithms applicable (or at least provably convergent) only for limited classes of matrices. In later sections we will describe the applicability of various methods in more detail.

The “explicit inverse” algorithm refers to precomputing the explicit inverse of $T_{N \times N}$, and computing $v = T_{N \times N}^{-1}f$ by a single matrix-vector multiplication (and not counting the flops to precompute $T_{N \times N}^{-1}$). Along with dense Cholesky, it uses n^2 space, vastly more than the other methods. It is not a good method. Band Cholesky was discussed in section 2.7.3; this is just Cholesky taking advantage of the fact that there are no entries to compute or store outside a band of $2N + 1$ diagonals.

Jacobi and Gauss–Seidel are classical iterative methods and not particularly fast, but they form the basis for other faster methods: successive overrelaxation, symmetric successive overrelaxation, and multigrid, our fastest algorithm. So we will study them in some detail in section 6.5.

Sparse Cholesky refers to the algorithm discussed in section 2.7.4: it is an implementation of Cholesky that avoids storing or operating on the zero entries of $T_{N \times N}$ or its Cholesky factor. Furthermore, we are assuming the rows and columns of $T_{N \times N}$ have been “optimally ordered” to minimize work and storage (using nested dissection [110, 111]). While sparse Cholesky is reasonably fast on Poisson’s equation in two dimensions, it is significantly worse in three dimensions (using $O(N^6) = O(n^2)$ time and $O(N^4) = O(n^{4/3})$ space), because there is more “fill-in” of zero entries during the algorithm.

Conjugate gradients, while not particularly fast on our model problem, are a representative of a much larger class of methods, called *Krylov subspace* methods, which are very widely applicable both for linear system solving and finding eigenvalues of sparse matrices. We will discuss these methods in more detail in section 6.6.

The fastest methods are block cyclic reduction, the fast Fourier transform (FFT), and multigrid. In particular, multigrid does only $O(1)$ operations per solution component, which is asymptotically optimal.

A final warning is that this table does not give a complete picture, since the constants are missing. For a particular size problem on a particular machine, one cannot immediately deduce which method is fastest. Still, it is clear that iterative methods such as Jacobi, Gauss–Seidel, conjugate gradients, and successive overrelaxation are inferior to the FFT, block cyclic reduction, and multigrid for large enough n . But they remain of interest because they are building blocks for some of the faster methods, and because they apply to larger classes of problems than the faster methods.

All of these algorithms can be implemented in parallel; see the lectures

on PARALLEL_HOMEPAGE for details. It is interesting that, depending on the parallel machine, multigrid may no longer be fastest. This is because on a parallel machine the time required for separate processors to communicate data to one another may be as costly as the floating point operations, and other algorithms may communicate less than multigrid.

6.5. Basic Iterative Methods

In this section we will talk about the most basic iterative methods:

Jacobi's
Gauss–Seidel,
successive overrelaxation (SOR(ω)),
Chebyshev acceleration with symmetric successive overrelaxation
(SSOR(ω)).

These methods are also discussed and their implementations are provided at NETLIB/ templates.

Given x_0 , these methods generate a sequence x_m converging to the solution $A^{-1}b$ of $Ax = b$, where x_{m+1} is cheap to compute from x_m .

DEFINITION 6.3. *A splitting of A is a decomposition $A = M - K$, with M nonsingular.*

A splitting yields an iterative method as follows: $Ax = b$ implies $Mx = Kx + b$ or $x = M^{-1}Kx + M^{-1}b \equiv Rx + c$. So we can take $x_{m+1} = Rx_m + c$ as our iterative method. Let us see when it converges.

LEMMA 6.4. *Let $\|\cdot\|$ be any operator norm ($\|R\| \equiv \max_{x \neq 0} \frac{\|Rx\|}{\|x\|}$). If $\|R\| < 1$, then $x_{m+1} = Rx_m + c$ converges for any x_0 .*

Proof. Subtract $x = Rx + c$ from $x_{m+1} = Rx_m + c$ to get $x_{m+1} - x = R(x_m - x)$. Thus $\|x_{m+1} - x\| \leq \|R\| \cdot \|x_m - x\| \leq \|R\|^{m+1} \cdot \|x_0 - x\|$, which converges to 0 since $\|R\| < 1$. \square

Our ultimate convergence criterion will depend on the following property of R .

DEFINITION 6.4. *The spectral radius of R is $\rho(R) \equiv \max |\lambda|$, where the maximum is taken over all eigenvalues λ of R .*

LEMMA 6.5. *For all operator norms $\rho(R) \leq \|R\|$. For all R and for all $\epsilon > 0$ there is an operator norm $\|\cdot\|_*$ such that $\|R\|_* \leq \rho(R) + \epsilon$. $\|\cdot\|_*$ depends on both R and ϵ .*

Proof. To show $\rho(R) \leq \|R\|$ for any operator norm, let x be an eigenvector for λ , where $\rho(R) = |\lambda|$ and so $\|R\| = \max_{y \neq 0} \frac{\|Ry\|}{\|y\|} \geq \frac{\|Rx\|}{\|x\|} = \frac{\|\lambda x\|}{\|x\|} = |\lambda|$.

To construct an operator norm $\|\cdot\|_*$ such that $\|R\|_* \leq \rho(R) + \epsilon$, let $S^{-1}RS = J$ be in Jordan form. Let $D_\epsilon = \text{diag}(1, \epsilon, \epsilon^2, \dots, \epsilon^{n-1})$. Then

$$\begin{aligned} (SD_\epsilon)^{-1}R(SD_\epsilon) &= D_\epsilon^{-1}JD_\epsilon \\ &= \begin{bmatrix} \lambda_1 & \epsilon & & & \\ & \ddots & \ddots & & \\ & & \ddots & \epsilon & \\ & & & \lambda_1 & \\ \hline & & & \lambda_2 & \epsilon \\ & & & \ddots & \ddots \\ & & & & \ddots & \epsilon \\ & & & & & \lambda_2 \\ \hline & & & & & \ddots \end{bmatrix}, \end{aligned}$$

i.e., a “Jordan form” with ϵ ’s above the diagonal. Now use the vector norm $\|x\|_* \equiv \|(SD_\epsilon)^{-1}x\|_\infty$ to generate the operator norm

$$\begin{aligned} \|R\|_* &\equiv \max_{x \neq 0} \frac{\|Rx\|_*}{\|x\|_*} \\ &= \max_{x \neq 0} \frac{\|(SD_\epsilon)^{-1}Rx\|_\infty}{\|(SD_\epsilon)^{-1}x\|_\infty} \\ &= \max_{y \neq 0} \frac{\|(SD_\epsilon)^{-1}R(SD_\epsilon)y\|_\infty}{\|y\|_\infty} \\ &= \|(SD_\epsilon)^{-1}R(SD_\epsilon)\|_\infty \\ &= \max_i |\lambda_i| + \epsilon \\ &= \rho(R) + \epsilon. \quad \square \end{aligned}$$

THEOREM 6.1. *The iteration $x_{m+1} = Rx_m + c$ converges to the solution of $Ax = b$ for all starting vectors x_0 and for all b if and only if $\rho(R) < 1$.*

Proof. If $\rho(R) \geq 1$, choose $x_0 - x$ to be an eigenvector of R with eigenvalue λ where $|\lambda| = \rho(R)$. Then

$$(x_{m+1} - x) = R(x_m - x) = \dots = R^{m+1}(x_0 - x) = \lambda^{m+1}(x_0 - x)$$

will not approach 0. If $\rho(R) < 1$, use Lemma 6.5 to choose an operator norm so $\|R\|_* < 1$ and then apply Lemma 6.4 to conclude that the method converges. \square

DEFINITION 6.5. *The rate of convergence of $x_{m+1} = Rx_m + c$ is $r(R) \equiv -\log_{10} \rho(R)$.*

$r(R)$ is the increase in the number of correct decimal places in the solution per iteration, since $\log_{10} \|x_m - x\|_* - \log_{10} \|x_{m+1} - x\|_* \geq r(R) + O(\epsilon)$. The smaller is $\rho(R)$, the higher is the rate of convergence, i.e., the greater is the number of correct decimal places computed per iteration.

Our goal is now to choose a splitting $A = M - K$ so that both

- (1) $Rx = M^{-1}Kx$ and $c = M^{-1}b$ are easy to evaluate,
- (2) $\rho(R)$ is small.

We will need to balance these conflicting goals. For example, choosing $M = I$ is good for goal (1) but may not make $\rho(R) < 1$. On the other hand, choosing $M = A$ and $K = 0$ is good for goal (2) but probably bad for goal (1).

The splittings for the methods discussed in this section all share the following notation. When A has no zeros on its diagonal, we write

$$A = D - \tilde{L} - \tilde{U} = D(I - L - U), \quad (6.19)$$

where D is the diagonal of A , $-\tilde{L}$ is the strictly lower triangular part of A , $DL = \tilde{L}$, $-\tilde{U}$ is the strictly upper triangular part of A , and $DU = \tilde{U}$.

6.5.1. Jacobi's Method

Jacobi's method can be described as repeatedly looping through the equations, changing variable j so that equation j is satisfied exactly. Using the notation of equation (6.19), the splitting for Jacobi's method is $A = D - (\tilde{L} + \tilde{U})$; we denote $R_J \equiv D^{-1}(\tilde{L} + \tilde{U}) = L + U$ and $c_J \equiv D^{-1}b$, so we can write one step of Jacobi's method as $x_{m+1} = R_J x_m + c_J$. To see that this formula corresponds to our first description of Jacobi's method, note that it implies $Dx_{m+1} = (\tilde{L} + \tilde{U})x_m + b$, $a_{jj}x_{m+1,j} = -\sum_{k \neq j} a_{jk}x_{m,k} + b_j$, or $a_{jj}x_{m+1,j} + \sum_{k \neq j} a_{jk}x_{m,k} = b_j$.

ALGORITHM 6.1. *One step of Jacobi's method:*

```

for  $j = 1$  to  $n$ 
     $x_{m+1,j} = \frac{1}{a_{jj}}(b_j - \sum_{k \neq j} a_{jk}x_{m,k})$ 
end for

```

In the special case of the model problem, the implementation of Jacobi's algorithm simplifies as follows. Working directly from equation (6.10) and letting $v_{m,i,j}$ denote the m th value of the solution at grid point i, j , Jacobi's method becomes the following.

ALGORITHM 6.2. *One step of Jacobi's method for two-dimensional Poisson's equation:*

```

for  $i = 1$  to  $N$ 
    for  $j = 1$  to  $N$ 
         $v_{m+1,i,j} = (v_{m,i-1,j} + v_{m,i+1,j} + v_{m,i,j-1} + v_{m,i,j+1} + h^2 f_{ij})/4$ 
    end for
end for

```

end for
end for

In other words, at each step the new value of v_{ij} is obtained by “averaging” its neighbors with $h^2 f_{ij}$. Note that all new values $v_{m+1,i,j}$ may be computed independently of one another. Indeed, Algorithm 6.2 can be implemented in one line of Matlab if the $v_{m+1,i,j}$ are stored in a square array \hat{V} that includes an extra first and last row of zeros and first and last column of zeros (see Question 6.6).

6.5.2. Gauss–Seidel Method

The motivation for this method is that at the j th step of the loop for Jacobi’s method, we have improved values of the first $j - 1$ components of the solution, so we should use them in the sum.

ALGORITHM 6.3. *One step of the Gauss–Seidel method:*

$$\begin{array}{l} \text{for } j = 1 \text{ to } n \\ \quad x_{m+1,j} = \frac{1}{a_{jj}} \left(b_j - \underbrace{\sum_{k=1}^{j-1} a_{jk} x_{m+1,k}}_{\text{updated } x \text{'s}} - \underbrace{\sum_{k=j+1}^n a_{jk} x_{m,k}}_{\text{older } x \text{'s}} \right) \\ \text{end for} \end{array}$$

For the purpose of later analysis, we want to write this algorithm in the form $x_{m+1} = R_{GS}x_m + c_{GS}$. To this end, note that it can first be rewritten as

$$\sum_{k=1}^j a_{jk} x_{m+1,k} = - \sum_{k=j+1}^n a_{jk} x_{m,k} + b_j. \quad (6.20)$$

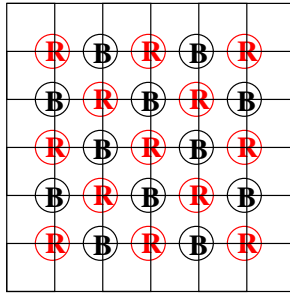
Then using the notation of equation (6.19), we can rewrite equation (6.20) as $(D - \tilde{L})x_{m+1} = \tilde{U}x_m + b$ or

$$\begin{aligned} x_{m+1} &= (D - \tilde{L})^{-1} \tilde{U}x_m + (D - \tilde{L})^{-1} b \\ &= (I - L)^{-1} Ux_m + (I - L)^{-1} D^{-1} b \\ &\equiv R_{GS}x_m + c_{GS}. \end{aligned}$$

As with Jacobi’s method, we consider how to implement the Gauss–Seidel method for our model problem. In principle it is quite similar, except that we have to keep track of which variables are new (numbered $m + 1$) and which are old (numbered m). But depending on the order in which we loop through the grid points i, j , we will get different (and valid) implementations of the

Gauss–Seidel method. This is unlike Jacobi’s method, in which the order in which we update the variables is irrelevant. For example, if we update $v_{m,1,1}$ first (before any other $v_{m,i,j}$), then all its neighboring values are necessarily old. But if we update $v_{m,1,1}$ last, then all its neighboring values are necessarily new, so we get a different value for $v_{m,1,1}$. Indeed, there are as many possible implementations of the Gauss–Seidel method as there are ways to order N^2 variables (namely, $N^2!$). But of all these orderings, only two are of interest. The first is the ordering shown in Figure 6.4; this is called the *natural ordering*.

The second ordering is called *red-black ordering*. It is important because our best convergence results in sections 6.5.4 and 6.5.5 depend on it. To explain red-black ordering, consider the chessboard-like coloring of the grid of unknowns below; the $\textcircled{\mathbf{B}}$ nodes correspond to the black squares on a chessboard, and the $\textcircled{\mathbf{R}}$ nodes correspond to the red squares.



The red-black ordering is to order the red nodes before the black nodes. Note that red nodes are adjacent to only black nodes. So if we update all the red nodes first, they will use only old data from the black nodes. Then when we update the black nodes, which are only adjacent to red nodes, they will use only new data from the red nodes. Thus the algorithm becomes the following.

ALGORITHM 6.4. *One step of the Gauss–Seidel method on two-dimensional Poisson’s equation with red-black ordering:*

for all nodes i, j that are red ($\textcircled{\mathbf{R}}$)

$$v_{m+1,i,j} = (v_{m,i-1,j} + v_{m,i+1,j} + v_{m,i,j-1} + v_{m,i,j+1} + h^2 f_{ij})/4$$

end for

for all nodes i, j that are black ($\textcircled{\mathbf{B}}$)

$$v_{m+1,i,j} = (v_{m+1,i-1,j} + v_{m+1,i+1,j} + v_{m+1,i,j-1} + v_{m+1,i,j+1} + h^2 f_{ij})/4$$

end for

6.5.3. Successive Overrelaxation

We refer to this method as $\text{SOR}(\omega)$, where ω is the *relaxation parameter*. The motivation is to improve the Gauss–Seidel loop by taking an appropriate

weighted average of the $x_{m+1,j}$ and $x_{m,j}$:

$$\text{SOR's } x_{m+1,j} = (1 - \omega)x_{m,j} + \omega x_{m+1,j},$$

yielding the following algorithm.

ALGORITHM 6.5. *SOR*:

for $j = 1$ to n

$$x_{m+1,j} = (1 - \omega)x_{m,j} + \frac{\omega}{a_{jj}} \left[b_j - \sum_{k=1}^{j-1} a_{jk}x_{m+1,k} - \sum_{k=j+1}^n a_{jk}x_{m,k} \right]$$

end for

We may rearrange this to get, for $j = 1$ to n ,

$$a_{jj}x_{m+1,j} + \omega \sum_{k=1}^{j-1} a_{jk}x_{m+1,k} = (1 - \omega)a_{jj}x_{m,j} - \omega \sum_{k=j+1}^n a_{jk}x_{m,k} + \omega b_j$$

or, again using the notation of equation (6.19),

$$(D - \omega\tilde{L})x_{m+1} = ((1 - \omega)D + \omega\tilde{U})x_m + \omega b$$

or

$$\begin{aligned} x_{m+1} &= (D - \omega\tilde{L})^{-1}((1 - \omega)D + \omega\tilde{U})x_m + \omega(D - \omega\tilde{L})^{-1}b \\ &= (I - \omega L)^{-1}((1 - \omega)I + \omega U)x_m + \omega(I - \omega L)^{-1}D^{-1}b \\ &\equiv R_{SOR(\omega)}x_m + c_{SOR(\omega)}. \end{aligned} \quad (6.21)$$

We distinguish three cases, depending on the values of ω : $\omega = 1$ is equivalent to the Gauss–Seidel method, $\omega < 1$ is called *underrelaxation*, and $\omega > 1$ is called *overrelaxation*. A somewhat superficial motivation for overrelaxation is that if the direction from x_m to x_{m+1} is a good direction in which to move the solution, then moving $\omega > 1$ times as far in that direction is better.

In the next two sections, we will show how to pick the optimal ω for the model problem. This optimality depends on using red-black ordering.

ALGORITHM 6.6. *One step of SOR(ω) on two-dimensional Poisson's equation with red-black ordering:*

for all nodes i, j that are red (**R**)

$$v_{m+1,i,j} = (1 - \omega)v_{m,i,j} + \omega(v_{m,i-1,j} + v_{m,i+1,j} + v_{m,i,j-1} + v_{m,i,j+1} + h^2 f_{ij})/4$$

end for

for all nodes i, j that are black (**B**)

$$v_{m+1,i,j} = (1 - \omega)v_{m,i,j} + \omega(v_{m+1,i-1,j} + v_{m+1,i+1,j} + v_{m+1,i,j-1} + v_{m+1,i,j+1} + h^2 f_{ij})/4$$

end for

6.5.4. Convergence of Jacobi's, Gauss–Seidel, and $\text{SOR}(\omega)$ Methods on the Model Problem

It is easy to compute how fast Jacobi's method converges on the model problem, since the corresponding splitting is $T_{N \times N} = 4I - (4I - T_{N \times N})$, and so $R_J = (4I)^{-1}(4I - T_{N \times N}) = I - T_{N \times N}/4$. Thus the eigenvalues of R_J are $1 - \lambda_{i,j}/4$, where the $\lambda_{i,j}$ are the eigenvalues of $T_{N \times N}$:

$$\lambda_{i,j} = \lambda_i + \lambda_j = 4 - 2 \left(\cos \frac{\pi i}{N+1} + \cos \frac{\pi j}{N+1} \right).$$

$\rho(R_J)$ is the largest of $|1 - \lambda_{i,j}/4|$, namely,

$$\rho(R_J) = |1 - \lambda_{1,1}/4| = |1 - \lambda_{N,N}/4| = \cos \frac{\pi}{N+1} \approx 1 - \frac{\pi^2}{2(N+1)^2}.$$

Note that as N grows and T becomes more ill-conditioned, the spectral radius $\rho(R_J)$ approaches 1. Since the error is multiplied by the spectral radius at each step, convergence slows down. To estimate the speed of convergence more precisely, let us compute the number m of Jacobi iterations required to decrease the error by $e^{-1} = \exp(-1)$. Then m must satisfy $(\rho(R_J))^m = e^{-1}$, $(1 - \frac{\pi^2}{2(N+1)^2})^m = e^{-1}$, or $m \approx \frac{2(N+1)^2}{\pi^2} = O(N^2) = O(n)$. Thus the number of iterations is proportional to the number of unknowns. Since one step of Jacobi costs $O(1)$ to update each solution component or $O(n)$ to update all of them, it costs $O(n^2)$ to decrease the error by e^{-1} (or by any constant factor less than 1). This explains the entry for Jacobi's method in Table 6.1.

This is a common phenomenon: the more ill-conditioned the original problem, the more slowly most iterative methods converge. There are important exceptions, such as multigrid and domain decomposition, which we discuss later.

In the next section we will show, provided that the variables in Poisson's equation are updated in red-black order (see Algorithm 6.4 and Corollary 6.1), that $\rho(R_{GS}) = \rho(R_J)^2 = \cos^2 \frac{\pi}{N+1}$. In other words, one Gauss–Seidel step decreases the error as much as two Jacobi steps. This is a general phenomenon for matrices arising from approximating differential equations with certain finite difference approximations. This also explains the entry for the Gauss–Seidel method in Table 6.1; since it is only twice as fast as Jacobi, it still has the same complexity in the $O(\cdot)$ sense.

For the same red-black update order (see Algorithm 6.6 and Theorem 6.7), we will also show that for the relaxation parameter $1 < \omega = 2/(1 + \sin \frac{\pi}{N+1}) < 2$

$$\rho(R_{\text{SOR}(\omega)}) = \frac{\cos^2 \frac{\pi}{N+1}}{(1 + \sin \frac{\pi}{N+1})^2} \approx 1 - \frac{2\pi}{N+1} \text{ for large } N.$$

This is in contrast to $\rho(R) = 1 - O(\frac{1}{N^2})$ for R_J and R_{GS} . This is the optimal value for ω ; i.e., it minimizes $R_{\text{SOR}(\omega)}$. With this choice of ω , $\text{SOR}(\omega)$ is

approximately N times faster than Jacobi's or the Gauss–Seidel method, since if $\text{SOR}(\omega)$ takes j steps to decrease the error as much as k steps of Jacobi's or the Gauss–Seidel method, then $(1 - \frac{1}{N^2})^k \approx (1 - \frac{1}{N})^j$, implying $1 - \frac{k}{N^2} \approx 1 - \frac{j}{N}$ or $k \approx j \cdot N$. This lowers the complexity of $\text{SOR}(\omega)$ from $O(n^2)$ to $O(n^{3/2})$, as shown in Table 6.1.

In the next section we will show generally for certain finite difference matrices how to choose ω to minimize $\rho(R_{\text{SOR}(\omega)})$.

6.5.5. Detailed Convergence Criteria for Jacobi's, Gauss–Seidel, and $\text{SOR}(\omega)$ Methods

We will give a sequence of conditions that guarantee the convergence of these methods. The first criterion is simple to apply but is not always applicable, in particular not to the model problem. Then we give several more complicated criteria, which place stronger conditions on the matrix A but in return give more information about convergence. These more complicated criteria are tailored to fit the matrices arising from discretizing certain kinds of partial differential equations such as Poisson's equation.

Here is a summary of the results of this section:

1. If A is strictly row diagonally dominant (Definition 6.6), then Jacobi's and the Gauss–Seidel methods both converge, and the Gauss–Seidel method is faster (Theorem 6.2). Strict row diagonal dominance means that each diagonal entry of A is larger in magnitude than the sum of the magnitudes of the other entries in its row.
2. Since our model problem is not strictly row diagonally dominant, the last result does not apply. So we ask for a weaker form of diagonal dominance (Definition 6.11) but impose a condition called *irreducibility* on the pattern of nonzero entries of A (Definition 6.7) to prove convergence of Jacobi's and the Gauss–Seidel methods. The Gauss–Seidel method again converges faster than Jacobi's method (Theorem 6.3). This result applies to the model problem.
3. Turning to $\text{SOR}(\omega)$, we show that $0 < \omega < 2$ is necessary for convergence (Theorem 6.4). If A is also positive definite (like the model problem), $0 < \omega < 2$ is also sufficient for convergence (Theorem 6.5).
4. To quantitatively compare Jacobi's, Gauss–Seidel, and $\text{SOR}(\omega)$ methods, we make one more assumption about the pattern of nonzero entries of A . This property is called *Property A* (Definition 6.12) and is equivalent to saying that the *graph of the matrix* is *bipartite*. Property A essentially says that we can update the variables using red-black ordering. Given Property A there is a simple algebraic formula relating the eigenvalues of R_J , R_{GS} , and $R_{\text{SOR}(\omega)}$ (Theorem 6.6), which lets us compare their

rates of convergence. This formula also lets us compute the optimal ω that makes $\text{SOR}(\omega)$ converge as fast as possible (Theorem 6.7).

DEFINITION 6.6. *A is strictly row diagonally dominant if $|a_{ii}| > \sum_{j \neq i} |a_{ij}|$ for all i .*

THEOREM 6.2. *If A is strictly row diagonally dominant, Jacobi's and the Gauss-Seidel methods both converge. In fact $\|R_{GS}\|_\infty \leq \|R_J\|_\infty < 1$.*

The inequality $\|R_{GS}\|_\infty \leq \|R_J\|_\infty$ implies that one step of the worst problem for the Gauss-Seidel method converges at least as fast as one step of the worst problem for Jacobi's method. It does *not* guarantee that for any particular $Ax = b$, the Gauss-Seidel method will be faster than Jacobi's method; Jacobi's method could “accidentally” have a smaller error at some step. *Proof.* Again using the notation of equation (6.19), we write $R_J = L + U$ and $R_{GS} = (I - L)^{-1}U$. We want to prove

$$\|R_{GS}\|_\infty = \|(R_{GS}|e)\|_\infty \leq \|(R_J|e)\|_\infty = \|R_J\|_\infty, \quad (6.22)$$

where $e = [1, \dots, 1]^T$ is the vector of all ones. Inequality (6.22) will be true if can prove the stronger componentwise inequality

$$|(I - L)^{-1}U| \cdot e = |R_{GS}| \cdot e \leq |R_J| \cdot e = (|L| + |U|) \cdot e. \quad (6.23)$$

Since

$$\begin{aligned} |(I - L)^{-1}U| \cdot e &\leq |(I - L)^{-1}| \cdot |U| \cdot e && \text{by the triangle inequality} \\ &= \left| \sum_{i=0}^{n-1} L^i \right| \cdot |U| \cdot e && \text{since } L^n = 0 \\ &\leq \sum_{i=0}^{n-1} |L|^i \cdot |U| \cdot e && \text{by the triangle inequality} \\ &= (I - |L|)^{-1} \cdot |U| \cdot e && \text{since } |L|^n = 0, \end{aligned}$$

inequality (6.23) will be true if can prove the even stronger componentwise inequality

$$(I - |L|)^{-1} \cdot |U| \cdot e \leq (|L| + |U|) \cdot e. \quad (6.24)$$

Since all entries of $(I - |L|)^{-1} = \sum_{i=0}^{n-1} |L|^i$ are nonnegative, inequality (6.24) will be true if we can prove

$$|U| \cdot e \leq (I - |L|) \cdot (|L| + |U|) \cdot e = (|L| + |U| - |L|^2 - |L| \cdot |U|) \cdot e$$

or

$$0 \leq (|L| - |L|^2 - |L| \cdot |U|) \cdot e = |L| \cdot (I - |L| - |U|) \cdot e. \quad (6.25)$$

Since all entries of $|L|$ are nonnegative, inequality (6.25) will be true if we can prove

$$0 \leq (I - |L| - |U|) \cdot e \quad \text{or} \quad |R_J| \cdot e = (|L| + |U|)e \leq e. \quad (6.26)$$

Finally, inequality (6.26) is true because by assumption $\| |R_J| \cdot e \|_\infty = \|R_J\|_\infty = \rho < 1$. \square

An analogous result holds when A is strictly column diagonally dominant (i.e., A^T is strictly row diagonally dominant).

The reader may easily confirm that this simple criterion does not apply to the model problem, so we need to weaken the assumption of strict diagonal dominance. Doing so requires looking at the *graph properties* of a matrix.

DEFINITION 6.7. *A is an irreducible matrix if there is no permutation matrix P such that*

$$PAP^T = \left[\begin{array}{c|c} A_{11} & A_{12} \\ \hline 0 & A_{22} \end{array} \right].$$

We connect this definition to *graph theory* as follows.

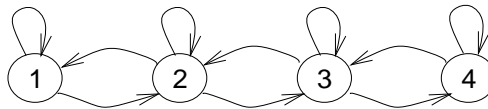
DEFINITION 6.8. *A directed graph is a finite collection of nodes connected by a finite collection of directed edges, i.e., arrows from one node to another. A path in a directed graph is a sequence of nodes n_1, \dots, n_m with an edge from each n_i to n_{i+1} . A self edge is an edge from a node to itself.*

DEFINITION 6.9. *The directed graph of A , $G(A)$, is a graph with nodes $1, 2, \dots, n$ and an edge from node i to node j if and only if $a_{ij} \neq 0$.*

EXAMPLE 6.1. The matrix

$$A = \begin{bmatrix} 2 & -1 & & \\ -1 & 2 & -1 & \\ & -1 & 2 & -1 \\ & & -1 & 2 \end{bmatrix}$$

has the directed graph



\diamond

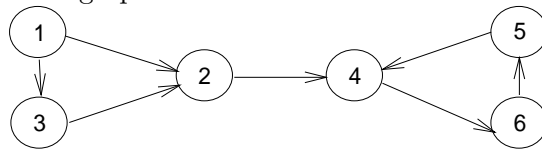
DEFINITION 6.10. *A directed graph is called strongly connected if there exists a path from every node i to every node j . A strongly connected component of a directed graph is a subgraph (a subset of the nodes with all edges connecting them) which is strongly connected and cannot be made larger yet still be strongly connected.*

EXAMPLE 6.2. The graph in Example 6.1 is strongly connected. \diamond

EXAMPLE 6.3. Let

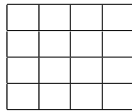
$$A = \left[\begin{array}{cc|cc} 1 & 1 & & \\ & & 1 & \\ \hline & 1 & & 1 \\ & & 1 & \\ & & & 1 \end{array} \right],$$

which has the directed graph



This graph is not strongly connected, since there is no path to node 1 from anywhere else. Nodes 4, 5, and 6 form a strongly connected component, since there is a path from any one of them to any other. \diamond

EXAMPLE 6.4. The graph of the model problem is strongly connected. The graph is essentially



except that each edge in the grid represents two edges (one in each direction), and the self edges are not shown. \diamond

LEMMA 6.6. A is irreducible if and only if $G(A)$ is strongly connected.

Proof. If $A = \begin{bmatrix} A_{11} & A_{12} \\ 0 & A_{22} \end{bmatrix}$ is reducible, then there is clearly no way to get from the nodes corresponding to A_{22} back to the ones corresponding to A_{11} ; i.e., $G(A)$ is not strongly connected. Similarly, if $G(A)$ is not strongly connected, renumber the rows (and columns) so that all the nodes in a particular strongly connected component come first; then the matrix PAP^T will be block upper triangular. \square

EXAMPLE 6.5. The matrix A in Example 6.3 is reducible.

DEFINITION 6.11. A is weakly row diagonally dominant if for all i , $|a_{ii}| \geq \sum_{k \neq i} |a_{ik}|$ with strict inequality at least once.

THEOREM 6.3. If A is irreducible and weakly row diagonally dominant, then both Jacobi's and Gauss-Seidel methods converge, and $\rho(R_{GS}) < \rho(R_J) < 1$.

For a proof of this theorem, see [247].

EXAMPLE 6.6. The model problem is weakly diagonally dominant and irreducible but not strongly diagonally dominant. (The diagonal is 4, and the offdiagonal sums are either 2, 3, or 4.) So Jacobi's and Gauss–Seidel methods converge on the model problem. \diamond

Despite the above results showing that under certain conditions the Gauss–Seidel method is faster than Jacobi's method, no such general result holds. This is because there are nonsymmetric matrices for which Jacobi's method converges and the Gauss–Seidel method diverges, as well as matrices for which the Gauss–Seidel method converges and Jacobi's method diverges [247].

Now we consider the convergence of $SOR(\omega)$ [247]. Recall its definition:

$$R_{SOR(\omega)} = (I - \omega L)^{-1}((1 - \omega)I + \omega U).$$

THEOREM 6.4. $\rho(R_{SOR(\omega)}) \geq |\omega - 1|$. Therefore $0 < \omega < 2$ is required for convergence.

Proof. Write the characteristic polynomial of $R_{SOR(\omega)}$ as $\varphi(\lambda) = \det(\lambda I - R_{SOR(\omega)}) = \det((I - \omega L)(\lambda I - R_{SOR(\omega)})) = \det((\lambda + \omega - 1)I - \omega \lambda L - \omega U)$ so that

$$\varphi(0) = \pm \prod_{i=1}^n \lambda_i(R_{SOR(\omega)}) = \pm \det((\omega - 1)I) = \pm(\omega - 1)^n,$$

implying $\max_i |\lambda_i(R_{SOR(\omega)})| \geq |\omega - 1|$. \square

THEOREM 6.5. If A is symmetric positive definite, then $\rho(R_{SOR(\omega)}) < 1$ for all $0 < \omega < 2$, so $SOR(\omega)$ converges for all $0 < \omega < 2$. Taking $\omega = 1$, we see that the Gauss–Seidel method also converges.

Proof. There are two steps. We abbreviate $R_{SOR(\omega)} = R$. Using the notation of equation (6.19), let $M = \omega^{-1}(D - \omega \tilde{L})$. Then we

(1) define $Q = A^{-1}(2M - A)$ and show $\Re \lambda_i(Q) > 0$ for all i ,

(2) show that $R = (Q - I)(Q + I)^{-1}$, implying $|\lambda_i(R)| < 1$ for all i .

For (1), note that $Qx = \lambda x$ implies $(2M - A)x = \lambda Ax$ or $x^*(2M - A)x = \lambda x^*Ax$. Add this last equation to its conjugate transpose to get $x^*(M + M^* - A)x = (\Re \lambda)(x^*Ax)$. So $\Re \lambda = x^*(M + M^* - A)x / x^*Ax = x^*(\frac{2}{\omega} - 1)Dx / x^*Ax > 0$ since A and $(\frac{2}{\omega} - 1)D$ are positive definite.

To prove (2), note that $(Q - I)(Q + I)^{-1} = (2A^{-1}M - 2I)(2A^{-1}M)^{-1} = I - M^{-1}A = R$, so by the spectral mapping theorem (Question 4.5)

$$|\lambda(R)| = \left| \frac{\lambda(Q) - 1}{\lambda(Q) + 1} \right| = \left| \frac{(\Re \lambda(Q) - 1)^2 + (\Im \lambda(Q))^2}{(\Re \lambda(Q) + 1)^2 + (\Im \lambda(Q))^2} \right|^{\frac{1}{2}} < 1. \quad \square$$

Together, Theorems 6.4 and 6.5 imply that if A is symmetric positive definite, then $SOR(\omega)$ converges if and only if $0 < \omega < 2$.

EXAMPLE 6.7. The model problem is symmetric positive definite, so $\text{SOR}(\omega)$ converges for $0 < \omega < 2$. \diamond

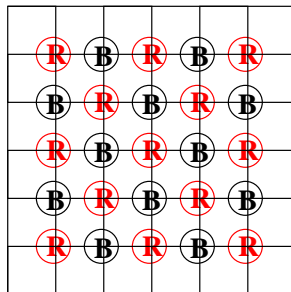
For the final comparison of the costs of Jacobi's, Gauss–Seidel, and $\text{SOR}(\omega)$ methods on the model problem we impose another graph theoretic condition on A that often arises from certain discretized partial differential equations, such as Poisson's equation. This condition will let us compute $\rho(R_{GS})$ and $\rho(R_{\text{SOR}(\omega)})$ explicitly in terms of $\rho(R_J)$.

DEFINITION 6.12. A matrix T has property A if there exists a permutation P such that

$$PTP^T = \left[\begin{array}{c|c} T_{11} & T_{12} \\ \hline T_{21} & T_{22} \end{array} \right],$$

where T_{11} and T_{22} are diagonal. In other words in the graph $G(A)$ the nodes divide into two sets $S_1 \cup S_2$, where there are no edges between two nodes both in S_1 or both in S_2 (ignoring self edges); such a graph is called bipartite.

EXAMPLE 6.8. *Red-black ordering* for the model problem. This was introduced in section 6.5.2, using the following chessboard-like depiction of the graph of the model problem: The black $\textcircled{\mathbf{B}}$ nodes are in S_1 , and the red $\textcircled{\mathbf{R}}$ nodes are in S_2 .



As described in section 6.5.2, each equation in the model problem relates the value at a grid point to the values at its left, right, top, and bottom neighbors, which are colored differently from the grid point in the middle. In other words, there is no direct connection from an $\textcircled{\mathbf{R}}$ node to an $\textcircled{\mathbf{R}}$ node or from a $\textcircled{\mathbf{B}}$ node to a $\textcircled{\mathbf{B}}$ node. So if we number the red nodes before the black nodes, the matrix will be in the form demanded by Definition 6.12. For

example, in the case of a 3-by-3 grid, we get the following:

$$\begin{aligned}
 P & \left[\begin{array}{ccc|ccc|ccc} 4 & -1 & & -1 & & & & & \\ -1 & 4 & -1 & & -1 & & & & \\ & -1 & 4 & & & -1 & & & \\ \hline -1 & & & 4 & -1 & & -1 & & \\ & -1 & & -1 & 4 & -1 & & -1 & \\ & & -1 & & -1 & 4 & & & \\ \hline & & & -1 & & & 4 & -1 & \\ & & & & -1 & & -1 & 4 & -1 \\ & & & & & -1 & & -1 & 4 \end{array} \right] P^T \\
 &= \left[\begin{array}{cccc|cccc} 4 & & & & -1 & -1 & & \\ & 4 & & & -1 & & -1 & \\ & & 4 & & -1 & -1 & -1 & -1 \\ & & & 4 & & -1 & & -1 \\ & & & & 4 & & -1 & -1 \\ \hline -1 & -1 & -1 & & 4 & & & \\ -1 & & -1 & -1 & & 4 & & \\ & -1 & -1 & & & & 4 & \\ & & -1 & -1 & -1 & & & 4 \end{array} \right] \cdot \diamond
 \end{aligned}$$

Now suppose that T has Property A , so we can write (where $D_i = T_{ii}$ is diagonal)

$$\begin{aligned}
 PTP^T &= \begin{bmatrix} D_1 & T_{12} \\ T_{21} & D_2 \end{bmatrix} = \begin{bmatrix} D_1 & \\ & D_2 \end{bmatrix} - \begin{bmatrix} 0 & 0 \\ -T_{21} & 0 \end{bmatrix} - \begin{bmatrix} 0 & -T_{12} \\ 0 & 0 \end{bmatrix} \\
 &= D - \tilde{L} - \tilde{U}.
 \end{aligned}$$

DEFINITION 6.13. Let $R_J(\alpha) = \alpha L + \frac{1}{\alpha}U$. Then $R_J(1) = R_J$ is the iteration matrix for Jacobi's method.

PROPOSITION 6.2. The eigenvalues of $R_J(\alpha)$ are independent of α .

Proof.

$$R_J(\alpha) = - \begin{bmatrix} 0 & \frac{1}{\alpha}D_1^{-1}T_{12} \\ \alpha D_2^{-1}T_{21} & 0 \end{bmatrix}$$

has the same eigenvalues as the similar matrix

$$\begin{bmatrix} I & \\ & \alpha I \end{bmatrix}^{-1} R_J(\alpha) \begin{bmatrix} I & \\ & \alpha I \end{bmatrix} = - \begin{bmatrix} 0 & D_1^{-1}T_{12} \\ D_2^{-1}T_{21} & 0 \end{bmatrix} = R_J(1). \quad \square$$

DEFINITION 6.14. Let T be any matrix, with $T = D - \tilde{L} - \tilde{U}$ and $R_J(\alpha) = \alpha D^{-1}\tilde{L} + \frac{1}{\alpha}D^{-1}\tilde{U}$. If $R_J(\alpha)$'s eigenvalues are independent of α , then T is called consistently ordered.

It is an easy fact that if T has Property A, such as the model problem, then PTP^T is consistently ordered for the permutation P that makes $PTP^T = \begin{bmatrix} T_{11} & T_{12} \\ T_{21} & T_{22} \end{bmatrix}$ have diagonal T_{11} and T_{22} . It is not true that consistent ordering implies a matrix has property A.

EXAMPLE 6.9. Any block tridiagonal matrix

$$\begin{bmatrix} D_1 & A_1 & & \\ B_1 & \ddots & \ddots & \\ & \ddots & \ddots & A_{n-1} \\ & & B_{n-1} & D_n \end{bmatrix}$$

is consistently ordered when the D_i are diagonal. \diamond

Consistent ordering implies that there are simple formulas relating the eigenvalues of R_J , R_{GS} , and $R_{SOR(\omega)}$ [247].

THEOREM 6.6. *If A is consistently ordered and $\omega = 0$, then the following are true:*

- 1) *The eigenvalues of R_J appear in \pm pairs.*
- 2) *If μ is an eigenvalue of R_J and*

$$(\lambda + \omega - 1)^2 = \lambda \omega^2 \mu^2, \quad (6.27)$$

then λ is an eigenvalue of $R_{SOR(\omega)}$.

- 3) *Conversely, if $\lambda = 0$ is an eigenvalue of $R_{SOR(\omega)}$, then μ in equation (6.27) is an eigenvalue of R_J .*

Proof.

- 1) Consistent ordering implies that the eigenvalues of $R_J(\alpha)$ are independent of α , so $R_J = R_J(1)$ and $R_J(-1) = -R_J(1)$ have same eigenvalues; hence they appear in \pm pairs.
- 2) If $\lambda = 0$ and equation (6.27) holds, then $\omega = 1$ and 0 is indeed an eigenvalue of $R_{SOR(1)} = R_{GS} = (I - L)^{-1}U$ since R_{GS} is singular. Otherwise

$$\begin{aligned} 0 &= \det(\lambda I - R_{SOR(\omega)}) \\ &= \det((I - \omega L)(\lambda I - R_{SOR(\omega)})) \\ &= \det((\lambda + \omega - 1)I - \omega \lambda L - \omega U) \\ &= \det\left(\sqrt{\lambda \omega} \left(\left(\frac{\lambda + \omega - 1}{\sqrt{\lambda \omega}} \right) I - \sqrt{\lambda} L - \frac{1}{\sqrt{\lambda}} U \right)\right) \\ &= \det\left(\left(\frac{\lambda + \omega - 1}{\sqrt{\lambda \omega}} \right) I - L - U\right) (\sqrt{\lambda \omega})^n, \end{aligned}$$

where the last equality is true because of Proposition 6.2. Therefore $\frac{\lambda + \omega - 1}{\sqrt{\lambda \omega}} = \mu$, an eigenvalue of $L + U = R_J$, and $(\lambda + \omega - 1)^2 = \mu^2 \omega^2 \lambda$.

3) If $\lambda = 0$, the last set of equalities works in the opposite direction. \square

COROLLARY 6.1. *If A is consistently ordered, then $\rho(R_{GS}) = (\rho(R_J))^2$. This means that the Gauss–Seidel method is twice as fast as Jacobi’s method.*

Proof. The choice $\omega = 1$ is equivalent to the Gauss–Seidel method, so $\lambda^2 = \lambda\mu^2$ or $\lambda = \mu^2$ \square

To get the most benefit from overrelaxation, we would like to find ω_{opt} minimizing $\rho(R_{SOR(\omega)})$ [247].

THEOREM 6.7. *Suppose that A is consistently ordered, R_J has real eigenvalues, and $\mu = \rho(R_J) < 1$. Then*

$$\begin{aligned}\omega_{opt} &= \frac{2}{1 + \sqrt{1 - \mu^2}}, \\ \rho(R_{SOR(\omega_{opt})}) &= \omega_{opt} - 1 = \frac{\mu^2}{[1 + \sqrt{1 - \mu^2}]^2}, \\ \rho(R_{SOR(\omega)}) &= \begin{cases} \omega - 1, & \omega_{opt} \leq \omega \leq 2, \\ 1 - \omega + \frac{1}{2}\omega^2\mu^2 + \omega\mu\sqrt{1 - \omega + \frac{1}{4}\omega^2\mu^2}, & 0 < \omega \leq \omega_{opt}. \end{cases}\end{aligned}$$

Proof. Solve $(\lambda + \omega - 1)^2 = \lambda\omega^2\mu^2$ for λ . \square

EXAMPLE 6.10. The model problem is an example: R_J is symmetric, so it has real eigenvalues. Figure 6.5 shows a plot of $\rho(R_{SOR(\omega)})$ versus ω , along with $\rho(R_{GS})$ and $\rho(R_J)$, for the model problem on an N -by- N grid with $N = 16$ and $N = 64$. The plots on the left are of $\rho(R)$, and the plots on the right are semilogarithmic plots of $1 - \rho(R)$. The main conclusion that we can draw is that the graph of $\rho(R_{SOR(\omega)})$ has a very narrow minimum, so if ω is even slightly different from ω_{opt} , the convergence will slow down significantly. The second conclusion is that if you have to guess ω_{opt} , a large value (near 2) is a better guess than a small value. \diamond

6.5.6. Chebyshev Acceleration and Symmetric SOR (SSOR)

Of the methods we have discussed so far, Jacobi’s and Gauss–Seidel methods require no information about the matrix to execute them (although proving that they converge requires some information). $SOR(\omega)$ depends on a parameter ω , which can be chosen depending on $\rho(R_J)$ to accelerate convergence. Chebyshev acceleration is useful when we know even more about the spectrum of R_J than just $\rho(R_J)$ and lets us further accelerate convergence.

Suppose that we convert $Ax = b$ to the iteration $x_{i+1} = Rx_i + c$ using some method (Jacobi’s, Gauss–Seidel, or $SOR(\omega)$). Then we get a sequence $\{x_i\}$ where $x_i \rightarrow x$ as $i \rightarrow \infty$ if $\rho(R) < 1$.

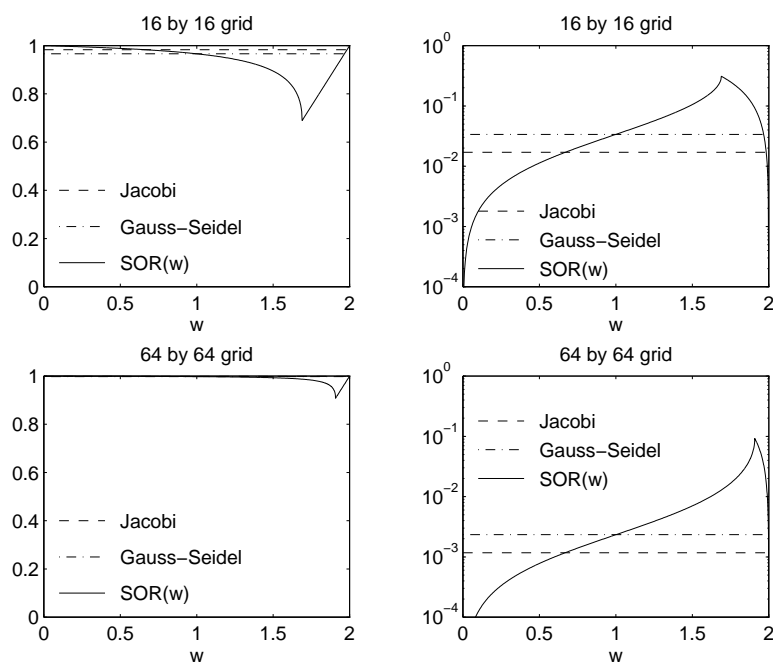


Fig. 6.5. Convergence of Jacobi's, Gauss-Seidel, and $SOR(\omega)$ methods versus ω on the model problem on a 16-by-16 grid and a 64-by-64 grid. The spectral radius $\rho(R)$ of each method ($\rho(R_J)$, $\rho(R_{GS})$, and $\rho(R_{SOR(\omega)})$) is plotted on the left, and $1 - \rho(R)$ on the right.

Given all these approximations x_i , it is natural to ask whether some linear combination of them, $y_m = \sum_{i=1}^m \gamma_{mi} x_i$, is an even better approximation of the solution x . Note that the scalars γ_{mi} must satisfy $\sum_{i=0}^m \gamma_{mi} = 1$, since if $x_0 = x_1 = \cdots = x$, we want $y_m = x$, too. So we can write the error in y_m as

$$\begin{aligned} y_m - x &= \sum_{i=0}^m \gamma_{mi} x_i - x \\ &= \sum_{i=0}^m \gamma_{mi} (x_i - x) \\ &= \sum_{i=0}^m \gamma_{mi} R^i (x_0 - x) \\ &= p_m(R)(x_0 - x), \end{aligned} \tag{6.28}$$

where $p_m(R) = \sum_{i=0}^m \gamma_{mi} R^i$ is a polynomial of degree m with $p_m(1) = \sum_{i=0}^m \gamma_{mi} = 1$.

EXAMPLE 6.11. If we could choose p_m to be the characteristic polynomial of R , then $p_m(R) = 0$ by the Cayley–Hamilton theorem, and we would converge in m steps. But this is not practical, because we seldom know the eigenvalues of R and we want to converge much faster than in $m = \dim(R)$ steps anyway. \diamond

Instead of seeking a polynomial such that $p_m(R)$ is zero, we will settle for making the spectral radius of $p_m(R)$ as small as we can. Suppose that we knew

- the eigenvalues of R were real,
- the eigenvalues of R lay in an interval $[-\rho, \rho]$ not containing 1.

Then we could try to choose a polynomial p_m where

- 1) $p_m(1) = 1$,
- 2) $\max_{-\rho \leq x \leq \rho} |p_m(x)|$ is as small as possible.

Since the eigenvalues of $p_m(R)$ are $p_m(\lambda(R))$ (see Problem 4.5), these eigenvalues would be small and so the spectral radius (the largest eigenvalue in absolute value) would be small.

Finding a polynomial p_m to satisfy conditions 1) and 2) above is a classical problem in approximation theory whose solution is based on *Chebyshev polynomials*.

DEFINITION 6.15. *The m th Chebyshev polynomial is defined by the recurrence $T_m(x) \equiv 2xT_{m-1}(x) - T_{m-2}(x)$, where $T_0(x) = 1$ and $T_1(x) = x$.*

Chebyshev polynomials have many interesting properties [238]. Here are a few, which are easy to prove from the definition (see Question 6.7).

LEMMA 6.7. *Chebyshev polynomials have the following properties:*

- $T_m(1) = 1$.
- $T_m(x) = 2^{m-1}x^m + O(x^{m-1})$.
- $T_m(x) = \begin{cases} \cos(m \cdot \arccos x) & \text{if } |x| \leq 1, \\ \cosh(m \cdot \operatorname{arccosh} x) & \text{if } |x| \geq 1. \end{cases}$
- $|T_m(x)| \leq 1$ if $|x| \leq 1$.
- The zeros of $T_m(x)$ are $x_i = \cos((2i-1)\pi/(2m))$ for $i = 1, \dots, m$.
- $T_m(x) = \frac{1}{2}[(x + \sqrt{x^2 - 1})^m + (x - \sqrt{x^2 - 1})^{-m}]$ if $|x| > 1$.
- $T_m(1 + \epsilon) \geq .5(1 + m\sqrt{2\epsilon})$ if $\epsilon > 0$.

Here is a table of values of $T_m(1 + \epsilon)$. Note how fast it grows as m grows, even when ϵ is tiny (see Figure 6.6).

m	ϵ		
	10^{-4}	10^{-3}	10^{-2}
10	1.0	1.1	2.2
100	2.2	44	$6.9 \cdot 10^5$
200	8.5	$3.8 \cdot 10^3$	$9.4 \cdot 10^{11}$
1000	$6.9 \cdot 10^5$	$1.3 \cdot 10^{19}$	$1.2 \cdot 10^{61}$

A polynomial with the properties we want is $p_m(x) = T_m(x/\rho)/T_m(1/\rho)$. To see why, note that $p_m(1) = 1$ and that if $x \in [-\rho, \rho]$, then $|p_m(x)| \leq 1/T_m(1/\rho)$. For example, if $\rho = 1/(1 + \epsilon)$, then $|p_m(x)| \leq 1/T_m(1 + \epsilon)$. As we have just seen, this bound is tiny for small ϵ and modest m .

To implement this cheaply, we use the three-term recurrence $T_m(x) = 2xT_{m-1}(x) - T_{m-2}(x)$ used to define Chebyshev polynomials. This means that we need only to save and combine three vectors y_m , y_{m-1} , and y_{m-2} , not all the previous x_m . To see how this works, let $\mu_m \equiv 1/T_m(1/\rho)$, so $p_m(R) = \mu_m T_m(R/\rho)$ and $\frac{1}{\mu_m} = \frac{2}{\rho\mu_{m-1}} - \frac{1}{\mu_{m-2}}$ by the three-term recurrence in Definition 6.15. Then

$$\begin{aligned}
 y_m - x &= p_m(R)(x_0 - x) \quad \text{by equation (6.28)} \\
 &= \mu_m T_m\left(\frac{R}{\rho}\right)(x_0 - x) \\
 &= \mu_m \left[2 \cdot \frac{R}{\rho} \cdot T_{m-1}\left(\frac{R}{\rho}\right)(x_0 - x) - T_{m-2}\left(\frac{R}{\rho}\right)(x_0 - x) \right] \\
 &\quad \text{by Definition 6.15}
 \end{aligned}$$

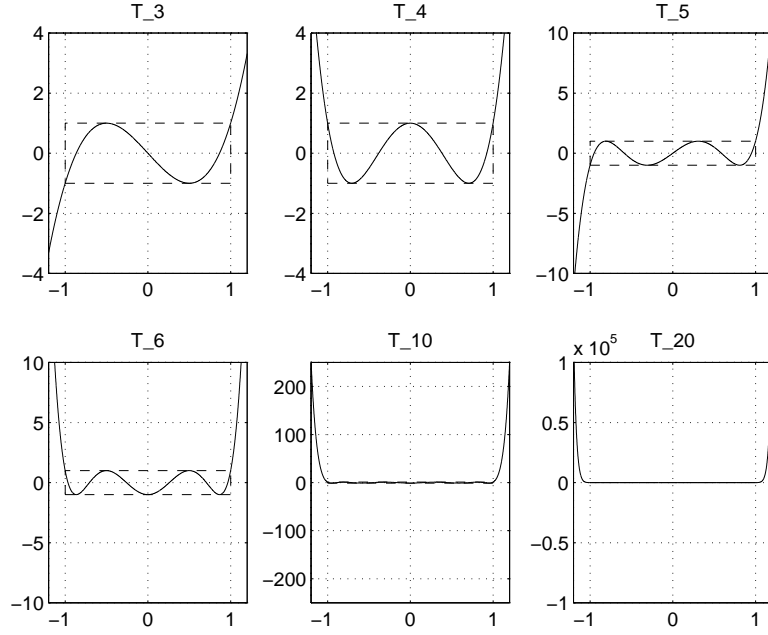


Fig. 6.6. Graph of $T_m(x)$ versus x . The dotted lines indicate that $|T_m(x)| \leq 1$ for $|x| \leq 1$.

$$\begin{aligned}
 &= \mu_m \left[2 \cdot \frac{R}{\rho} \cdot \frac{p_{m-1}(\frac{R}{\rho})(x_0 - x)}{\mu_{m-1}} - \frac{p_{m-2}(\frac{R}{\rho})(x_0 - x)}{\mu_{m-2}} \right] \\
 &= \mu_m \left[2 \cdot \frac{R}{\rho} \cdot \frac{y_{m-1} - x}{\mu_{m-1}} - \frac{y_{m-2} - x}{\mu_{m-2}} \right] \quad \text{by equation (6.28)}
 \end{aligned}$$

or

$$y_m = \frac{2\mu_m}{\mu_{m-1}} \frac{R}{\rho} y_{m-1} - \frac{\mu_m}{\mu_{m-2}} y_{m-2} + d_m,$$

where

$$\begin{aligned}
 d_m &= x - \frac{2\mu_m}{\mu_{m-1}} \left(\frac{R}{\rho} \right) x + \frac{\mu_m}{\mu_{m-2}} x \\
 &= x - \frac{2\mu_m}{\mu_{m-1}} \left(\frac{x - c}{\rho} \right) + \frac{\mu_m}{\mu_{m-2}} x \quad \text{since } x = Rx + c \\
 &= \mu_m \left(\frac{1}{\mu_m} - \frac{2}{\rho\mu_{m-1}} + \frac{1}{\mu_{m-2}} \right) x + \frac{2\mu_m}{\rho\mu_{m-1}} c \\
 &= \frac{2\mu_m}{\rho\mu_{m-1}} c \quad \text{by the definition of } \mu_m.
 \end{aligned}$$

This yields the algorithm.

ALGORITHM 6.7. Chebyshev acceleration of $x_{i+1} = Rx_i + c$:

$\mu_0 = 1; \mu_1 = \rho; y_0 = x_0; y_1 = Rx_0 + c$
 for $m = 2, 3, \dots$

$$\mu_m = 1 / \left(\frac{2}{\rho\mu_{m-1}} - \frac{1}{\mu_{m-2}} \right)$$

$$y_m = \frac{2\mu_m}{\rho\mu_{m-1}} Ry_{m-1} - \frac{\mu_m}{\mu_{m-2}} y_{m-2} + \frac{2\mu_m}{\rho\mu_{m-1}} c$$

 end for

Note that each iteration takes just one application of R , so if this is significantly more expensive than the other scalar and vector operations, this algorithm is no more expensive per step than the original iteration $x_{m+1} = Rx_m + c$.

Unfortunately, we cannot apply this directly to $\text{SOR}(\omega)$ for solving $Ax = b$, because $R_{\text{SOR}(\omega)}$ generally has complex eigenvalues, and Chebyshev acceleration requires that R have real eigenvalues in the interval $[-\rho, \rho]$. But we can fix this by using the following algorithm.

ALGORITHM 6.8. *SSOR*:

1. Take one step of $\text{SOR}(\omega)$ computing the components of x in the usual increasing order: $x_{i,1}, x_{i,2}, \dots, x_{i,n}$,
2. Take one step of $\text{SOR}(\omega)$ computing backwards: $x_{i,n}, x_{i,n-1}, \dots, x_{i,1}$.

We will reexpress this algorithm as $x_{i+1} = E_\omega x_i + c_\omega$ and show that E_ω has real eigenvalues, so we can use Chebyshev acceleration.

Suppose A is symmetric as in the model problem and again write $A = D - \tilde{L} - \tilde{U} = D(I - L - U)$ as in equation (6.19). Since $A = A^T$, $U = L^T$. Use equation (6.21) to rewrite the two steps of SSOR as

1. $x_{i+\frac{1}{2}} = (I - \omega L)^{-1}((1 - \omega)I + \omega U)x_i + c_{1/2} \equiv L_\omega x_i + c_{1/2}$,
2. $x_i = (I - \omega U)^{-1}((1 - \omega)I + \omega L)x_{i+\frac{1}{2}} + c_1 \equiv U_\omega x_{i+\frac{1}{2}} + c_1$.

Eliminating $x_{i+\frac{1}{2}}$ yields $x_{i+1} = E_\omega x_i + \hat{c}$, where

$$\begin{aligned}
 E_\omega &= U_\omega L_\omega \\
 &= I + (\omega - 2)^2 (I - \omega U)^{-1} (I - \omega L)^{-1} + (\omega - 2)(I - \omega U)^{-1} \\
 &\quad + (\omega - 2)(I - \omega U)^{-1} (I - \omega L)^{-1} (I - \omega U).
 \end{aligned}$$

We claim that E_ω has real eigenvalues, since it has the same eigenvalues as the similar matrix

$$\begin{aligned}
 &(I - \omega U)E_\omega(I - \omega U)^{-1} \\
 &= I + (2 - \omega)^2 (I - \omega L)^{-1} (I - \omega U)^{-1} + (\omega - 2)(I - \omega U)^{-1} \\
 &\quad + (\omega - 2)(I - \omega L)^{-1} \\
 &= I + (2 - \omega)^2 (I - \omega L)^{-1} (I - \omega L^T)^{-1} + (\omega - 2)(I - \omega L^T)^{-1} \\
 &\quad + (\omega - 2)(I - \omega L)^{-1},
 \end{aligned}$$

which is clearly symmetric and so must have real eigenvalues.

EXAMPLE 6.12. Let us apply SSOR(ω) with Chebyshev acceleration to the model problem. We need to both choose ω and estimate the spectral radius $\rho = \rho(E_\omega)$. The optimal ω that minimizes ρ is not known but Young [265, 135] has shown that the choice $\omega = \frac{2}{1+[2(1-\rho(R_J))]^{1/2}}$ is a good one, yielding $\rho(E_\omega) \approx 1 - \frac{\pi}{2N}$. With Chebyshev acceleration the error is multiplied by $\mu_m \approx \frac{1}{T_m(1+\frac{\pi}{2N})} \leq 2/(1+m\sqrt{\frac{\pi}{N}})$ at step m . Therefore, to decrease the error by a fixed factor < 1 requires $m = O(N^{1/2}) = O(n^{1/4})$ iterations. Since each iteration has the same cost as an iteration of SOR(ω), $O(n)$, the overall cost is $O(n^{5/4})$. This explains the entry for SSOR with Chebyshev acceleration in Table 6.1.

In contrast, after m steps of SOR(ω_{opt}), the error would decrease only by $(1 - \frac{\pi}{N})^m$. For example, consider $N = 1000$. Then SOR(ω_{opt}) requires $m = 220$ iterations to cut the error in half, whereas SSOR(ω_{opt}) with Chebyshev acceleration requires only $m = 17$ iterations. \diamond

6.6. Krylov Subspace Methods

These methods are used both to solve $Ax = b$ and to find eigenvalues of A . They assume that A is accessible only via a “black-box” subroutine that returns $y = Az$ given any z (and perhaps $y = A^T z$ if A is nonsymmetric). In other words, no direct access or manipulation of matrix entries is used. This is a reasonable assumption for several reasons. First, the cheapest nontrivial operation that one can perform on a (sparse) matrix is to multiply it by a vector; if A has m nonzero entries, matrix-vector multiplication costs m multiplications and (at most) m additions. Second, A may not be represented explicitly as a matrix but may be available only as a subroutine for computing Ax .

EXAMPLE 6.13. Suppose that we have a physical device whose behavior is modeled by a program, which takes a vector x of input parameters and produces a vector y of output parameters describing the device’s behavior. The output y may be an arbitrarily complicated function $y = f(x)$, perhaps requiring the solution of nonlinear differential equations. For example, x could be parameters describing the shape of a wing and $f(x)$ could be the drag on the wing, computed by solving the Navier–Stokes equations for the airflow over the wing. A common engineering design problem is to pick the input x to optimize the device behavior $f(x)$, where for concreteness we assume that this means making $f(x)$ as small as possible. Our problem is then to try to solve $f(x) = 0$ as nearly as we can. Assume for illustration that x and y are vectors of equal dimension. Then Newton’s method is an obvious candidate, yielding the iteration $x^{(m+1)} = x^{(m)} - (\nabla f(x^{(m)}))^{-1} f(x^{(m)})$, where $\nabla f(x^{(m)})$ is the Jacobian of f at $x^{(m)}$. We can rewrite this as solving the linear system $(\nabla f(x^{(m)})) \cdot \delta^{(m)} = f(x^{(m)})$ for $\delta^{(m)}$ and then computing $x^{(m+1)} = x^{(m)} - \delta^{(m)}$.

But how do we solve this linear system with coefficient matrix $\nabla f(x^{(m)})$ when computing $f(x^{(m)})$ is already complicated? It turns out that we can compute the matrix-vector product $(\nabla f(x)) \cdot z$ for an arbitrary vector z so that we can use Krylov subspace methods to solve the linear system. One way to compute $(\nabla f(x)) \cdot z$ is with *divided differences* or by using a Taylor expansion to see that $[f(x + hz) - f(x)]/h \approx (\nabla f(x)) \cdot z$. Thus, computing $(\nabla f(x)) \cdot z$ requires two calls to the subroutine that computes $f(\cdot)$, once with argument x and once with $x + hz$. However, sometimes it is difficult to choose h to get an accurate approximation of the derivative (choosing h too small results in a loss of accuracy due to roundoff). Another way to compute $(\nabla f(x)) \cdot z$ is to actually differentiate the function f . If f is simple enough, this can be done by hand. For complicated f , compiler tools can take a (nearly) arbitrary subroutine for computing $f(x)$ and automatically produce another subroutine for computing $(\nabla f(x)) \cdot z$ [29]. This can also be done by using the operator overloading facilities of C++ or Fortran 90, although this is less efficient. \diamond

A variety of different Krylov subspace methods exist. Some are suitable for nonsymmetric matrices, and others assume symmetry or positive definiteness. Some methods for nonsymmetric matrices assume that $A^T z$ can be computed as well as Az ; depending on how A is represented, $A^T z$ may or may not be available (see Example 6.13). The most efficient and best understood method, the conjugate gradient method (CG), is suitable only for symmetric positive definite matrices, including the model problem. We will concentrate on CG in this chapter.

Given a matrix that is not symmetric positive definite, it can be difficult to pick the best method from the many available. In section 6.6.6 we will give a short summary of the other methods available, besides CG, along with advice on which method to use in which situation. We also refer the reader to the more comprehensive on-line help at NETLIB/templates, which includes a book [24] and implementations in Matlab, Fortran, and C++. For a survey of current research in Krylov subspace methods, see [15, 105, 134, 212].

In Chapter 7, we will also discuss Krylov subspace methods for finding eigenvalues.

6.6.1. Extracting Information about A via Matrix-Vector Multiplication

Given a vector b and a subroutine for computing $A \cdot x$, what can we deduce about A ? The most obvious thing that we can do is compute the sequence of matrix-vector products $y_1 = b$, $y_2 = Ay_1$, $y_3 = Ay_2 = A^2 y_1$, \dots , $y_n = Ay_{n-1} = A^{n-1} y_1$, where A is n -by- n . Let $K = [y_1, y_2, \dots, y_n]$. Then we can write

$$A \cdot K = [Ay_1, \dots, Ay_{n-1}, Ay_n] = [y_2, \dots, y_n, A^n y_1]. \quad (6.29)$$

Note that the leading $n - 1$ columns of $A \cdot K$ are the same as the trailing $n - 1$ columns of K , shifted left by one. Assume for the moment that K is

nonsingular, so we can compute $c = -K^{-1}A^n y_1$. Then

$$A \cdot K = K \cdot [e_2, e_3, \dots, e_n, -c] \equiv K \cdot C,$$

where e_i is the i th column of the identity matrix, or

$$K^{-1}AK = C = \begin{bmatrix} 0 & 0 & \cdots & 0 & -c_1 \\ 1 & 0 & \cdots & 0 & -c_2 \\ 0 & 1 & \cdots & \vdots & \vdots \\ \vdots & 0 & \cdots & \vdots & \vdots \\ \vdots & \vdots & \cdots & 0 & \vdots \\ \vdots & \vdots & \cdots & 1 & -c_n \end{bmatrix}.$$

Note that C is upper Hessenberg. In fact, it is a *companion matrix* (see section 4.5.3), which means that its characteristic polynomial is $p(x) = x^n + \sum_{i=1}^n c_i x^{i-1}$. Thus, just by matrix-vector multiplication, we have reduced A to a very simple form, and in principle we could now find the eigenvalues of A by finding the zeros of $p(x)$.

However, this simple form is not useful in practice, for the following reasons:

1. Finding c requires $n - 1$ matrix-vector multiplications by A and then solving a linear system with K . Even if A is sparse, K is likely to be dense, so there is no reason to expect solving a linear system with K will be any easier than solving the original problem $Ax = b$.
2. K is likely to be very ill-conditioned, so c would be very inaccurately computed. This is because the algorithm is performing the power method (Algorithm 4.1) to get the columns y_i of K , so that y_i is converging to an eigenvector corresponding to the largest eigenvalue of A . Thus, the columns of K tend to get more and more parallel.

We will overcome these problems as follows: We will replace K with an orthogonal matrix Q such that for all k , the leading k columns of K and Q span the same space. This space is called a *Krylov subspace*. In contrast to K , Q is well conditioned and easy to invert. Furthermore, we will compute only as many leading columns of Q as needed to get an accurate solution (for $Ax = b$ or $Ax = \lambda x$). In practice we usually need very few columns compared to the matrix dimension n .

We proceed by writing $K = QR$, the QR decomposition of K . Then

$$K^{-1}AK = (R^{-1}Q^T)A(QR) = C,$$

implying

$$Q^T A Q = R C R^{-1} \equiv H.$$

Since R and R^{-1} are both upper triangular and C is upper Hessenberg, it is easy to confirm that $H = RCR^{-1}$ is also upper Hessenberg (see Question 6.11). In other words, we have reduced A to upper Hessenberg form by an orthogonal transformation Q . (This is the first step of the algorithm for finding eigenvalues of nonsymmetric matrices discussed in section 4.4.6.) Note that if A is symmetric, so is $Q^T A Q = H$, and a symmetric matrix which is upper Hessenberg must also be lower Hessenberg, i.e., tridiagonal. In this case we write $Q^T A Q = T$.

We still need to show how to compute the columns of Q one at a time, rather than all of them: Let $Q = [q_1, \dots, q_n]$. Since $Q^T A Q = H$ implies $AQ = QH$, we can equate column j on both sides of $AQ = QH$, yielding

$$Aq_j = \sum_{i=1}^{j+1} h_{i,j} q_i.$$

Since the q_i are orthonormal, we can multiply both sides of this last equality by q_m^T to get

$$q_m^T Aq_j = \sum_{i=1}^{j+1} h_{i,j} q_m^T q_i = h_{m,j} \quad \text{for } 1 \leq m \leq j$$

and so

$$h_{j+1,j} q_{j+1} = Aq_j - \sum_{i=1}^j h_{i,j} q_i.$$

This justifies the following algorithm.

ALGORITHM 6.9. *The Arnoldi algorithm for (partial) reduction to Hessenberg form:*

```

 $q_1 = b / \|b\|_2$ 
/*  $k$  is the number of columns of  $Q$  and  $H$  to compute */
for  $j = 1$  to  $k$ 
     $z = Aq_j$ 
    for  $i = 1$  to  $j$ 
         $h_{i,j} = q_i^T z$ 
         $z = z - h_{i,j} q_i$ 
    end for
     $h_{j+1,j} = \|z\|_2$ 
    if  $h_{j+1,j} = 0$ , quit
     $q_{j+1} = z / h_{j+1,j}$ 
end for
    
```

The q_j computed by Arnoldi's algorithm are often called *Arnoldi vectors*. The loop over i updating z can be also be described as applying the *modified Gram-Schmidt algorithm* (Algorithm 3.1) to subtract the components in the directions q_1 through q_j away from z , leaving z orthogonal to them. Computing q_1 through q_k costs k matrix-vector multiplications by A , plus $O(k^2n)$ other work. If we stop the algorithm here, what have we learned about A ? Let us write $Q = [Q_k, Q_u]$, where $Q_k = [q_1, \dots, q_k]$ and $Q_u = [q_{k+1}, \dots, q_n]$. Note that we have computed only Q_k and q_{k+1} ; the other columns of Q_u are unknown. Then

$$\begin{aligned} H &= Q^T A Q = [Q_k, Q_u]^T A [Q_k, Q_u] = \begin{bmatrix} Q_k^T A Q_k & Q_k^T A Q_u \\ Q_u^T A Q_k & Q_u^T A Q_u \end{bmatrix} \\ &\equiv \begin{matrix} & k & n-k \\ k & H_k & H_{uk} \\ n-k & H_{ku} & H_u \end{matrix}. \end{aligned} \quad (6.30)$$

Note that H_k is upper Hessenberg, because H has the same property. For the same reason, H_{ku} has a single (possibly) nonzero entry in its upper right corner, namely, $h_{k+1,k}$. Thus, H_u and H_{uk} are unknown; we know only H_k and H_{ku} .

When A is symmetric, $H = T$ is symmetric and tridiagonal, and the Arnoldi algorithm simplifies considerably, because most of the $h_{i,j}$ are zero: Write

$$T = \begin{bmatrix} \alpha_1 & \beta_1 & & & \\ \beta_1 & \ddots & \ddots & & \\ & \ddots & \ddots & \beta_{n-1} & \\ & & \beta_{n-1} & \alpha_n & \end{bmatrix}.$$

Equating column j on both sides of $AQ = QT$ yields

$$Aq_j = \beta_{j-1}q_{j-1} + \alpha_jq_j + \beta_jq_{j+1}.$$

Since the columns of Q are orthonormal, multiplying both sides this equation by q_j^T yields $q_j^T A q_j = \alpha_j$. This justifies the following version of the Arnoldi algorithm, called the *Lanczos algorithm*.

ALGORITHM 6.10. *The Lanczos algorithm for (partial) reduction to symmetric tridiagonal form.*

```

 $q_1 = b/\|b\|_2, \beta_0 = 0, q_0 = 0$ 
for  $j = 1$  to  $k$ 
     $z = Aq_j$ 
     $\alpha_j = q_j^T z$ 
     $z = z - \alpha_j q_j - \beta_{j-1} q_{j-1}$ 
     $\beta_j = \|z\|_2$ 

```


if $\beta_j = 0$, *quit*
 $q_{j+1} = z/\beta_j$
end for

The q_j computed by the Lanczos algorithm are often called *Lanczos vectors*. After k steps of Lanczos, here is what we have learned about A :

$$\begin{aligned}
 T &= Q^T A Q = [Q_k, Q_u]^T A [Q_k, Q_u] \\
 &= \begin{bmatrix} Q_k^T A Q_k & Q_k^T A Q_u \\ Q_u^T A Q_k & Q_u^T A Q_u \end{bmatrix} \\
 &\quad \begin{matrix} k & n-k \\ n-k & \end{matrix} \\
 &\equiv \begin{matrix} k \\ n-k \end{matrix} \begin{pmatrix} T_k & T_{uk} \\ T_{ku} & T_u \end{pmatrix} \\
 &= \begin{bmatrix} T_k & T_{ku}^T \\ T_{ku} & T_u \end{bmatrix}. \tag{6.31}
 \end{aligned}$$

Because A is symmetric, we know T_k and $T_{ku} = T_{uk}^T$ but not T_u . T_{ku} has a single (possibly) nonzero entry in its upper right corner, namely, β_k . Note that β_k is nonnegative, because it is computed as the norm of z .

We define some standard notation associated with the partial factorization of A computed by the Arnoldi and Lanczos algorithms.

DEFINITION 6.16. *The Krylov subspace $\mathcal{K}_k(A, b)$ is $\text{span}[b, Ab, A^2b, \dots, A^{k-1}b]$.*

We will write \mathcal{K}_k instead of $\mathcal{K}_k(A, b)$ if A and b are implicit from the context. Provided that the algorithm does not quit because $z = 0$, the vectors Q_k computed by the Arnoldi or Lanczos algorithms form an orthonormal basis of the Krylov subspace \mathcal{K}_k . (One can show that \mathcal{K}_k has dimension k if and only if the Arnoldi or Lanczos algorithm can compute q_k without quitting first; see Question 6.12.) We also call H_k (or T_k) the *projection* of A onto the Krylov subspace \mathcal{K}_k .

Our goal is to design algorithms to solve $Ax = b$ using only the information computed by k steps of the Arnoldi or Lanczos algorithm. We hope that k can be much smaller than n , so the algorithms are efficient.

(In Chapter 7 we will use this same information for find eigenvalues of A . We can already sketch how we will do this: Note that if $h_{k+1,k}$ happens to be zero, then H (or T) is block upper triangular and so all the eigenvalues of H_k are also eigenvalues of H , and therefore also of A , since A and H are similar. The (right) eigenvectors of H_k are eigenvectors of H , and if we multiply them by Q_k , we get eigenvectors of A . When $h_{k+1,k}$ is nonzero but small, we expect the eigenvalues and eigenvectors of H_k to provide good approximations to the eigenvalues and eigenvectors of A .)

We finish this introduction by noting that roundoff error causes a number of the algorithms that we discuss to behave *entirely differently* from how they would in exact arithmetic. In particular, the vectors q_i computed by

the Lanczos algorithm can quickly lose orthogonality and in fact often become linearly dependent. This apparently disastrous numerical instability led researchers to abandon these algorithms for several years after their discovery. But eventually researchers learned either how to stabilize the algorithms or that convergence occurred despite instability! We return to these points in section 6.6.4, where we analyze the convergence of the conjugate gradient method for solving $Ax = b$ (which is “unstable” but converges anyway), and in Chapter 7, especially in sections 7.4 and 7.5, where we show how to compute eigenvalues (and the basic algorithm is modified to ensure stability).

6.6.2. Solving $Ax = b$ Using the Krylov Subspace \mathcal{K}_k

How do we solve $Ax = b$, given only the information available from k steps of either the Arnoldi or the Lanczos algorithm?

Since the only vectors we know are the columns of Q_k , the only place to “look” for an approximate solution is in the Krylov subspace \mathcal{K}_k spanned by these vectors. In other words, we see the “best” approximate solution of the form

$$x_k = \sum_{j=1}^k z_j q_j = Q_k \cdot z, \quad \text{where } z = [z_1, \dots, z_k]^T.$$

Now we have to define “best.” There are several natural but different definitions, leading to different algorithms. We let $x = A^{-1}b$ denote the true solution and $r_k = b - Ax_k$ denote the residual.

1. The “best” x_k minimizes $\|x_k - x\|_2$. Unfortunately, we do not have enough information in our Krylov subspace to compute this x_k .
2. The “best” x_k minimizes $\|r_k\|_2$. This is implementable, and the corresponding algorithms are called MINRES (for *minimum residual*) when A is symmetric [192] and GMRES (for *generalized minimum residual*) when A is nonsymmetric [213].
3. The “best” x_k makes $r_k \perp \mathcal{K}_k$, i.e., $Q_k^T r_k = 0$. This is sometimes called the *orthogonal residual* property, or a *Galerkin condition*, by analogy to a similar condition in the theory of finite elements. When A is symmetric, the corresponding algorithm is called SYMMLQ [192]. When A is nonsymmetric, a variation of GMRES works [209].
4. When A is symmetric and positive definite, it defines a norm $\|r\|_{A^{-1}} = (r^T A^{-1} r)^{1/2}$ (see Lemma 1.3). We say the “best” x_k minimizes $\|r_k\|_{A^{-1}}$. This norm is the same as $\|x_k - x\|_A$. The algorithm is called the conjugate gradient algorithm [143].

When A is symmetric positive definite, the last two definitions of “best” also turn out to be equivalent.

THEOREM 6.8. *Let A be symmetric, $T_k = Q_k^T A Q_k$, and $r_k = b - Ax_k$, where $x_k \in \mathcal{K}_k$. If T_k is nonsingular and $x_k = Q_k T_k^{-1} e_1 \|b\|_2$, where $e_1^{k \times 1} = [1, 0, \dots, 0]^T$, then $Q_k^T r_k = 0$. If A is also positive definite, then T_k must be nonsingular, and this choice of x_k also minimizes $\|r_k\|_{A^{-1}}$ over all $x_k \in \mathcal{K}_k$. We also have that $r_k = \pm \|r_k\|_{2q_{k+1}}$.*

Proof. We drop the subscripts k for ease of notation. Let $x = QT^{-1}e_1\|b\|_2$ and $r = b - Ax$, and assume that $T = Q^T A Q$ is nonsingular. We confirm that $Q^T r = 0$ by computing

$$\begin{aligned} Q^T r &= Q^T (b - Ax) = Q^T b - Q^T Ax \\ &= e_1 \|b\|_2 - Q^T A (QT^{-1}e_1\|b\|_2) \\ &\quad \text{because the first column of } Q \text{ is } b/\|b\|_2 \\ &\quad \text{and its other columns are orthogonal to } b \\ &= e_1 \|b\|_2 - (Q^T A Q)T^{-1}e_1\|b\|_2 \\ &= e_1 \|b\|_2 - (T)T^{-1}e_1\|b\|_2 \quad \text{because } Q^T A Q = T \\ &= 0. \end{aligned}$$

Now assume that A is also positive definite. Then T must be positive definite and thus nonsingular too (see Question 6.13). Let $\hat{x} = x + Qz$ be another candidate solution in \mathcal{K} , and let $\hat{r} = b - A\hat{x}$. We need to show that $\|\hat{r}\|_{A^{-1}}$ is minimized when $z = 0$. But

$$\begin{aligned} \|\hat{r}\|_{A^{-1}}^2 &= \hat{r}^T A^{-1} \hat{r} \quad \text{by definition} \\ &= (r - AQz)^T A^{-1} (r - AQz) \\ &\quad \text{since } \hat{r} = b - A\hat{x} = b - A(x + Qz) = r - AQz \\ &= r^T A^{-1} r - 2(AQz)^T A^{-1} r + (AQz)^T A^{-1} (AQz) \\ &= \|r\|_{A^{-1}}^2 - 2z^T Q^T r + \|AQz\|_{A^{-1}}^2 \\ &\quad \text{since } (AQz)^T A^{-1} r = z^T Q^T A A^{-1} r = z^T Q^T r \\ &= \|r\|_{A^{-1}}^2 + \|AQz\|_{A^{-1}}^2 \quad \text{since } Q^T r = 0, \end{aligned}$$

so $\|\hat{r}\|_{A^{-1}}$ is minimized if and only if $AQz = 0$. But $AQz = 0$ if and only if $z = 0$ since A is nonsingular and Q has full column rank.

To show that $r_k = \pm \|r_k\|_{2q_{k+1}}$, we reintroduce subscripts. Since $x_k \in \mathcal{K}_k$, we must have $r_k = b - Ax_k \in \mathcal{K}_{k+1}$, so r_k is a linear combination of the columns of Q_{k+1} , since these columns span \mathcal{K}_{k+1} . But since $Q_k^T r_k = 0$, the only column of Q_{k+1} to which r_k is not orthogonal is q_{k+1} . \square

6.6.3. Conjugate Gradient Method

The algorithm of choice for symmetric positive definite matrices is CG. Theorem 6.8 characterizes the solution x_k computed by CG. While MINRES might seem more natural than CG because it minimizes $\|r_k\|_2$ instead of $\|r_k\|_{A^{-1}}$, it

turns out that MINRES requires more work to implement, is more susceptible to numerical instabilities, and thus often produces less accurate answers than CG. We will see that CG has the particularly attractive property that it can be implemented by keeping only four vectors in memory at one time, and not k (q_1 through q_k). Furthermore, the work in the inner loop, beyond the matrix-vector product, is limited to two dot products, three “saxpy” operations (adding a multiple of one vector to another), and a handful of scalar operations. This is a very small amount of work and storage.

Now we derive CG. There are several ways to do this. We will start with the Lanczos algorithm (Algorithm 6.10), which computes the columns of the orthogonal matrix Q_k and the entries of the tridiagonal matrix T_k , along with the formula $x_k = Q_k T_k^{-1} e_1 \|b\|_2$ from Theorem 6.8. We will show how to compute x_k directly via recurrences for three sets of vectors. We will keep only the most recent vector from each set in memory at one time, overwriting the old ones. The first set of vectors are the approximate solutions x_k . The second set of vectors are the residuals $r_k = b - Ax_k$, which Theorem 6.8 showed were parallel to the Lanczos vectors q_{k+1} . The third set of vectors are the *conjugate gradients* p_k . The p_k are called *gradients* because a single step of CG can be interpreted as choosing a scalar ν so that the new solution $x_k = x_{k-1} + \nu p_k$ minimizes the residual norm $\|r_k\|_{A^{-1}} = (r_k^T A^{-1} r_k)^{1/2}$. In other words, the p_k are used as *gradient search directions*. The p_k are called *conjugate*, or more precisely *A-conjugate*, because $p_k^T A p_j = 0$ if $j \neq k$. In other words, the p_k are orthogonal with respect to the inner product defined by A (see Lemma 1.3).

Since A is symmetric positive definite, so is $T_k = Q_k^T A Q_k$ (see Question 6.13). This means we can perform Cholesky on T_k to get $T_k = \hat{L}_k \hat{L}_k^T = L_k D_k L_k^T$, where L_k is unit lower bidiagonal and D_k is diagonal. Then using the formula for x_k from Theorem 6.8, we get

$$\begin{aligned} x_k &= Q_k T_k^{-1} e_1 \|b\|_2 \\ &= Q_k (L_k^{-T} D_k^{-1} L_k^{-1}) e_1 \|b\|_2 \\ &= (Q_k L_k^{-T}) (D_k^{-1} L_k^{-1} e_1 \|b\|_2) \\ &\equiv (\tilde{P}_k)(y_k), \end{aligned}$$

where $\tilde{P}_k \equiv Q_k L_k^{-T}$ and $y_k \equiv D_k^{-1} L_k^{-1} e_1 \|b\|_2$. Write $\tilde{P}_k = [\tilde{p}_1, \dots, \tilde{p}_k]$. The conjugate gradients p_i will turn out to be parallel to the columns \tilde{p}_i of \tilde{P}_k . We know enough to prove the following lemma.

LEMMA 6.8. *The columns \tilde{p}_i of \tilde{P}_k are A-conjugate. In other words, $\tilde{P}_k^T A \tilde{P}_k$ is diagonal.*

Proof. We compute

$$\begin{aligned} \tilde{P}_k^T A \tilde{P}_k &= (Q_k L_k^{-T})^T A (Q_k L_k^{-T}) = L_k^{-1} (Q_k^T A Q_k) L_k^{-T} = L_k^{-1} (T_k) L_k^{-T} \\ &= L_k^{-1} (L_k D_k L_k^T) L_k^{-T} = D_k. \quad \square \end{aligned}$$

Now we derive simple recurrences for the columns of \tilde{P}_k and entries of y_k . We will show that $y_{k-1} \equiv [\eta_1, \dots, \eta_{k-1}]^T$ is identical to the leading $k-1$ entries of $y_k = [\eta_1, \dots, \eta_{k-1}, \eta_k]^T$ and that \tilde{P}_{k-1} is identical to the leading $k-1$ columns of \tilde{P}_k . Therefore we can let

$$x_k = \tilde{P}_k \cdot y_k = [\tilde{P}_{k-1}, \tilde{p}_k] \cdot \begin{bmatrix} y_{k-1} \\ \eta_k \end{bmatrix} = \tilde{P}_{k-1} y_{k-1} + \tilde{p}_k \eta_k = x_{k-1} + \tilde{p}_k \eta_k \quad (6.32)$$

be our recurrence for x_k .

The recurrence for the η_k is derived as follows. Since T_{k-1} is the leading $(k-1)$ -by- $(k-1)$ submatrix of T_k , L_{k-1} and D_{k-1} are also the leading $(k-1)$ -by- $(k-1)$ submatrices of L_k and D_k , respectively:

$$\begin{aligned} T_k &= \begin{bmatrix} \alpha_1 & \beta_1 & & \\ \beta_1 & \ddots & \ddots & \\ & \ddots & \ddots & \beta_{k-1} \\ & & \beta_{k-1} & \alpha_k \end{bmatrix} \\ &= L_k D_k L_k^T \\ &= \begin{bmatrix} 1 & & & \\ l_1 & \ddots & & \\ & \ddots & \ddots & \\ & & l_{k-1} & 1 \end{bmatrix} \cdot \begin{bmatrix} d_1 & & & \\ & \ddots & & \\ & & d_{k-1} & \\ & & & d_k \end{bmatrix} \cdot \begin{bmatrix} 1 & & & \\ l_1 & \ddots & & \\ & \ddots & \ddots & \\ & & l_{k-1} & 1 \end{bmatrix}^T \\ &= \begin{bmatrix} L_{k-1} & \\ l_{k-1} \hat{e}_{k-1}^T & 1 \end{bmatrix} \cdot \text{diag}(D_{k-1}, d_k) \cdot \begin{bmatrix} L_{k-1} & \\ l_{k-1} \hat{e}_{k-1}^T & 1 \end{bmatrix}^T, \end{aligned}$$

where $\hat{e}_{k-1}^T = [0, \dots, 0, 1]$ has dimension $k-1$. Similarly, D_{k-1}^{-1} and L_{k-1}^{-1} are also the leading $(k-1)$ -by- $(k-1)$ submatrices of $D_k^{-1} = \text{diag}(D_{k-1}^{-1}, d_k^{-1})$ and

$$L_k^{-1} = \begin{bmatrix} L_{k-1}^{-1} & \\ \star & 1 \end{bmatrix},$$

respectively, where the details of the last row \star do not concern us. This means that $y_{k-1} = D_{k-1}^{-1} L_{k-1}^{-1} \hat{e}_1 \|b\|_2$, where \hat{e}_1 has dimension $k-1$, is identical to the leading $k-1$ components of

$$\begin{aligned} y_k &= D_k^{-1} L_k^{-1} e_1 \|b\|_2 = \begin{bmatrix} D_{k-1}^{-1} & \\ & d_k^{-1} \end{bmatrix} \cdot \begin{bmatrix} L_{k-1}^{-1} & \\ \star & 1 \end{bmatrix} \cdot e_1 \|b\|_2 \\ &= \begin{bmatrix} D_{k-1}^{-1} L_{k-1}^{-1} \hat{e}_1 \|b\|_2 \\ \eta_k \end{bmatrix} = \begin{bmatrix} y_{k-1} \\ \eta_k \end{bmatrix}. \end{aligned}$$

Now we need a recurrence for the columns of $\tilde{P}_k = [\tilde{p}_1, \dots, \tilde{p}_k]$. Since L_{k-1}^T is upper triangular, so is L_{k-1}^{-T} , and it forms the leading $(k-1)$ -by- $(k-1)$

submatrix of L_k^{-T} . Therefore \tilde{P}_{k-1} is identical to the leading $k-1$ columns of

$$\tilde{P}_k = Q_k L_k^{-T} = [Q_{k-1}, q_k] \begin{bmatrix} L_{k-1}^{-T} & \star \\ 0 & 1 \end{bmatrix} = [Q_{k-1} L_{k-1}^{-T}, \tilde{p}_k] = [\tilde{P}_{k-1}, \tilde{p}_k].$$

From $\tilde{P}_k = Q_k L_k^{-T}$ we get $\tilde{P}_k L_k^T = Q_k$ or, equating the k th column on both sides, the recurrence

$$\tilde{p}_k = q_k - l_{k-1} \tilde{p}_{k-1}. \quad (6.33)$$

Altogether, we have recursions for q_k (from the Lanczos algorithm), for \tilde{p}_k (from equation (6.33)), and for the approximate solution x_k (from equation (6.32)). All these recursions are *short*; i.e., they require only the previous iterate or two to implement. Thus, they together provide the means to compute x_k while storing a small number of vectors and doing a small number of dot products, saxpys, and scalar work in the inner loop.

We still have to simplify these recursions slightly to get the ultimate CG algorithm. Since Theorem 6.8 tells us that r_k and q_{k+1} are parallel, we can replace the Lanczos recurrence for q_{k+1} with the recurrence $r_k = b - Ax_k$ or equivalently $r_k = r_{k-1} - \eta_k A \tilde{p}_k$ (gotten from multiplying the recurrence $x_k = x_{k-1} + \eta_k \tilde{p}_k$ by A and subtracting from $b = b$). This yields the three vector recurrences

$$r_k = r_{k-1} - \eta_k A \tilde{p}_k, \quad (6.34)$$

$$x_k = x_{k-1} + \eta_k \tilde{p}_k \quad \text{from equation (6.32)}, \quad (6.35)$$

$$\tilde{p}_k = q_k - l_{k-1} \tilde{p}_{k-1} \quad \text{from equation (6.33)}. \quad (6.36)$$

In order to eliminate q_k , substitute $q_k = r_{k-1} / \|r_{k-1}\|_2$ and $p_k \equiv \|r_{k-1}\|_2 \tilde{p}_k$ into the above recurrences to get

$$\begin{aligned} r_k &= r_{k-1} - \frac{\eta_k}{\|r_{k-1}\|_2} A p_k \\ &\equiv r_{k-1} - \nu_k A p_k, \end{aligned} \quad (6.37)$$

$$\begin{aligned} x_k &= x_{k-1} + \frac{\eta_k}{\|r_{k-1}\|_2} p_k \\ &\equiv x_{k-1} + \nu_k p_k, \end{aligned} \quad (6.38)$$

$$\begin{aligned} p_k &= r_{k-1} - \frac{\|r_{k-1}\|_2 l_{k-1}}{\|r_{k-2}\|_2} \cdot p_{k-1} \\ &\equiv r_{k-1} + \mu_k \cdot p_{k-1}. \end{aligned} \quad (6.39)$$

We still need formulas for the scalars ν_k and μ_k . As we will see, there are several equivalent mathematical expression for them in terms of dot products of vectors computed by the algorithm. Our ultimate formulas are chosen to minimize the number of dot products needed and because they are more stable than the alternatives.

To get a formula for ν_k , first we multiply both sides of equation (6.39) on the left by $p_k^T A$, and use the fact that p_k and p_{k-1} are A-conjugate (Lemma 6.8) to get

$$p_k^T A p_k = p_k^T A r_{k-1} + 0 = r_{k-1}^T A p_k. \quad (6.40)$$

Then, multiply both sides of equation (6.37) on the left by r_{k-1}^T and use the fact that $r_{k-1}^T r_k = 0$ (since the r_i are parallel to the columns of the orthogonal matrix Q) to get

$$\begin{aligned} \nu_k &= \frac{r_{k-1}^T r_{k-1}}{r_{k-1}^T A p_k} \\ &= \frac{r_{k-1}^T r_{k-1}}{p_k^T A p_k} \quad \text{by equation (6.40)}. \end{aligned} \quad (6.41)$$

(Equation (6.41) can also be derived from a property of ν_k in Theorem 6.8, namely, that it minimizes the residual norm

$$\begin{aligned} \|r_k\|_{A^{-1}}^2 &= r_k^T A^{-1} r_k \\ &= (r_{k-1} - \nu_k A p_k)^T A^{-1} (r_{k-1} - \nu_k A p_k) \quad \text{by equation (6.37)} \\ &= r_{k-1}^T A^{-1} r_{k-1} - 2\nu_k p_k^T r_{k-1} + \nu_k^2 p_k^T A p_k. \end{aligned}$$

This expression is a quadratic function of ν_k , so it can be easily minimized by setting its derivative with respect to ν_k to zero and solving for ν_k . This yields

$$\begin{aligned} \nu_k &= \frac{p_k^T r_{k-1}}{p_k^T A p_k} \\ &= \frac{(r_{k-1} + \mu_k \cdot p_{k-1})^T r_{k-1}}{p_k^T A p_k} \quad \text{by equation (6.39)} \\ &= \frac{r_{k-1}^T r_{k-1}}{p_k^T A p_k}, \end{aligned}$$

where we have used the fact that $p_{k-1}^T r_{k-1} = 0$, which holds since r_{k-1} is orthogonal to all vectors in \mathcal{K}_{k-1} , including p_{k-1} .)

To get a formula for μ_k , multiply both sides of equation (6.39) on the left by $p_{k-1}^T A$ and use the fact that p_k and p_{k-1} are A-conjugate (Lemma 6.8) to get

$$\mu_k = -\frac{p_{k-1}^T A r_{k-1}}{p_{k-1}^T A p_{k-1}}. \quad (6.42)$$

The trouble with this formula for μ_k is that it requires another dot product, $p_{k-1}^T A r_{k-1}$, besides the two required for ν_k . So we will derive another formula requiring no new dot products.

We do this by deriving an alternate formula for ν_k : Multiply both sides of equation (6.37) on the left by r_k^T , again use the fact that $r_{k-1}^T r_k = 0$, and solve for ν_k to get

$$\nu_k = -\frac{r_k^T r_k}{r_k^T A p_k}. \quad (6.43)$$

Equating the two expressions (6.41) and (6.43) for ν_{k-1} (note that we have subtracted 1 from the subscript), rearranging, and comparing to equation (6.42) yield our ultimate formula for μ_k :

$$\begin{aligned} \mu_k &= -\frac{p_{k-1}^T A r_{k-1}}{p_{k-1}^T A p_{k-1}} \\ &= \frac{r_{k-1}^T r_{k-1}}{r_{k-2}^T r_{k-2}}. \end{aligned} \quad (6.44)$$

Combining recurrences (6.37), (6.38), and (6.39) and formulas (6.41) and (6.44) yields our final implementation of the conjugate gradient algorithm.

ALGORITHM 6.11. *Conjugate gradient algorithm:*

```

k = 0; x0 = 0; r0 = b; p1 = b;
repeat
  k = k + 1
  z = A · pk
  νk = (rk-1T rk-1) / (pkT z)
  xk = xk-1 + νk pk
  rk = rk-1 - νk z
  μk+1 = (rkT rk) / (rk-1T rk-1)
  pk+1 = rk + μk+1 pk
until ||rk||2 is small enough

```

The cost of the inner loop for CG is one matrix-vector product $z = A \cdot p_k$, two inner products (by saving the value of $r_k^T r_k$ from one loop iteration to the next), three saxpys, and a few scalar operations. The only vectors that need to be stored are the current values of r , x , p , and $z = Ap$. For more implementation details, including how to decide if “ $\|r_k\|_2$ is small enough,” see NETLIB/templates/templates.html.

6.6.4. Convergence Analysis of the Conjugate Gradient Method

We begin with a convergence analysis of CG that depends only on the condition number of A . This analysis will show that the number of CG iterations needed to reduce the error by a fixed factor less than 1 is proportional to the square root of the condition number. This worst-case analysis is a good estimate for the speed of convergence on our model problem, Poisson’s equation. But it

severely *underestimates* the speed of convergence in many other cases. After presenting the bound based on the condition number, we describe when we can expect faster convergence.

We start with the initial approximate solution $x_0 = 0$. Recall that x_k minimizes the A^{-1} -norm of the residual $r_k = b - Ax_k$ over all possible solutions $x_k \in \mathcal{K}_k(A, b)$. This means x_k minimizes

$$\|b - Az\|_{A^{-1}}^2 \equiv f(z) = (b - Az)^T A^{-1}(b - Az) = (x - z)^T A(x - z)$$

over all $z \in \mathcal{K}_k = \text{span}[b, Ab, A^2b, \dots, A^{k-1}b]$. Any $z \in \mathcal{K}_k(A, b)$ may be written $z = \sum_{j=0}^{k-1} \alpha_j A^j b = p_{k-1}(A)b = p_{k-1}(A)Ax$, where $p_{k-1}(\xi) = \sum_{j=0}^{k-1} \alpha_j \xi^j$ is a polynomial of degree $k-1$. Therefore,

$$\begin{aligned} f(z) &= [(I - p_{k-1}(A)A)x]^T A[(I - p_{k-1}(A)A)x] \\ &\equiv (q_k(A)x)^T A(q_k(A)x) \\ &= x^T q_k(A)Aq_k(A)x, \end{aligned}$$

where $q_k(\xi) \equiv 1 - p_{k-1}(\xi) \cdot \xi$ is a degree- k polynomial with $q_k(0) = 1$. Note that $(q_k(A))^T = q_k(A)$ because $A = A^T$. Letting \mathcal{Q}_k be the set of all degree- k polynomials which take the value 1 at 0, this means

$$f(x_k) = \min_{z \in \mathcal{K}_k} f(z) = \min_{q_k \in \mathcal{Q}_k} x^T q_k(A)Aq_k(A)x. \quad (6.45)$$

To simplify this expression, write the eigendecomposition $A = Q\Lambda Q^T$ and let $Q^T x = y$ so that

$$\begin{aligned} f(x_k) = \min_{z \in \mathcal{K}_k} f(z) &= \min_{q_k \in \mathcal{Q}_k} x^T (q_k(Q\Lambda Q^T))(Q\Lambda Q^T)(q_k(Q\Lambda Q^T))x \\ &= \min_{q_k \in \mathcal{Q}_k} x^T (Qq_k(\Lambda)Q^T)(Q\Lambda Q^T)(Qq_k(\Lambda)Q^T)x \\ &= \min_{q_k \in \mathcal{Q}_k} y^T q_k(\Lambda)\Lambda q_k(\Lambda)y \\ &= \min_{q_k \in \mathcal{Q}_k} y^T \cdot \text{diag}(q_k(\lambda_i)\lambda_i q_k(\lambda_i)) \cdot y \\ &= \min_{q_k \in \mathcal{Q}_k} \sum_{i=1}^n y_i^2 \lambda_i (q_k(\lambda_i))^2 \\ &\leq \min_{q_k \in \mathcal{Q}_k} \left(\max_{\lambda_i \in \lambda(A)} (q_k(\lambda_i))^2 \right) \sum_{i=1}^n y_i^2 \lambda_i \\ &= \min_{q_k \in \mathcal{Q}_k} \left(\max_{\lambda_i \in \lambda(A)} (q_k(\lambda_i))^2 \right) f(x_0) \end{aligned}$$

since $x_0 = 0$ implies $f(x_0) = x^T Ax = y^T \Lambda y = \sum_{i=1}^n y_i^2 \lambda_i$. Therefore,

$$\frac{\|r_k\|_{A^{-1}}^2}{\|r_0\|_{A^{-1}}^2} = \frac{f(x_k)}{f(x_0)} \leq \min_{q_k \in \mathcal{Q}} \max_{\lambda_i \in \lambda(A)} (q_k(\lambda_i))^2$$

or

$$\frac{\|r_k\|_{A^{-1}}}{\|r_0\|_{A^{-1}}} \leq \min_{q_k \in \mathcal{Q}} \max_{\lambda_i \in \lambda(A)} |q_k(\lambda_i)|.$$

We have thus reduced the question of how fast CG converges to a question about polynomials: How small can a degree- k polynomial $q_k(\xi)$ be when ξ ranges over the eigenvalues of A , while simultaneously satisfying $q_k(0) = 1$? Since A is positive definite, its eigenvalues lie in the interval $[\lambda_{\min}, \lambda_{\max}]$, where $0 < \lambda_{\min} \leq \lambda_{\max}$, so to get a simple upper bound we will instead seek a degree- k polynomial $\hat{q}_k(\xi)$ that is small on the whole interval $[\lambda_{\min}, \lambda_{\max}]$ and 1 at 0. A polynomial $\hat{q}_k(\xi)$ that has this property is easily constructed from the Chebyshev polynomials $T_k(\xi)$ discussed in section 6.5.6. Recall that $|T_k(\xi)| \leq 1$ when $|\xi| \leq 1$ and increases rapidly when $|\xi| > 1$ (see Figure 6.6). Now let

$$\hat{q}_k(\xi) = T_k \left(\frac{\lambda_{\max} + \lambda_{\min} - 2\xi}{\lambda_{\max} - \lambda_{\min}} \right) / T_k \left(\frac{\lambda_{\max} + \lambda_{\min}}{\lambda_{\max} - \lambda_{\min}} \right)$$

It is easy to see that $\hat{q}_k(0) = 1$, and if $\xi \in [\lambda_{\min}, \lambda_{\max}]$, then

$$\left| \frac{\lambda_{\max} + \lambda_{\min} - 2\xi}{\lambda_{\max} - \lambda_{\min}} \right| \leq 1,$$

so

$$\begin{aligned} \frac{\|r_k\|_{A^{-1}}}{\|r_0\|_{A^{-1}}} &\leq \min_{q_k \in \mathcal{Q}} \max_{\lambda_i \in \lambda(A)} |q_k(\lambda_i)| \\ &\leq \frac{1}{T_k \left(\frac{\lambda_{\max} + \lambda_{\min}}{\lambda_{\max} - \lambda_{\min}} \right)} = \frac{1}{T_k \left(\frac{\kappa + 1}{\kappa - 1} \right)} = \frac{1}{T_k \left(1 + \frac{2}{\kappa - 1} \right)}, \end{aligned} \quad (6.46)$$

where $\kappa = \lambda_{\max}/\lambda_{\min}$ is the condition number of A .

If the condition number κ is near 1, $1 + 2/(\kappa - 1)$ is large, $1/T_k(1 + \frac{2}{\kappa - 1})$ is small, and convergence is rapid. If κ is large, convergence slows down, with the convergence rate

$$\frac{1}{T_k \left(1 + \frac{2}{\kappa - 1} \right)} \leq \frac{2}{1 + \frac{2k}{\sqrt{\kappa - 1}}}.$$

EXAMPLE 6.14. For the N -by- N model problem, $\kappa = O(N^2)$, so after k steps of CG the residual is multiplied by about $(1 - O(N^{-1}))^k$, the same as SOR with optimal overrelaxation parameter ω . In other words, CG takes $O(N) = O(n^{1/2})$ iterations to converge. Since each iteration costs $O(n)$, the overall cost is $O(n^{3/2})$. This explains the entry for CG in Table 6.1. \diamond

This analysis using the condition number does not explain all the important convergence behavior of CG. The next example shows that the entire distribution of eigenvalues of A is important, not just the ratio of the largest to the smallest one.

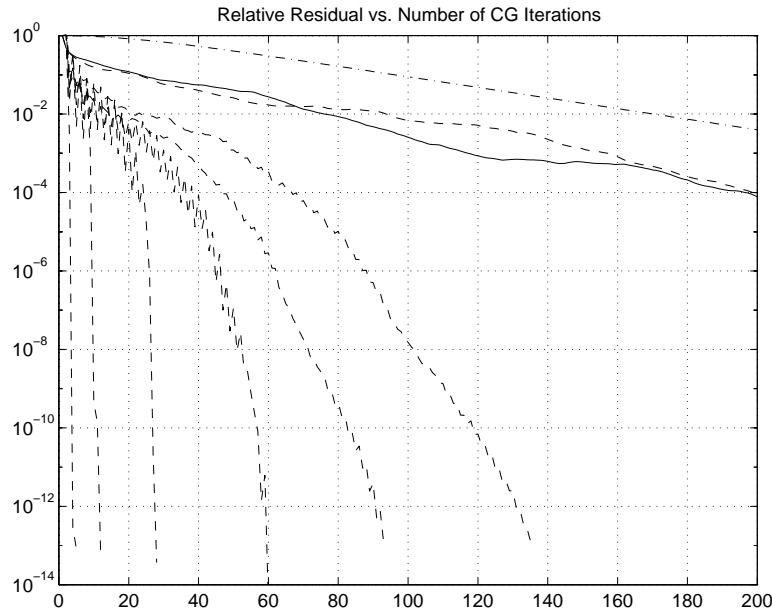


Fig. 6.7. Graph of relative residuals computed by CG.

EXAMPLE 6.15. Let us consider Figure 6.7, which plots the relative residual $\|r_k\|_2/\|r_0\|_2$ at each CG step for eight different linear systems. The relative residual $\|r_k\|_2/\|r_0\|_2$ measures the speed of convergence; our implementation of CG terminates when this ratio sinks below 10^{-13} , or after $k = 200$ steps, whichever comes first.

All eight linear systems shown have the same dimension $n = 10^4$ and the same condition number $\kappa \approx 4134$, yet their convergence behaviors are radically different. The uppermost (dash-dot) line is $1/T_k(1 + \frac{2}{\kappa-1})$, which inequality (6.46) tells us is an upper bound on $\|r_k\|_{A^{-1}}/\|r_0\|_{A^{-1}}$. It turns out the graphs of $\|r_k\|_2/\|r_0\|_2$ and the graphs of $\|r_k\|_{A^{-1}}/\|r_0\|_{A^{-1}}$ are nearly the same, so we plot only the former, which are easier to interpret.

The solid line is $\|r_k\|_2/\|r_0\|_2$ for Poisson's equation on a 100-by-100 grid with a random right-hand side b . We see that the upper bound captures its general convergence behavior. The seven dashed lines are plots of $\|r_k\|_2/\|r_0\|_2$ for seven diagonal linear systems $D_i x = b$, numbered from D_1 on the left to D_7 on the right. Each D_i has the same dimension and condition number as Poisson's equation, so we need to study them more closely to understand their differing convergence behaviors.

We have constructed each D_i so that its smallest m_i and largest m_i eigenvalues are identical to those of Poisson's equation, with the remaining $n - 2m_i$ eigenvalues equal to the geometric mean of the largest and smallest eigenvalues. In other words, D_i has only $d_i = 2m_i + 1$ distinct eigenvalues. We let k_i denote the number of CG iterations it takes for the solution of $D_i x = b$ to

reach $\|r_k\|_2/\|r_0\|_2 \leq 10^{-13}$. The convergence properties are summarized in the following table:

Example number	i	1	2	3	4	5	6	7
Number of distinct eigenvalues	d_i	3	11	41	81	201	401	5000
Number of steps to converge	k_i	3	11	27	59	94	134	> 200

We see that the number k_i of steps required to converge grows with the number d_i of distinct eigenvalues. D_7 has the same spectrum as Poisson's equation, and converges about as slowly.

In the absence of roundoff, we claim that CG would take *exactly* $k_i = d_i$ steps to converge. The reason is that we can find a polynomial $q_{d_i}(\xi)$ of degree d_i that is zero at the eigenvalues α_j of A , while $q_{d_i}(0) = 1$, namely,

$$q_{d_i}(\xi) = \frac{\prod_{j=1}^{d_i}(\alpha_j - \xi)}{\prod_{j=1}^{d_i}(\alpha_j)}.$$

Equation (6.45) tells us that after d_i steps, CG minimizes $\|r_{d_i}\|_{A^{-1}}^2 = f(x_{d_i})$ over all possible degree- d_i polynomials equaling 1 at 0. Since q_{d_i} is one of those polynomials and $q_{d_i}(A) = 0$, we must have $\|r_{d_i}\|_{A^{-1}}^2 = 0$, or $r_{d_i} = 0$. \diamond

One lesson of Example 6.15 is that if the largest and smallest eigenvalues of A are few in number (or clustered closely together), then CG will converge much more quickly than an analysis based just on A 's condition number would indicate.

Another lesson is that the behavior of CG in floating point arithmetic can differ significantly from its behavior in exact arithmetic. We saw this because the number d_i of distinct eigenvalues frequently differed from the number k_i of steps required to converge, although in theory we showed that they should be identical. Still, d_i and k_i were of the same order of magnitude.

Indeed, if one were to perform CG in exact arithmetic and compare the computed solutions and residuals with those computed in floating point arithmetic, they would very probably diverge and soon be quite different. Still, as long as A is not too ill-conditioned, the floating point result will eventually converge to the desired solution of $Ax = b$, and so CG is still very useful. The fact that the exact and floating point results can differ dramatically is interesting but does not prevent the practical use of CG.

When CG was discovered, it was proven that in exact arithmetic it would provide the exact answer after n steps, since then r_{n+1} would be orthogonal to n other orthogonal vectors r_1 through r_n , and so must be zero. In other words, CG was thought of as a *direct method* rather than an *iterative method*. When convergence after n steps did not occur in practice, CG was considered unstable and then abandoned for many years. Eventually it was recognized as a perfectly good iterative method, often providing quite accurate answers after $k \ll n$ steps.

Recently, a subtle backward error analysis was devised to explain the observed behavior of CG in floating point and explain how it can differ from exact arithmetic [121]. This behavior can also include long “plateaus” in the convergence, with $\|r_k\|_2$ decreasing little for many iterations, interspersed with periods of rapid convergence. This behavior can be explained by showing that CG applied to $Ax = b$ in floating point arithmetic behaves *exactly* like CG applied to $\tilde{A}\tilde{x} = \tilde{b}$ in exact arithmetic, where \tilde{A} is close to A in the following sense: \tilde{A} has a much larger dimension than A , but \tilde{A} ’s eigenvalues all lie in narrow clusters around the eigenvalues of A . Thus the plateaus in convergence correspond to the polynomial q_k underlying CG developing more and more zeros near the eigenvalues of \tilde{A} lying in a cluster.

6.6.5. Preconditioning

In the previous section we saw that the convergence rate of CG depended on the condition number of A , or more generally the distribution of A ’s eigenvalues. Other Krylov subspace methods have the same property. *Preconditioning* means replacing the system $Ax = b$ with the system $M^{-1}Ax = M^{-1}b$, where M is an approximation to A with the properties that

1. M is symmetric and positive definite,
2. $M^{-1}A$ is well conditioned or has few extreme eigenvalues,
3. $Mx = b$ is easy to solve.

A careful, problem-dependent choice of M can often make the condition number of $M^{-1}A$ much smaller than the condition number of A and thus accelerate convergence dramatically. Indeed, a good preconditioner is often necessary for an iterative method to converge at all, and much current research in iterative methods is directed at finding better preconditioners (see also section 6.10).

We cannot apply CG directly to the system $M^{-1}Ax = M^{-1}b$, because $M^{-1}A$ is generally not symmetric. We derive the *preconditioned conjugate gradient method* as follows. Let $M = Q\Lambda Q^T$ be the eigendecomposition of M , and define $M^{1/2} \equiv Q\Lambda^{1/2}Q^T$. Note that $M^{1/2}$ is also symmetric positive definite, and $(M^{1/2})^2 = M$. Now multiply $M^{-1}Ax = M^{-1}b$ through by $M^{1/2}$ to get the new symmetric positive definite system $(M^{-1/2}AM^{-1/2})(M^{1/2}x) = M^{-1/2}b$, or $\hat{A}\hat{x} = \hat{b}$. Note that \hat{A} and $M^{-1}A$ have the same eigenvalues since they are similar ($M^{-1}A = M^{-1/2}\hat{A}M^{1/2}$). We now apply CG *implicitly* to the system $\hat{A}\hat{x} = \hat{b}$ in such a way that avoids the need to multiply by $M^{-1/2}$. This yields the following algorithm.

ALGORITHM 6.12. *Preconditioned CG algorithm:*

$k = 0; x_0 = 0; r_0 = b; p_1 = M^{-1}b; y_0 = M^{-1}r_0$
repeat

$k = k + 1$
 $z = A \cdot p_k$
 $\nu_k = (y_{k-1}^T r_{k-1}) / (p_k^T z)$
 $x_k = x_{k-1} + \nu_k p_k$
 $r_k = r_{k-1} - \nu_k z$
 $y_k = M^{-1} r_k$
 $\mu_{k+1} = (y_k^T r_k) / (y_{k-1}^T r_{k-1})$
 $p_{k+1} = y_k + \mu_{k+1} p_k$
until $\|r_k\|_2$ is small enough

THEOREM 6.9. *Let A and M be symmetric positive definite, $\hat{A} = M^{-1/2} A M^{1/2}$, and $\hat{b} = M^{-1/2} b$. The CG algorithm applied to $\hat{A}\hat{x} = \hat{b}$,*

$k = 0; \hat{x}_0 = 0; \hat{r}_0 = \hat{b}; \hat{p}_1 = \hat{b};$
repeat
 $k = k + 1$
 $\hat{z} = \hat{A} \cdot \hat{p}_k$
 $\hat{\nu}_k = (\hat{r}_{k-1}^T \hat{r}_{k-1}) / (\hat{p}_k^T \hat{z})$
 $\hat{x}_k = \hat{x}_{k-1} + \hat{\nu}_k \hat{p}_k$
 $\hat{r}_k = \hat{r}_{k-1} - \hat{\nu}_k \hat{z}$
 $\hat{\mu}_{k+1} = (\hat{r}_k^T \hat{r}_k) / (\hat{r}_{k-1}^T \hat{r}_{k-1})$
 $\hat{p}_{k+1} = \hat{r}_k + \hat{\mu}_{k+1} \hat{p}_k$
until $\|\hat{r}_k\|_2$ is small enough

and Algorithm 6.12 are related as follows:

$$\begin{aligned}
 \hat{\mu}_k &= \mu_k, \\
 \hat{\nu}_k &= \nu_k, \\
 \hat{z} &= M^{-1/2} z, \\
 \hat{x}_k &= M^{1/2} x_k, \\
 \hat{r}_k &= M^{-1/2} r_k, \\
 \hat{p}_k &= M^{1/2} p_k.
 \end{aligned}$$

Therefore, x_k converges to $M^{-1/2}$ times the solution of $\hat{A}\hat{x} = \hat{b}$, i.e., to $M^{-1/2} \hat{A}^{-1} \hat{b} = A^{-1} b$.

For a proof, see Question 6.14.

Now we describe some common preconditioners. Note that our twin goals of minimizing the condition number of $M^{-1}A$ and keeping $Mx = b$ easy to solve are in conflict with one another: Choosing $M = A$ minimizes the condition number of $M^{-1}A$ but leaves $Mx = b$ as hard to solve as the original problem. Choosing $M = I$ makes solving $Mx = b$ trivial but leaves the condition number of $M^{-1}A$ unchanged. Since we need to solve $Mx = b$ in the inner loop of the algorithm, we restrict our discussion to those M for which solving $Mx = b$ is easy, and describe when they are likely to decrease the condition number of $M^{-1}A$.

- If A has widely varying diagonal entries, we may use the simple *diagonal preconditioner* $M = \text{diag}(a_{11}, \dots, a_{nn})$. One can show that among all possible diagonal preconditioners, this choice reduces the condition number of $M^{-1}A$ to within a factor of n of its minimum value [242]. This is also called *Jacobi preconditioning*.
- As a generalization of the first preconditioner, let

$$A = \begin{bmatrix} A_{11} & \cdots & A_{1b} \\ \vdots & \ddots & \vdots \\ A_{b1} & \cdots & A_{bb} \end{bmatrix}$$

be a block matrix, where the diagonal blocks A_{ii} are square. Then among all block diagonal preconditioners

$$M = \begin{bmatrix} M_{11} & & \\ & \ddots & \\ & & M_{bb} \end{bmatrix},$$

where M_{ii} and A_{ii} have the same dimensions, the choice $M_{ii} = A_{ii}$ minimizes the condition number of $M^{-1/2}AM^{-1/2}$ to within a factor of b [68]. This is also called *block Jacobi preconditioning*.

- Like Jacobi, SSOR can also be used to create a (block) preconditioner.
- An *incomplete Cholesky factorization* LL^T of A is an approximation $A \approx LL^T$, where L is limited to a particular sparsity pattern, such as the original pattern of A . In other words, no fill-in is allowed during Cholesky. Then $M = LL^T$ is used. (For nonsymmetric problems, there is a corresponding *incomplete LU preconditioner*.)
- *Domain decomposition* is used when A represents an equation (such as Poisson's equation) on a physical region Ω . So far, for Poisson's equation, we have let Ω be the unit square. More generally, the region Ω may be broken up into disjoint (or slightly overlapping) subregions $\Omega = \cup_j \Omega_j$, and the equation may be solved on each subregion independently. For example, if we are solving Poisson's equation and if the subregions are squares or rectangles, these subproblems can be solved very quickly using FFTs. Solving these subproblem corresponds to a block diagonal M (if the subregions are disjoint) or a product of block diagonal M (if the subregions overlap). This is discussed in more detail in section 6.10.

A number of these preconditioners have been implemented in the software packages PETSc [230] and PARPRE (NETLIB/scalapack/parpre.tar.gz).

6.6.6. Other Krylov Subspace Algorithms for Solving $Ax = b$

So far we have concentrated on the symmetric positive definite linear systems and minimized the A^{-1} -norm of the residual. In this section we describe methods for other kinds of linear systems and offer advice on which method to use, based on simple properties of the matrix. See Figure 6.8 for a summary, [15, 105, 134, 212] and NETLIB/templates for details, and NETLIB/templates in particular for more comprehensive advice on choosing a method, along with software.

Any system $Ax = b$ can be changed to a symmetric positive definite system by solving the normal equations $A^T Ax = A^T b$ (or $AA^T y = b$, $x = A^T y$). This includes the least squares problem $\min_x \|Ax - b\|_2$. This lets us use CG, provided that we can multiply vectors both by A and A^T . Since the condition number of $A^T A$ or AA^T is the square of the condition number of A , this method can lead to slow convergence if A is ill conditioned but is fast if A is well-conditioned (or $A^T A$ has a “good” distribution of eigenvalues, as discussed in section 6.6.4).

We can minimize the two-norm of the residual instead of the A^{-1} -norm when A is symmetric positive definite. This is called the minimum residual algorithm, or MINRES [192]. Since MINRES is more expensive than CG and is often less accurate because of numerical instabilities, it is not used for positive definite systems. But MINRES can be used when the matrix is symmetric indefinite, whereas CG cannot. In this case, we can also use the SYMMLQ algorithm of Paige and Saunders [192], which produces a residual $r_k \perp \mathcal{K}_k(A, b)$ at each step.

Unfortunately, there are few matrices other than symmetric matrices where algorithms like CG exist that simultaneously

1. either minimize the residual $\|r_k\|_2$ or keep it orthogonal $r_k \perp \mathcal{K}_k$,
2. require a fixed number of dot products and saxpy's in the inner loop, independent of k .

Essentially, algorithms satisfying these two properties exist only for matrices of the form $e^{i\theta}(T + \sigma I)$, where $T = T^T$ (or $TH = (HT)^T$ for some symmetric positive definite H), θ is real, and σ is complex [100, 249]. For these symmetric and special nonsymmetric A , it turns out we can find a short recurrence, as in the Lanczos algorithm, for computing an orthogonal basis $[q_1, \dots, q_k]$ of $\mathcal{K}_k(A, b)$. The fact that there are just a few terms in the recurrence for updating q_k means that it can be computed very efficiently.

This existence of short recurrences no longer holds for general nonsymmetric A . In this case, we can use Arnoldi's algorithm. So instead of the tridiagonal matrix $T_k = Q_k^T A Q_k$, we get a fully upper Hessenberg matrix $H_k = Q_k^T A Q_k$. The *GMRES algorithm* (*generalized minimum residual*) uses this decomposition to choose $x_k = Q_k y_k \in \mathcal{K}_k(A, b)$ to minimize the residual

$$\|r_k\|_2 = \|b - Ax_k\|_2$$

$$\begin{aligned}
&= \|b - AQ_k y_k\|_2 \\
&= \|b - (QH Q^T) Q_k y_k\|_2 \quad \text{by equation (6.30)} \\
&= \|Q^T b - H Q^T Q_k y_k\|_2 \quad \text{since } Q \text{ is orthogonal} \\
&= \left\| e_1 \|b\|_2 - \begin{bmatrix} H_k & H_{uk} \\ H_{ku} & H_u \end{bmatrix} \cdot \begin{bmatrix} y_k \\ 0 \end{bmatrix} \right\|_2 \\
&\quad \text{by equation (6.30) and since the first column of} \\
&\quad Q = [Q_k, Q_u] \text{ is } b/\|b\|_2 \\
&= \left\| e_1 \|b\|_2 - \begin{bmatrix} H_k \\ H_{ku} \end{bmatrix} y_k \right\|_2.
\end{aligned}$$

Since only the first row of H_{ku} is nonzero, this is a $(k+1)$ -by- k upper Hessenberg least squares problem for the entries of y_k . Since it is upper Hessenberg, the QR decomposition needed to solve it can be accomplished with k Givens rotations, at a cost of $O(k^2)$ instead of $O(k^3)$. Also, the storage required is $O(kn)$, since Q_k must be stored. One way to limit the growth in cost and storage is to *restart* GMRES, i.e., taking the answer x_k computed after k steps, restarting GMRES to solve the linear system $Ad = r_k = b - Ax_k$, and updating the solution to get $x_k + d$; this is called GMRES(k). Still, even GMRES(k) is more expensive than CG, where the cost of the inner loop does not depend on k at all.

Another approach to nonsymmetric linear systems is to abandon computing an orthonormal basis of $\mathcal{K}_k(A, b)$ and compute a nonorthonormal basis that again reduces A to (nonsymmetric) tridiagonal form. This is called the *nonsymmetric Lanczos method* and requires matrix-vector multiplication by both A and A^T . This is important because $A^T z$ is sometimes harder (or impossible) to compute (see Example 6.13). The advantage of tridiagonal form is that it is much easier to solve with a tridiagonal matrix than a Hessenberg one. The disadvantage is that the basis vectors may be very ill conditioned and may in fact fail to exist at all, a phenomenon called *breakdown*. The potential efficiency has led to a great deal of research on avoiding or alleviating this instability (*look-ahead Lanczos*) and to competing methods, including *biconjugate gradients* and *quasi-minimum residuals*. There are also some versions that do not require multiplication by A^T , including *conjugate gradients squared*, and *bi-conjugate gradient stabilized*. No one method is best in all cases.

Figure 6.8 shows a decision tree giving simple advice on which method to try first, assuming that we have no other deep knowledge of the matrix A (such as that it arises from the Poisson equation).

6.7. Fast Fourier Transform

In this section i will always denote $\sqrt{-1}$.

We begin by showing how to solve the two-dimensional Poisson's equation in a way requiring multiplication by the matrix of eigenvectors of T_N .

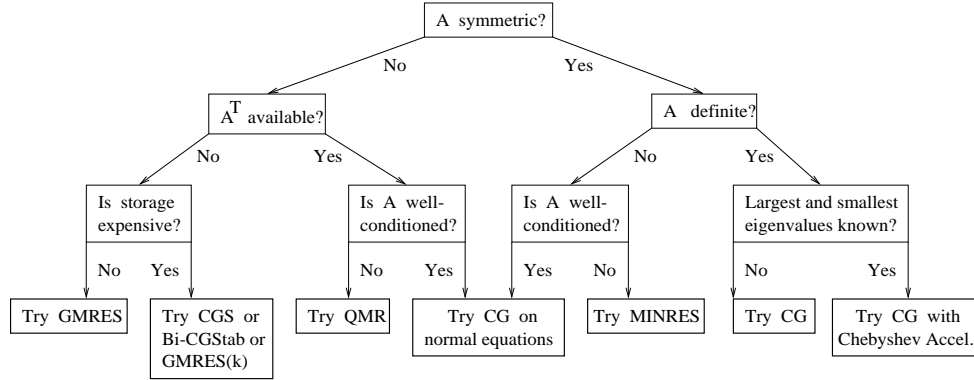


Fig. 6.8. Decision tree for choosing an iterative algorithm for $Ax = b$. *Bi-CGSTab* = bi-conjugate gradient stabilized. *QMR* = quasi-minimum residuals.

A straightforward implementation of this matrix-matrix multiplication would cost $O(N^3) = O(n^{3/2})$ operations, which is expensive. Then we show how this multiplication can be implemented using the FFT in only $O(N^2 \log N) = O(n \log n)$ operations, which is within a factor of $\log n$ of optimal.

This solution is a discrete analogue of the Fourier series solution of the original differential equation (6.1) or (6.6). Later we will make this analogy more precise.

Let $T_N = Z\Lambda Z^T$ be the eigendecomposition of T_N , as defined in Lemma 6.1. We begin with the formulation of the two-dimensional Poisson's equation in equation (6.11):

$$T_N V + V T_N = h^2 F.$$

Substitute $T_N = Z\Lambda Z^T$ and multiply by the Z^T on the left and Z on the right to get

$$Z^T(Z\Lambda Z^T)VZ + Z^T V(Z\Lambda Z^T)Z = Z^T(h^2 F)Z$$

or

$$\Lambda V' + V' \Lambda = h^2 F',$$

where $V' = Z^T V Z$ and $F' = Z^T F Z$. The (j, k) th entry of this last equation is

$$(\Lambda V' + V' \Lambda)_{jk} = \lambda_j v'_{jk} + v'_{jk} \lambda_k = h^2 f'_{jk},$$

which can be solved for v'_{jk} to get

$$v'_{jk} = \frac{h^2 f'_{jk}}{\lambda_j + \lambda_k}.$$

This yields the first version of our algorithm.

ALGORITHM 6.13. Solving the two-dimensional Poisson's equation using the eigendecomposition $T_N = Z\Lambda Z^T$:

- 1) $F' = Z^T F Z$
- 2) For all j and k , $v'_{jk} = \frac{h^2 f'_{jk}}{\lambda_j + \lambda_k}$
- 3) $V = Z V' Z^T$

The cost of step 2 is $3N^2 = 3n$ operations, and the cost of steps 1 and 3 is 4 matrix-matrix multiplications by Z and $Z^T = Z$, which is $8N^3 = 8n^{3/2}$ operations using a conventional algorithm. In the next section we show how multiplication by Z is essentially the same as computing a *discrete Fourier transform*, which can be done in $O(N^2 \log N) = O(n \log n)$ operations using the FFT.

(Using the language of Kronecker products introduced in section 6.3.3, and in particular the eigendecomposition of $T_{N \times N}$ from Proposition 6.1,

$$T_{N \times N} = I \otimes T_N + T_N \otimes I = (Z \otimes Z) \cdot (I \otimes \Lambda + \Lambda \otimes I) \cdot (Z \otimes Z)^T,$$

we can rewrite the formula justifying Algorithm 6.13 as follows:

$$\begin{aligned} \text{vec}(V) &= (T_{N \times N})^{-1} \cdot \text{vec}(h^2 F) \\ &= ((Z \otimes Z) \cdot (I \otimes \Lambda + \Lambda \otimes I) \cdot (Z \otimes Z)^T)^{-1} \cdot \text{vec}(h^2 F) \\ &= (Z \otimes Z)^{-T} \cdot (I \otimes \Lambda + \Lambda \otimes I)^{-1} \cdot (Z \otimes Z)^{-1} \cdot \text{vec}(h^2 F) \\ &= (Z \otimes Z) \cdot (I \otimes \Lambda + \Lambda \otimes I)^{-1} \cdot (Z^T \otimes Z^T) \cdot \text{vec}(h^2 F). \end{aligned} \quad (6.47)$$

We claim that doing the indicated matrix-vector multiplications from right to left is mathematically the same as Algorithm 6.13; see Question 6.9. This also shows how to extend the algorithm to Poisson's equation in higher dimensions.)

6.7.1. The Discrete Fourier Transform

In this subsection, we will number the rows and columns of matrices from 0 to $N - 1$ instead of from 1 to N .

DEFINITION 6.17. *The discrete Fourier transform (DFT) of an N -vector x is the vector $y = \Phi x$, where Φ is an N -by- N matrix defined as follows. Let $\omega = e^{\frac{-2\pi i}{N}} = \cos \frac{2\pi}{N} - i \cdot \sin \frac{2\pi}{N}$, a principal N th root of unity. Then $\phi_{jk} = \omega^{jk}$. The inverse discrete Fourier transform (IDFT) of y is the vector $x = \Phi^{-1} y$.*

LEMMA 6.9. $\frac{1}{\sqrt{N}} \Phi$ is a symmetric unitary matrix, so $\Phi^{-1} = \frac{1}{N} \Phi^* = \frac{1}{N} \bar{\Phi}$.

Proof. Clearly $\Phi = \Phi^T$, so $\bar{\Phi} = \Phi^*$, and we need only show $\Phi \cdot \bar{\Phi} = N \cdot I$. Compute $(\Phi \bar{\Phi})_{lj} = \sum_{k=0}^{N-1} \phi_{lk} \bar{\phi}_{kj} = \sum_{k=0}^{N-1} \omega^{lk} \bar{\omega}^{kj} = \sum_{k=0}^{N-1} \omega^{k(l-j)}$, since $\bar{\omega} = \omega^{-1}$. If $l = j$, this sum is clearly N . If $l \neq j$, it is a geometric sum with value $\frac{1 - \omega^{N(l-j)}}{1 - \omega^{l-j}} = 0$, since $\omega^N = 1$. \square

Thus, both the DFT and IDFT are just matrix-vector multiplications and can be straightforwardly implemented in $2N^2$ flops. This operation is called

a DFT because of its close mathematical relationship to two other kinds of Fourier analyses:

the Fourier transform	$F(\zeta) = \int_{-\infty}^{\infty} e^{-2\pi i \zeta x} f(x) dx$
and its inverse	$f(x) = \int_{-\infty}^{\infty} e^{+2\pi i \zeta x} F(\zeta) d\zeta$
the Fourier series	$c_j = \int_0^1 e^{-2\pi i j x} f(x) dx$
where f is periodic on $[0, 1]$	
and its inverse	$f(x) = \sum_{j=-\infty}^{\infty} e^{+2\pi i j x} c_j$
the DFT	$y_j = (\Phi x)_j = \sum_{k=0}^{N-1} e^{-2\pi i j k / N} x_k$
and its inverse	$x_k = (\Phi^{-1} y)_k = \frac{1}{N} \sum_{j=0}^{N-1} e^{+2\pi i j k / N} y_j$

We will make this close relationship more concrete in two ways. First, we will show how to solve the model problem using the DFT and then the original Poisson's equation (6.1) using Fourier series. This example will motivate us to find a fast way to multiply by Φ , because this will give us a fast way to solve the model problem. This fast way is called the *fast Fourier transform* or *FFT*. Instead of $2N^2$ flops, it will require only about $\frac{3}{2}N \log_2 N$ flops, which is much less. We will derive the FFT by stressing a second mathematical relationship shared among the different kinds of Fourier analyses: reducing convolution to multiplication.

In Algorithm 6.13 we showed that to solve the discrete Poisson equation $T_N V + V T_N = h^2 F$ for V required the ability to multiply by the N -by- N matrix Z , where

$$z_{jk} = \sqrt{\frac{2}{N+1}} \sin \frac{\pi(j+1)(k+1)}{N+1}.$$

(Recall that we number rows and columns from 0 to $N-1$ in this section.) Now consider the $(2N+2)$ -by- $(2N+2)$ DFT matrix Φ , whose j, k entry is

$$\exp\left(\frac{-2\pi i j k}{2N+2}\right) = \exp\left(\frac{-\pi i j k}{N+1}\right) = \cos \frac{\pi j k}{N+1} - i \cdot \sin \frac{\pi j k}{N+1}.$$

Thus the N -by- N matrix Z consists of $-\sqrt{\frac{2}{N+1}}$ times the imaginary part of the second through $(N+1)$ st rows and columns of Φ . So if we can multiply efficiently by Φ using the FFT, then we can multiply efficiently by Z . (To be most efficient, one modifies the FFT algorithm, which we describe below, to multiply by Z directly; this is called the *fast sine transform*. But one can also just use the FFT.) Thus, multiplying ZF quickly requires an FFT-like operation on each column of F , and multiplying FZ requires the same operation on each row. (In three dimensions, we would let V be an N -by- N -by- N array of unknowns and apply the same operation to each of the $3N^2$ sections parallel to the coordinate axes.)

6.7.2. Solving the Continuous Model Problem Using Fourier Series

We now return to numbering rows and columns of matrices from 1 to N .

In this section we show how the algorithm for solving the discrete model problem is a natural analogue of using Fourier series to solve the original differential equation (6.1). We will do this for the one-dimensional model problem.

Recall that Poisson's equation on $[0, 1]$ is $-\frac{d^2v}{dx^2} = f(x)$ with boundary conditions $v(0) = v(1)$. To solve this, we will expand $v(x)$ in a Fourier series: $v(x) = \sum_{j=1}^{\infty} \alpha_j \sin(j\pi x)$. (The boundary condition $v(1) = 0$ tells us that no cosine terms appear.) Plugging $v(x)$ into Poisson's equation yields

$$\sum_{j=1}^{\infty} \alpha_j (j^2 \pi^2) \sin(j\pi x) = f(x).$$

Multiply both sides by $\sin(k\pi x)$, integrate from 0 to 1, and use the fact that $\int_0^1 \sin(j\pi x) \sin(k\pi x) dx = 0$ if $j \neq k$ and $1/2$ if $j = k$ to get

$$\alpha_k = \frac{2}{k^2 \pi^2} \int_0^1 \sin(k\pi x) f(x) dx$$

and finally

$$v(x) = \sum_{j=1}^{\infty} \left(\frac{2}{j^2 \pi^2} \int_0^1 \sin(j\pi y) f(y) dy \right) \sin(j\pi x). \quad (6.48)$$

Now consider the discrete model problem $T_N v = h^2 f$. Since $T_N = Z \Lambda Z^T$, we can write $v = T_N^{-1} h^2 f = Z \Lambda^{-1} Z^T h^2 f$, so

$$v_k = \sum_{j=1}^N z_{kj} \frac{h^2}{\lambda_j} (Z^T f)_j = \sum_{j=1}^N \sin \frac{\pi j k}{N+1} \left(\frac{h^2}{\lambda_j} \sqrt{\frac{2}{N+1}} (Z^T f)_j \right), \quad (6.49)$$

where

$$\begin{aligned} \sqrt{\frac{2}{N+1}} (Z^T f)_j &= \sqrt{\frac{2}{N+1}} \sum_{l=1}^N \sqrt{\frac{2}{N+1}} \sin \left(\frac{\pi j l}{N+1} \right) f_l \\ &= 2 \sum_{l=1}^N \frac{1}{N+1} \sin \left(\frac{\pi j l}{N+1} \right) f_l \\ &\approx 2 \int_0^1 \sin(\pi j y) f(y) dy, \end{aligned}$$

since the last sum is just a Riemann sum approximation of the integral. Furthermore, for small j , recall that $\frac{h^2}{\lambda_j} \approx \frac{1}{j^2 \pi^2}$. So we see how the solution of the discrete problem (6.49) approximates the solution of the continuous problem (6.48), with multiplication by Z^T corresponding to multiplication by $\sin(j\pi x)$ and integration, and multiplication by Z corresponding to summing the different Fourier components.

6.7.3. Convolutions

The *convolution* is an important operation in Fourier analysis, whose definition depends on whether we are doing Fourier transforms, Fourier series, or the DFT:

Fourier transform	$(f * g)(x) \equiv \int_{-\infty}^{\infty} f(x-y)g(y)dy$
Fourier series	$(f * g)(x) \equiv \int_0^1 f(x-y)g(y)dy$
DFT	If $a = [a_0, \dots, a_{N-1}, 0, \dots, 0]^T$ and $b = [b_0, \dots, b_{N-1}, 0, \dots, 0]^T$ are $2N$ -vectors then $a * b \equiv c = [c_0, \dots, c_{2N-1}]^T$, where $c_k = \sum_{j=0}^k a_j b_{k-j}$

To illustrate the use of the discrete convolution, consider polynomial multiplication. Let $a(x) = \sum_{k=0}^{N-1} a_k x^k$ and $b(x) = \sum_{k=0}^{N-1} b_k x^k$ be degree- $(N-1)$ polynomials. Then their product $c(x) \equiv a(x) \cdot b(x) = \sum_{k=0}^{2N-1} c_k x^k$, where the coefficients c_0, \dots, c_{2N-1} are given by the discrete convolution.

One purpose of the Fourier transform, Fourier series, or DFT is to convert convolution into multiplication. In the case of the Fourier transform, $\mathcal{F}(f * g) = \mathcal{F}(f) \cdot \mathcal{F}(g)$; i.e., the Fourier transform of the convolution is the product of the Fourier transforms. In the case of Fourier series, $c_j(f * g) = c_j(f) \cdot c_j(g)$; i.e., the Fourier coefficients of the convolution are the product of the Fourier coefficients. The same is true of the discrete convolution.

THEOREM 6.10. *Let $a = [a_0, \dots, a_{N-1}, 0, \dots, 0]^T$ and $b = [b_0, \dots, b_{N-1}, 0, \dots, 0]^T$ be vectors of dimension $2N$, and let $c = a * b = [c_0, \dots, c_{2N-1}]^T$. Then $(\Phi c)_k = (\Phi a)_k \cdot (\Phi b)_k$.*

Proof. If $a' = \Phi a$, then $a'_k = \sum_{j=0}^{2N-1} a_j \omega^{kj}$, the value of the polynomial $a(x) \equiv \sum_{j=0}^{N-1} a_j x^j$ at $x = \omega^k$. Similarly $b' = \Phi b$ means $b'_k = \sum_{j=0}^{N-1} b_j \omega^{kj} = b(\omega^k)$ and $c' = \Phi c$ means $c'_k = \sum_{j=0}^{2N-1} c_j \omega^{kj} = c(\omega^k)$. Therefore

$$a'_k \cdot b'_k = a(\omega^k) \cdot b(\omega^k) = c(\omega^k) = c'_k$$

as desired. \square

In other words, the DFT is polynomial evaluation at the points $\omega^0, \dots, \omega^{N-1}$, and conversely the IDFT is polynomial interpolation, producing the coefficients of a polynomial given its values at $\omega^0, \dots, \omega^{N-1}$.

6.7.4. Computing the Fast Fourier Transform

We will derive the FFT via its interpretation as polynomial evaluation just discussed. The goal is to evaluate $a(x) = \sum_{k=0}^{N-1} a_k x^k$ at $x = \omega^j$ for $0 \leq j \leq N-1$. For simplicity we will assume $N = 2^m$. Now write

$$\begin{aligned} a(x) &= a_0 + a_1 x + a_2 x^2 + \dots + a_{N-1} x^{N-1} \\ &= (a_0 + a_2 x^2 + a_4 x^4 + \dots) + x(a_1 + a_3 x^2 + a_5 x^4 + \dots) \\ &\equiv a_{\text{even}}(x^2) + x \cdot a_{\text{odd}}(x^2). \end{aligned}$$

Thus, we need to evaluate two polynomials a_{even} and a_{odd} of degree $\frac{N}{2} - 1$ at $(\omega^j)^2$, $0 \leq j \leq N-1$. But this is really just $\frac{N}{2}$ points ω^{2j} for $0 \leq j \leq \frac{N}{2} - 1$, since $\omega^{2j} = \omega^{2(j+\frac{N}{2})}$.

Thus evaluating a polynomial of degree $N-1 = 2^m-1$ at all N N th roots of unity is the same as evaluating two polynomials of degree $\frac{N}{2} - 1$ at all $\frac{N}{2}$ th roots of unity and then combining the results with N multiplications and additions. This can be done recursively.

ALGORITHM 6.14. *FFT (recursive version):*

```
function FFT(a, N)
  if N = 1
    return a
  else
    a'_{\text{even}} = FFT(a_{\text{even}}, N/2)
    a'_{\text{odd}} = FFT(a_{\text{odd}}, N/2)
     $\omega = e^{-2\pi i/N}$ 
     $w = [\omega^0, \dots, \omega^{N/2-1}]$ 
    return  $a' = [a'_{\text{even}} + w.*a'_{\text{odd}}, a'_{\text{even}} - w.*a'_{\text{odd}}]$ 
  endif
```

Here $.*$ means componentwise multiplication of arrays (as in Matlab), and we have used the fact that $\omega^{j+N/2} = -\omega^j$.

Let the cost of this algorithm be denoted $C(N)$. Then we see that $C(N)$ satisfies the recurrence $C(N) = 2C(N/2) + 3N/2$ (assuming that the powers of ω are precomputed and stored in tables). To solve this recurrence write

$$\begin{aligned} C(N) &= 2C\left(\frac{N}{2}\right) + \frac{3N}{2} = 4C\left(\frac{N}{4}\right) + 2 \cdot \frac{3N}{2} = 8C\left(\frac{N}{8}\right) + 3 \cdot \frac{3N}{2} \\ &= \dots \\ &= \log_2 N \cdot \frac{3N}{2}. \end{aligned}$$

To compute the FFT of each column (or each row) of an N -by- N matrix therefore costs $\log_2 N \cdot \frac{3N^2}{2}$. This complexity analysis justifies the entry for the FFT in Table 6.1.

In practice, implementations of the FFT use simple nested loops rather than recursion in order to be as efficient as possible; see NETLIB/fftpack. In addition, these implementations sometimes return the components in *bit-reversed* order: This means that instead of returning y_0, y_1, \dots, y_{N-1} , where $y = \Phi x$, the subscripts j are reordered so that the bit patterns are reversed. For example, if $N = 8$, the subscripts run from $0 = 000_2$ to $7 = 111_2$. The following table shows the normal order and the bit-reversed order:

normal increasing order	bit-reversed order
0 = 000 ₂	0 = 000 ₂
1 = 001 ₂	4 = 100 ₂
2 = 010 ₂	2 = 010 ₂
3 = 011 ₂	6 = 110 ₂
4 = 100 ₂	1 = 001 ₂
5 = 101 ₂	5 = 101 ₂
6 = 110 ₂	3 = 011 ₂
7 = 111 ₂	7 = 111 ₂

The inverse FFT undoes this reordering and returns the results in their original order. Therefore, these algorithms can be used for solving the model problem, provided that we divide by the appropriate eigenvalues, whose subscripts correspond to bit-reversed order. (Note that Matlab always returns results in normal increasing order.)

6.8. Block Cyclic Reduction

Block cyclic reduction is another fast ($O(N^2 \log_2 N)$) method for the model problem but is slightly more generally applicable than the FFT-based solution. The fastest algorithms for the model problem on vector computers are often a hybrid of block cyclic reduction and FFT.

First we describe a simple but numerically unstable version of the algorithm; then we say a little about how to stabilize it. Write the model problem as

$$\begin{bmatrix} A & -I & & \\ -I & \ddots & \ddots & \\ & \ddots & \ddots & -I \\ & & -I & A \end{bmatrix} \begin{bmatrix} x_1 \\ \vdots \\ x_N \end{bmatrix} = \begin{bmatrix} b_1 \\ \vdots \\ b_N \end{bmatrix},$$

where we assume that N , the dimension of $A = T_N + 2I_N$, is odd. Note also that x_i and b_i are N -vectors.

We use block Gaussian elimination to combine three consecutive sets of equations,

$$\begin{array}{rcl} + & \begin{bmatrix} -x_{j-2} & +Ax_{j-1} & -x_j & & \\ & -x_{j-1} & +Ax_j & -x_{j+1} & \\ & & -x_j & +Ax_{j+1} & -x_{j+2} \end{bmatrix} & = \begin{bmatrix} b_{j-1} \\ b_j \\ b_{j+1} \end{bmatrix}, \\ +A* & & \\ + & & \end{array}$$

thus eliminating x_{j-1} and x_{j+1} :

$$-x_{j-2} + (A^2 - 2I)x_j - x_{j+2} = b_{j-1} + Ab_j + b_{j+1}.$$

Doing this for every set of three consecutive equations yields two sets of equations: one for the x_j with j even,

$$\begin{bmatrix} B & -I & & & \\ -I & B & -I & & \\ & -I & \ddots & \ddots & \\ & & \ddots & \ddots & -I \\ & & & -I & B \end{bmatrix} \begin{bmatrix} x_2 \\ x_4 \\ \vdots \\ x_{N-1} \end{bmatrix} = \begin{bmatrix} b_1 + Ab_2 + b_3 \\ b_3 + Ab_4 + b_5 \\ \vdots \\ b_{N-2} + Ab_{N-1} + b_N \end{bmatrix}, \quad (6.50)$$

where $B = 2I - A^2$, and one set of equations for the x_j with j odd, which we can solve after solving equation (6.50) for the odd x_j :

$$\begin{bmatrix} A & & & \\ & A & & \\ & & \ddots & \\ & & & A \end{bmatrix} \begin{bmatrix} x_1 \\ x_3 \\ \vdots \\ x_N \end{bmatrix} = \begin{bmatrix} b_1 + x_2 \\ b_3 + x_2 + x_4 \\ \vdots \\ b_N + x_{N-1} \end{bmatrix}.$$

Note that equation (6.50) has the same form as the original problem, so we may repeat this process recursively. For example, at the next step we get

$$\begin{bmatrix} C & -I & & & \\ -I & C & -I & & \\ & -I & \ddots & \ddots & \\ & & \ddots & \ddots & -I \\ & & & -I & C \end{bmatrix} \begin{bmatrix} x_4 \\ x_8 \\ \vdots \end{bmatrix} = \begin{bmatrix} \vdots \\ \vdots \\ \vdots \\ \vdots \end{bmatrix}, \quad \text{where } C = B^2 - 2I,$$

and

$$\begin{bmatrix} B & & & \\ & B & & \\ & & \ddots & \\ & & & B \end{bmatrix} \begin{bmatrix} x_2 \\ x_6 \\ \vdots \end{bmatrix} = \begin{bmatrix} \vdots \\ \vdots \\ \vdots \\ \vdots \end{bmatrix}.$$

We repeat this until only one equation is left, which we solve another way.

We formalize this algorithm as follows: Assume $N = N_0 = 2^{k+1} - 1$, and let $N_r = 2^{k+1-r} - 1$. Let $A^{(0)} = A$ and $b_j^{(0)} = b_j$ for $j = 1, \dots, N$.

ALGORITHM 6.15. *Block cyclic reduction:*

1) *Reduce:*

```

for  $r = 0$  to  $k - 1$ 
   $A^{(r+1)} = (A^{(r)})^2 - 2I$ 
  for  $j = 1$  to  $N_{r+1}$ 
     $b_j^{(r+1)} = b_{2j-1}^{(r)} + A^{(r)}b_{2j}^{(r)} + b_{2j+1}^{(r)}$ 
  end for
end for
```

Comment: at the r th step the problem is reduced to

$$\begin{bmatrix} A^{(r)} & -I & & \\ -I & \ddots & \ddots & \\ & \ddots & \ddots & -I \\ & & -I & A^{(r)} \end{bmatrix} \begin{bmatrix} x_1^{(r)} \\ \vdots \\ x_{N_r}^{(r)} \end{bmatrix} = \begin{bmatrix} b_1^{(r)} \\ \vdots \\ b_{N_r}^{(r)} \end{bmatrix}$$

2) $A^{(k)}x^{(k)} = b^{(k)}$ is solved another way.

3) *Backsolve:*

```

for  $r = k - 1, \dots, 0$ 
  for  $j = 1$  to  $N_{r+1}$ 
     $x_{2j}^{(r)} = x_j^{(r+1)}$ 
  end for
  for  $j = 1$  to  $N_r$  step 2
    solve  $A^{(r)}x_j^{(r)} = b_j^{(r)} + x_{j-1}^{(r)} + x_{j+1}^{(r)}$  for  $x_j^{(r)}$ 
    (we take  $x_0^{(r)} = x_{N_r+1}^{(r)} \equiv 0$ )
  end for
end for

```

Finally, $x = x^{(0)}$ is the desired result.

This simple approach has two drawbacks:

- 1) It is numerically unstable because $A^{(r)}$ grows quickly: $\|A^{(r)}\| \sim \|A^{(r-1)}\|^2 \approx 4^{2^r}$, so in computing $b_j^{(r+1)}$, the $b_{2j\pm 1}^{(r)}$ are lost in roundoff.
- 2) $A^{(r)}$ has bandwidth $2^r + 1$ if A is tridiagonal, so it soon becomes dense and thus expensive to multiply or solve.

Here is a fix for the second drawback. Note that $A^{(r)}$ is a polynomial $p_r(A)$ of degree 2^r :

$$p_0(A) = A \text{ and } p_{r+1}(A) = (p_r(A))^2 - 2I.$$

LEMMA 6.10. Let $t = 2 \cos \theta$. Then $p_r(t) = p_r(2 \cos \theta) = 2 \cos(2^r \theta)$.

Proof. This is a simple trigonometric identity. \square

Note that $p_r(t) = 2 \cos(2^r \arccos(\frac{t}{2})) = 2T_{2^r}(\frac{t}{2})$ where $T_{2^r}(\cdot)$ is a *Chebyshev polynomial* (see section 6.5.6).

LEMMA 6.11. $p_r(t) = \prod_{j=1}^{2^r} (t - t_j)$, where $t_j = 2 \cos(\pi \frac{2j-1}{2^r})$.

Proof. The zeros of the Chebyshev polynomials are given in Lemma 6.7. \square

Thus $A^{(r)} = \prod_{j=1}^{2^r} (A - 2 \cos(\pi \frac{2j-1}{2^{r+1}}))$, so solving $A^{(r)}z = c$ is equivalent to solving 2^r tridiagonal systems with tridiagonal coefficient matrices $A + 2 \cos(\pi \frac{2j-1}{2^{r+1}})$, each of which costs $O(N)$ via tridiagonal Gaussian elimination or Cholesky.

More changes are needed to have a numerically stable algorithm. The final algorithm is due to Buneman and described in [46, 45].

We analyze the cost of the simple algorithm as follows; the stable algorithm is analogous. Multiplying by a tridiagonal matrix or solving a tridiagonal system of size N costs $O(N)$ flops. Therefore multiplying by $A^{(r)}$ or solving a system with $A^{(r)}$ costs $O(2^r N)$ flops, since $A^{(r)}$ is the product of 2^r tridiagonal matrices. The inner loop of step 1) of the algorithm therefore costs $\frac{N}{2^{r+1}} \cdot O(2^r N) = O(N^2)$ flops to update the $N_{r+1} \approx \frac{N}{2^{r+1}}$ vectors $b_j^{(r+1)}$. $A^{(r+1)}$ is not computed explicitly. Since the loop in step 1) is executed $k \approx \log_2 N$ times, the total cost of step 1) is $O(N^2 \log_2 N)$. For similar reasons, step 2) costs $O(2^k N) = O(N^2)$ flops, and step 3) costs $O(N^2 \log_2 N)$ flops, for a total cost of $O(N^2 \log_2 N)$ flops. This justifies the entry for block cyclic reduction in Table 6.1.

This algorithm generalizes to any block tridiagonal matrix with a symmetric matrix A repeated along the diagonal and a symmetric matrix F that commutes with A ($FA = AF$) repeated along the offdiagonals. See also Question 6.10. This is a common situation when solving linear systems arising from discretized differential equations such as Poisson's equation.

6.9. Multigrid

Multigrid methods were invented for partial differential equations such as Poisson's equation, but they work on a wider class of problems too. In contrast to other iterative schemes that we have discussed so far, multigrid's convergence rate is *independent* of the problem size N , instead of slowing down for larger problems. As a consequence, it can solve problems with n unknowns in $O(n)$ time or for a constant amount of work per unknown. This is optimal, modulo the (modest) constant hidden inside the $O(\cdot)$.

Here is why the other iterative algorithms that we have discussed *cannot* be optimal for the model problem. In fact, this is true of *any* iterative algorithm that computes approximation x_{m+1} by averaging values of x_m and the right-hand side b from neighboring grid points. This includes Jacobi's, Gauss-Seidel, SOR(ω), SSOR with Chebyshev acceleration (the last three with red-black ordering), and any Krylov subspace method based on matrix-vector multiplication with the matrix $T_{N \times N}$; this is because multiplying a vector by $T_{N \times N}$ is also equivalent to averaging neighboring grid point values. Suppose that we start with a right-hand side b on a 31-by-31 grid, with a single nonzero entry, as shown in the upper left of Figure 6.9. The true solution x is shown

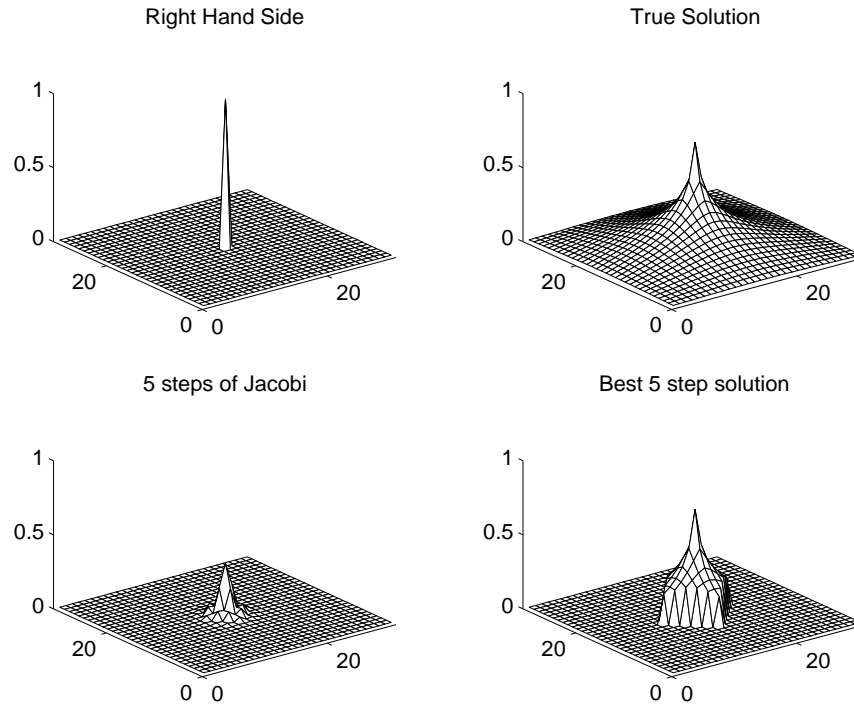


Fig. 6.9. *Limits of averaging neighboring grid points.*

in the upper right of the same figure; note that it is everywhere nonzero and gets smaller as we get farther from the center. The bottom left plot in Figure 6.9 shows the solution $x_{J,5}$ after 5 steps of Jacobi's method, starting with an initial solution of all zeros. Note that the solution $x_{J,5}$ is zero more than 5 grid points away from the center, because averaging with neighboring grid points can “propagate information” only one grid point per iteration, and the only nonzero value is initially in the center of the grid. More generally, after k iterations only grid points within k of the center can be nonzero. The bottom right figure shows the best possible solution $x_{Best,5}$ obtainable by any “nearest neighbor” method after 5 steps: it agrees with x on grid points within 5 of the center and is necessarily 0 farther away. We see graphically that the error $x_{Best,5} - x$ is equal to the size of x at the sixth grid point away from the center. This is still a large error; by formalizing this argument, one can show that it would take at least $O(\log n)$ steps on an n -by- n grid to decrease the error by a constant factor less than 1, no matter what “nearest-neighbor” algorithm is used. If we want to do better than $O(\log n)$ steps (and $O(n \log n)$ cost), we need to “propagate information” farther than one grid point per iteration. Multigrid does this by communicating with nearest neighbors on coarser grids, where a nearest neighbor on a coarse grid can be much farther away than a nearest neighbor on a fine grid.

Multigrid uses coarse grids to do *divide-and-conquer* in two related senses.

First, it obtains an initial solution for an N -by- N grid by using an $(N/2)$ -by- $(N/2)$ grid as an approximation, taking every other grid point from the N -by- N grid. The coarser $(N/2)$ -by- $(N/2)$ grid is in turn approximated by an $(N/4)$ -by- $(N/4)$ grid, and so on recursively. The second way multigrid uses divide-and-conquer is in the *frequency domain*. This requires us to think of the error as a sum of eigenvectors, or sine-curves of different frequencies. Then the work that we do on a particular grid will eliminate the error in half of the frequency components not eliminated on other grids. In particular, the work performed on a particular grid—averaging the solution at each grid point with its neighbors, a variation of Jacobi’s method—makes the solution smoother, which is equivalent to getting rid of the high-frequency error. We will illustrate these notions further below.

6.9.1. Overview of Multigrid on Two-Dimensional Poisson’s Equation

We begin by stating the algorithm at a high level and then fill in details. As with block cyclic reduction (section 6.8), it turns out to be convenient to consider a $(2^k - 1)$ -by- $(2^k - 1)$ grid of unknowns rather than the 2^k -by- 2^k grid favored by the FFT (section 6.7). For understanding and implementation, it is convenient to add the nodes at the boundary, which have the known value 0, to get a $(2^k + 1)$ -by- $(2^k + 1)$ grid, as shown in Figures 6.10 and 6.13. We also let $N_k = 2^k - 1$.

We will let $P^{(i)}$ denote the problem of solving a discrete Poisson equation on a $(2^i + 1)$ -by- $(2^i + 1)$ grid with $(2^i - 1)^2$ unknowns, or equivalently a $(N_i + 2)$ -by- $(N_i + 2)$ grid with N_i^2 unknowns. The problem $P^{(i)}$ is specified by the right-hand side $b^{(i)}$ and implicitly the grid size $2^i - 1$ and the coefficient matrix $T^{(i)} \equiv T_{N_i \times N_i}$. An approximate solution of $P^{(i)}$ will be denoted $x^{(i)}$. Thus, $b^{(i)}$ and $x^{(i)}$ are $(2^i - 1)$ -by- $(2^i - 1)$ arrays of values at each grid point. (The zero boundary values are implicit.) We will generate a sequence of related problems $P^{(i)}, P^{(i-1)}, P^{(i-2)}, \dots, P^{(1)}$ on increasingly coarse grids, where the solution to $P^{(i-1)}$ is a good approximation to the error in the solution of $P^{(i)}$.

To explain how multigrid works, we need some operators that take a problem on one grid and either improve it or transform it to a related problem on another grid:

- The *solution operator* S takes a problem $P^{(i)}$ and its approximate solution $x^{(i)}$ and computes an improved $x^{(i)}$:

$$\text{improved } x^{(i)} = S(b^{(i)}, x^{(i)}). \quad (6.51)$$

The improvement is to damp the “high-frequency components” of the error. We will explain what this means below. It is implemented by averaging each grid point value with its nearest neighbors and is a variation of Jacobi’s method.

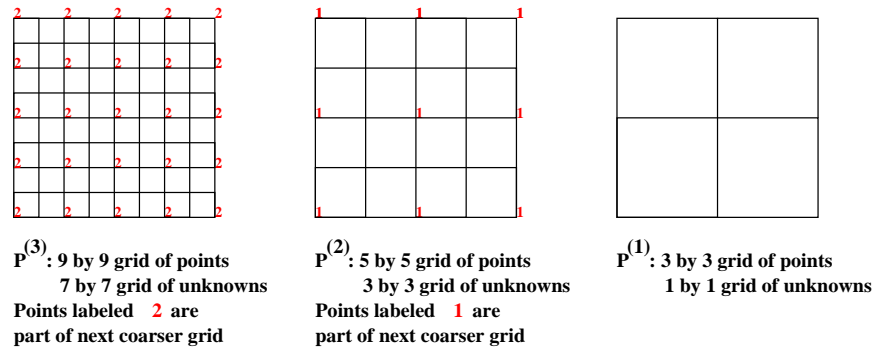


Fig. 6.10. Sequence of grids used by two-dimensional multigrid.

- The *restriction operator* R takes a right-hand side $b^{(i)}$ from problem $P^{(i)}$ and maps it to $b^{(i-1)}$, which is an approximation on the coarser grid:

$$b^{(i-1)} = R(b^{(i)}). \quad (6.52)$$

Its implementation also requires just a weighted average with nearest neighbors on the grid.

- The *interpolation operator* In takes an approximate solution $x^{(i-1)}$ for $P^{(i-1)}$ and converts it to an approximate solution $x^{(i)}$ for the problem $P^{(i)}$ on the next finer grid:

$$x^{(i)} = In(x^{(i-1)}). \quad (6.53)$$

Its implementation also requires just a weighted average with nearest neighbors on the grid.

Since all three operators are implemented by replacing values at each grid point by some weighted averages of nearest neighbors, each operation costs just $O(1)$ per unknown, or $O(n)$ for n unknowns. This is the key to the low cost of the ultimate algorithm.

Multigrid V-Cycle

This is enough to state the basic algorithm, the *multigrid V-cycle* (MGV).

ALGORITHM 6.16. *MGV (the lines are numbered for later reference):*

```

function MGV( $b^{(i)}, x^{(i)}$ )    ... replace an approximate solution  $x^{(i)}$ 
                                ... of  $P^{(i)}$  with an improved one
    if  $i = 1$                   ... only one unknown
        compute the exact solution  $x^{(1)}$  of  $P^{(1)}$ 
        return  $x^{(1)}$ 
    else

```

```

1)       $x^{(i)} = S(b^{(i)}, x^{(i)})$     ... improve the solution
2)       $r^{(i)} = T^{(i)} \cdot x^{(i)} - b^{(i)}$     ... compute the residual
3)       $d^{(i)} = In(MGV(4 \cdot R(r^{(i)}), 0))$  ... solve recursively
                                         ... on coarser grids
4)       $x^{(i)} = x^{(i)} - d^{(i)}$     ... correct fine grid solution
5)       $x^{(i)} = S(b^{(i)}, x^{(i)})$     ... improve the solution again
         return  $x^{(i)}$ 
endif

```

In words, the algorithm does the following:

1. Starts with a problem on a fine grid $(b^{(i)}, x^{(i)})$.
2. Improves it by damping the high-frequency error: $x^{(i)} = S(b^{(i)}, x^{(i)})$.
3. Computes the residual $r^{(i)}$ of the approximate solution $x^{(i)}$.
4. Approximates the fine grid residual $r^{(i)}$ on the next coarser grid: $R(r^{(i)})$.
5. Solves the coarser problem recursively, with a zero initial guess: $MGV(4 \cdot R(r^{(i)}), 0)$. The factor 4 appears because of the h^2 factor in the right-hand side of Poisson's equation, which changes by a factor of 4 from fine grid to coarse grid.
6. Maps the coarse solution back to the fine grid: $d_i = In(MGV(R(r^{(i)}), 0))$
7. Subtracts the correction computed on the coarse grid from the fine grid solution: $x^{(i)} = x^{(i)} - d^{(i)}$.
8. Improves the solution some more: $x^{(i)} = S(b^{(i)}, x^{(i)})$.

We justify the algorithm briefly as follows (we do the details later). Suppose (by induction) that $d^{(i)}$ is the *exact* solution to the equation

$$T^{(i)} \cdot d^{(i)} = r^{(i)} = T^{(i)} \cdot x^{(i)} - b^{(i)}.$$

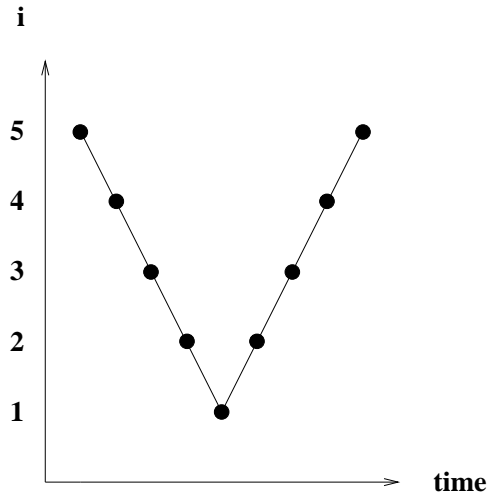
Rearranging, we get

$$T^{(i)} \cdot (x^{(i)} - d^{(i)}) = b^{(i)}$$

so that $x^{(i)} - d^{(i)}$ is the desired solution.

The algorithm is called a V-cycle, because if we draw it schematically in (grid number i , time) space, with a point for each recursive call to MGV , it looks like Figure 6.11, starting with a call to $MGV(b^{(5)}, x^{(5)})$ in the upper left corner. This calls MGV on grid 4, then 3, and so on down to the coarsest grid 1 and then back up to grid 5 again.

Knowing only that the building blocks S , R , and In replace values at grid points by certain weighted averages of their neighbors, we know enough to do

Fig. 6.11. *MGV*.

a $O(\cdot)$ complexity analysis of *MGV*. Since each building block does a constant amount of work per grid point, it does a total amount of work proportional to the number of grid points. Thus, each point at grid level i on the “V” in the V-cycle will cost $O((2^i - 1)^2) = O(4^i)$ operations. If the finest grid is at level k with $n = O(4^k)$ unknowns, then the total cost will be given by the geometric sum

$$\sum_{i=1}^k O(4^i) = O(4^k) = O(n).$$

Full Multigrid

The ultimate multigrid algorithm uses the *MGV* just described as a building block. It is called *full multigrid (FMG)*:

ALGORITHM 6.17. *FMG*:

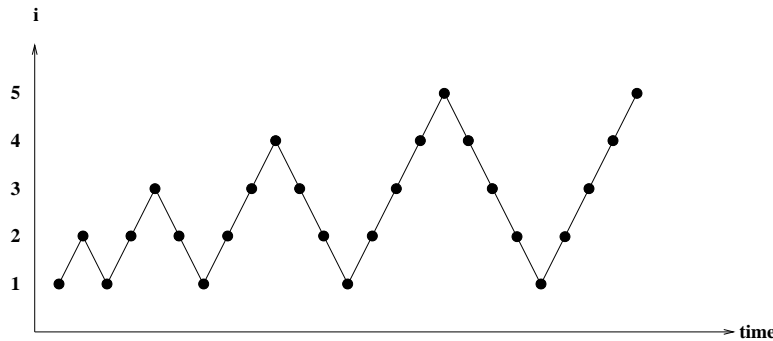
```

function FMG( $b^{(k)}, x^{(k)}$ ) ... return an accurate solution  $x^{(k)}$  of  $P^{(k)}$ 
  solve  $P^{(1)}$  exactly to get  $x^{(1)}$ 
  for  $i = 2$  to  $k$ 
     $x^{(i)} = \text{MGV}(b^{(i)}, \text{In}(x^{(i-1)}))$ 
  end for

```

In words, the algorithm does the following:

1. Solves the simplest problem $P^{(1)}$ exactly.
2. Given a solution $x^{(i-1)}$ of the coarse problem $P^{(i-1)}$, maps it to a starting guess $x^{(i)}$ for the next finer problem $P^{(i)}$: $\text{In}(x^{(i-1)})$.


 Fig. 6.12. *FMG*.

3. Solves the finer problem using the MGW with this starting guess: $MGV(b^{(i)}, In(x^{(i-1)}))$.

Now we can do the overall $O(\cdot)$ complexity analysis of FMG. A picture of FMG in (grid number i , time) space is shown in Figure 6.12. There is one “V” in this picture for each call to MGW in the inner loop of FMG. The “V” starting at level i costs $O(4^i)$ as before. Thus the total cost is again given by the geometric sum

$$\sum_{i=1}^k O(4^i) = O(4^k) = O(n),$$

which is optimal, since it does a constant amount of work for each of the n unknowns. This explains the entry for multigrid in Table 6.1.

A Matlab implementation of multigrid (both for the one and two-dimensional model problems) is available at HOMEPAGE/Matlab/MG_README.html.

6.9.2. Detailed Description of Multigrid on One-Dimensional Poisson’s Equation

Now we will explain in detail the various operators S , R , and In composing the multigrid algorithm and sketch the convergence proof. We will do this for Poisson’s equation in one dimension, since this will capture all the relevant behavior but is simpler to write. In particular, we can now consider a nested set of one-dimensional problems instead of two-dimensional problems, as shown in Figure 6.13.

As before we denote by $P^{(i)}$ the problem to be solved on grid i , namely, $T^{(i)} \cdot x^{(i)} = b^{(i)}$, where as before $N_i = 2^i - 1$ and $T^{(i)} \equiv T_{N_i}$. We begin by describing the solution operator S , which is a form of *weighted Jacobi convergence*.

Solution Operator in One Dimension

In this subsection we drop the superscripts on $T^{(i)}$, $x^{(i)}$, and $b^{(i)}$ for simplicity of notation. Let $T = Z\Lambda Z^T$ be the eigendecomposition of T , as defined in

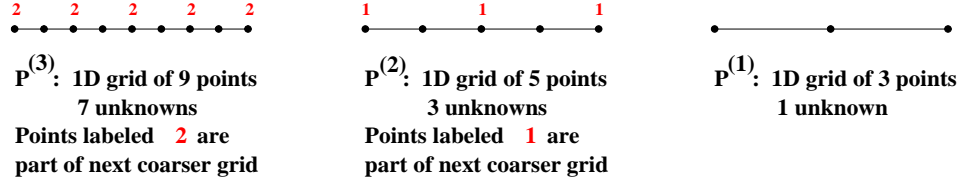


Fig. 6.13. Sequence of grids used by one-dimensional multigrid.

Lemma 6.1. The standard Jacobi's method for solving $Tx = b$ is $x_{m+1} = Rx_m + c$, where $R = I - T/2$ and $c = b/2$. We consider *weighted Jacobi convergence* $x_{m+1} = R_w x_m + c_w$, where $R_w = I - wT/2$ and $c_w = wb/2$; $w = 1$ corresponds to the standard Jacobi's method. Note that $R_w = Z(I - w\Lambda/2)Z^T$ is the eigendecomposition of R_w . The eigenvalues of R_w determine the convergence of weighted Jacobi in the usual way: Let $e_m = x_m - x$ be the error at the m th iteration of weighted Jacobi convergence so that

$$\begin{aligned}
 e_m &= R_w e_{m-1} \\
 &= R_w^m e_0 \\
 &= (Z(I - w\Lambda/2)Z^T)^m e_0 \\
 &= Z(I - w\Lambda/2)^m Z^T e_0
 \end{aligned}$$

so

$$Z^T e_m = (I - w\Lambda/2)^m Z^T e_0 \quad \text{or} \quad (Z^T e_m)_j = (I - w\Lambda/2)_{jj}^m (Z^T e_0)_j.$$

We call $(Z^T e_m)_j$ the j th frequency component of the error e_m , since $e_m = Z(Z^T e_m)$ is a sum of columns of Z weighted by the $(Z^T e_m)_j$, i.e., a sum of sinusoids of varying frequencies (see Figure 6.2). The eigenvalues $\lambda_j(R_w) = 1 - w\lambda_j/2$ determine how fast each frequency component goes to zero. Figure 6.14 plots $\lambda_j(R_w)$ for $N = 99$ and varying values of the weight w .

When $w = \frac{2}{3}$ and $j > \frac{N}{2}$, i.e., for the upper half of the frequencies λ_j , we have $|\lambda_j(R_w)| \leq \frac{1}{3}$. This means that the upper half of the error components $(Z^T e_m)_j$ are multiplied by $\frac{1}{3}$ or less at every iteration, independently of N . Low-frequency error components are not decreased as much, as we will see in Figure 6.15. So weighted Jacobi convergence with $w = \frac{2}{3}$ is good at decreasing the high-frequency error.

Thus, our solution operator S in equation (6.51) consists of taking one step of weighted Jacobi convergence with $w = \frac{2}{3}$:

$$S(b, x) = R_{2/3} \cdot x + b/3. \quad (6.54)$$

When we want to indicate the grid i on which $R_{2/3}$ operates, we will instead write $R_{2/3}^{(i)}$.

Figure 6.15 shows the effect of taking two steps of S for $i = 6$, where we have $2^i - 1 = 63$ unknowns. There are three rows of pictures, the first row

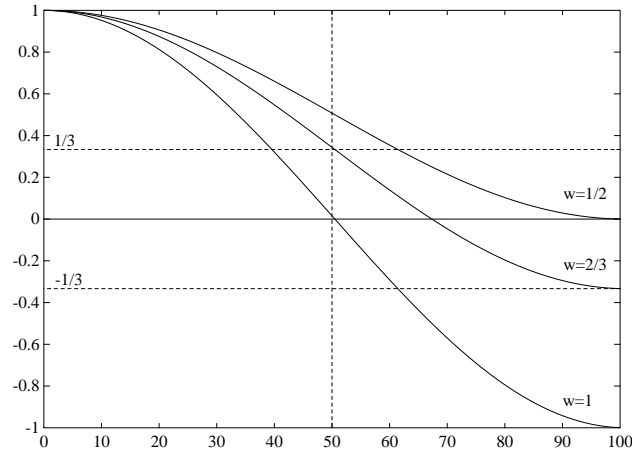


Fig. 6.14. Graph of the spectrum of R_w for $N = 99$ and $w = 1$ (Jacobi's method), $w = 1/2$ and $w = 2/3$.

showing the initial solution and error and the following two rows showing the solution x_m and error e_m after successive applications of S . The true solution is a sine curve, shown as a dotted line in the leftmost plot in each row. The approximate solution is shown as a solid line in the same plot. The middle plot shows the error alone, including its two-norm in the label at the bottom. The rightmost plot shows the frequency components of the error $Z^T e_m$. One can see in the rightmost plots that as S is applied, the right (upper) half of the frequency components are damped out. This can also be seen in the middle and left plots, because the approximate solution grows smoother. This is because high-frequency error looks like “rough” error and low-frequency error looks like “smooth” error. Initially, the norm of the vector decreases rapidly, from 1.65 to 1.055, but then decays more gradually, because there is little more error in the high frequencies to damp. Thus, it only makes sense to do a few iterations of S at a time.

Recursive Structure of Multigrid

Using this terminology, we can describe the recursive structure of multigrid as follows. What multigrid does on the finest grid $P^{(k)}$, is to damp the upper half of the frequency components of the error in the solution. This is accomplished by the solution operator S , as just described. On the next coarser grid, with half as many points, multigrid damps the upper half of the remaining frequency components in the error. This is because taking a coarser grid, with half as many points, makes frequencies appear twice as high, as illustrated in the example below.

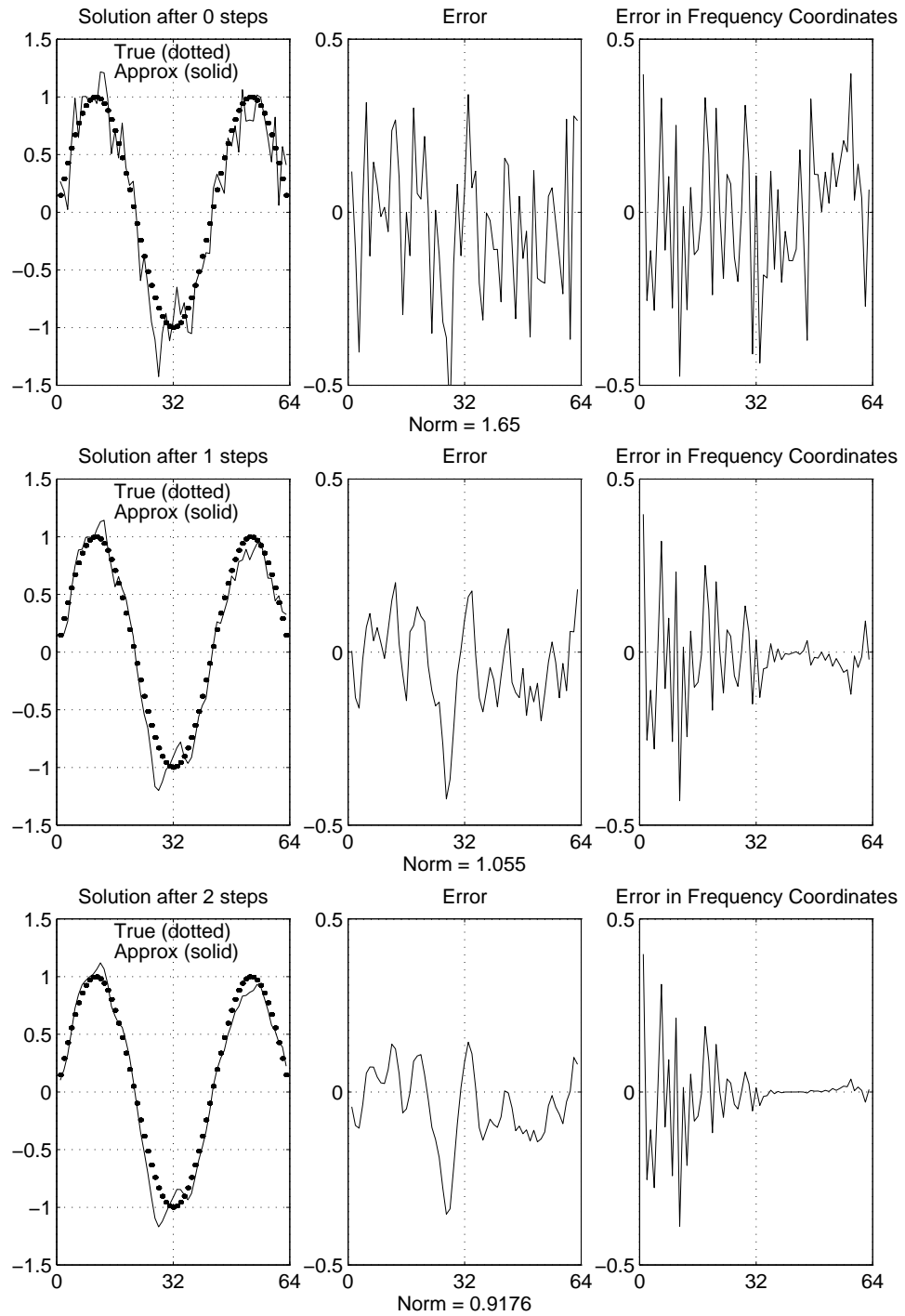


Fig. 6.15. Illustration of weighted Jacobi convergence.

Schematic Description of Multigrid

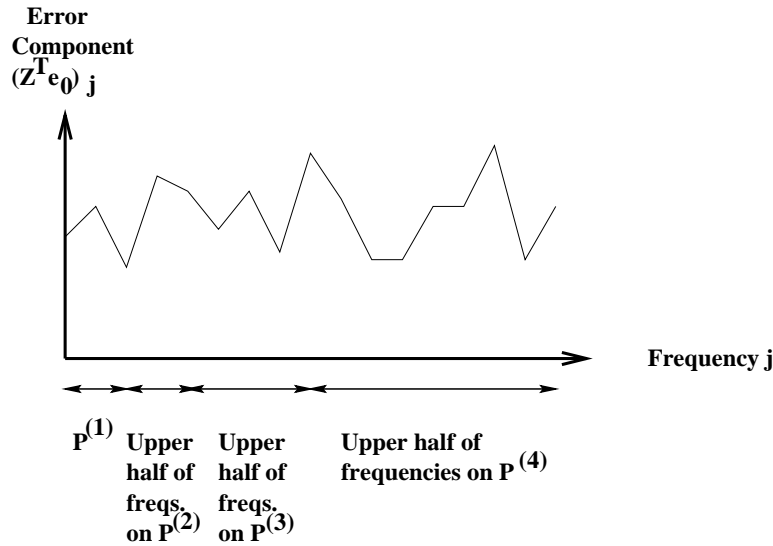
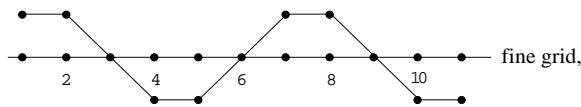


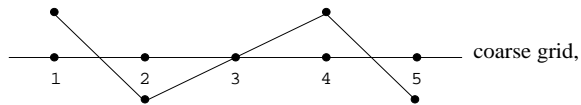
Fig. 6.16. Schematic description of how multigrid damps error components.

EXAMPLE 6.16.

$N = 12, k = 4$
 low frequency, $k < \frac{N}{2}$
 $\sin \frac{\pi \cdot k \cdot j}{12}$
 for $1 \leq j \leq 11$



$N = 6, k = 4$
 high frequency, $k > \frac{N}{2}$
 $\sin \frac{\pi \cdot 4 \cdot j}{6}$
 for $1 \leq j \leq 5$



◇

On the next coarser grid, the upper half of the remaining frequency components are damped, and so on, until we solve the exact (one unknown) problem $P^{(1)}$. This is shown schematically in Figure 6.16. The purpose of the restriction and interpolation operators is to change an approximate solution on one grid to one on the next coarser or next finer grid.

Restriction Operator in One Dimension

Now we turn to the restriction operator R , which takes a right-hand side $r^{(i)}$ from problem $P^{(i)}$ and approximates it on the next coarse grid, yielding $r^{(i-1)}$.

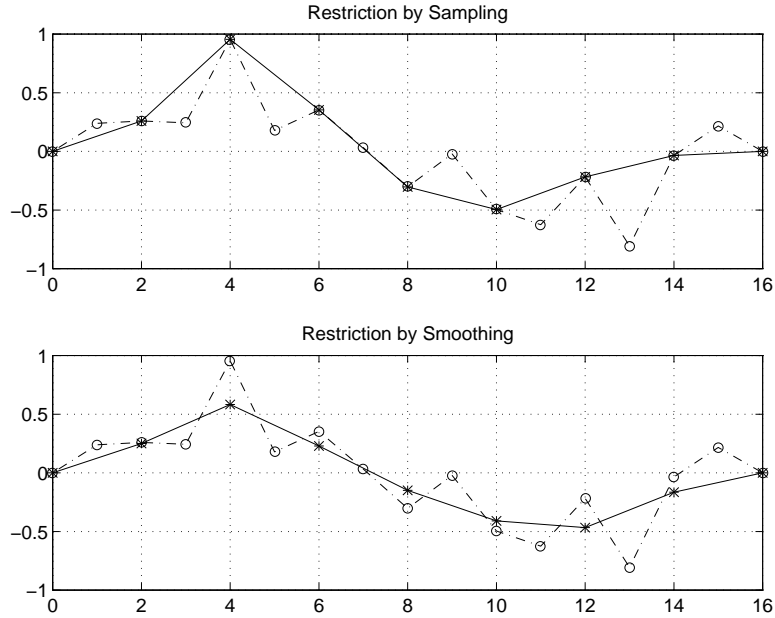


Fig. 6.17. Restriction from a grid with $2^4 - 1 = 15$ points to a grid with $2^3 - 1 = 7$ points. (0 boundary values also shown.)

The simplest way to compute $r^{(i-1)}$ would be to simply *sample* $r^{(i)}$ at the common grid points of the coarse and fine grids. But it is better to compute $r^{(i-1)}$ at a coarse grid point by averaging values of $r^{(i)}$ on neighboring fine grid points: the value at a coarse grid point is .5 times the value at the corresponding fine grid point, plus .25 times each of the fine grid point neighbors. We call this *smoothing*. Both methods are illustrated in Figure 6.17.

So altogether, we write the restriction operation as

$$\begin{aligned}
 r^{(i-1)} &= R(r^{(i)}) \\
 &\equiv P_i^{i-1} \cdot r^{(i)} \\
 &= \begin{bmatrix} \frac{1}{4} & \frac{1}{2} & \frac{1}{4} & & & & & \\ & & \frac{1}{4} & \frac{1}{2} & \frac{1}{4} & & & \\ & & & \frac{1}{4} & \frac{1}{2} & \frac{1}{4} & & \\ & & & & \frac{1}{4} & \frac{1}{2} & \frac{1}{4} & \\ & & & & & \ddots & \ddots & \ddots \\ & & & & & & \frac{1}{4} & \frac{1}{2} & \frac{1}{4} \end{bmatrix} \cdot r^{(i)}. \quad (6.55)
 \end{aligned}$$

The subscript i and superscript $i-1$ on the matrix P_i^{i-1} indicate that it maps from the grid with $2^i - 1$ points to the grid with $2^{i-1} - 1$ points.

In two dimensions, restriction involves averaging with the eight nearest neighbors of each grid points: $\frac{1}{4}$ times the grid cell value itself, plus $\frac{1}{8}$ times the four neighbors to the left, right, top, and bottom, plus $\frac{1}{16}$ times the four remaining neighbors at the upper left, lower left, upper right, and lower right.

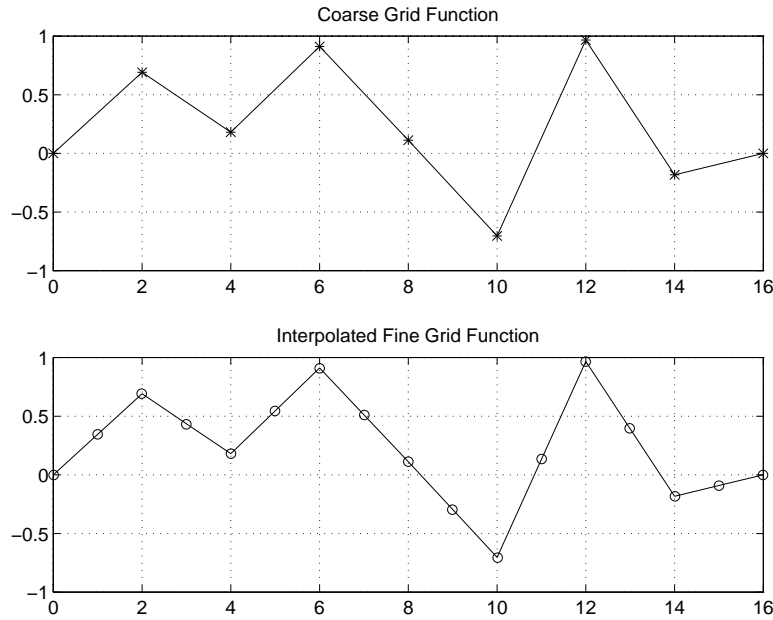


Fig. 6.18. Interpolation from a grid with $2^3 - 1 = 7$ points to a grid with $2^4 - 1 = 15$ points. (0 boundary values also shown.)

Interpolation Operator in One Dimension

The interpolation operator In takes an approximate solution $d^{(i-1)}$ on a coarse grid and maps it to a function $d^{(i)}$ on the next finer grid. The solution $d^{(i-1)}$ is interpolated to the finer grid as shown in Figure 6.18: we do simple linear interpolation to fill in the values on the fine grid (using the fact that the boundary values are known to be zero). Mathematically, we write this as

$$d^{(i)} = In(d^{(i-1)}) \equiv P_{i-1}^i \cdot d^{(i-1)} = \begin{bmatrix} \frac{1}{2} \\ 1 \\ \frac{1}{2} & \frac{1}{2} \\ & 1 & \ddots \\ & \frac{1}{2} & \ddots & \frac{1}{2} \\ & & \ddots & 1 \\ & & & \frac{1}{2} \end{bmatrix} \cdot x^{(i-1)}. \quad (6.56)$$

The subscript $i - 1$ and superscript i on the matrix P_{i-1}^i indicate that it maps from the grid with $2^{i-1} - 1$ points to the grid with $2^i - 1$ points.

Note that $P_{i-1}^i = 2 \cdot (P_i^{i-1})^T$. In other words, interpolation and smoothing are essentially transposes of one another. This fact will be important in the convergence analysis later.

In two dimensions, interpolation again involves averaging the values at coarse nearest neighbors of a fine grid point (one neighbor if the fine grid point

is also a coarse grid point; two neighbors if the fine grid point's nearest coarse neighbors are to the left and right or top and bottom; and four neighbors otherwise).

Putting It All Together

Now we run the algorithm just described for eight iterations on the problem pictured in the top two plots of Figure 6.19; both the true solution x (on the top left) and right-hand side b (on the top right) are shown. The number of unknowns is $2^7 - 1 = 127$. We show how multigrid converges in the bottom three plots. The middle left plot shows the ratio of consecutive residuals $\|r_{m+1}\|/\|r_m\|$, where the subscript m is the number of iterations of multigrid (i.e., calls to FMG, or Algorithm 6.17). These ratios are about .15, indicating that the residual decreases by more than a factor of 6 with each multigrid iteration. This quick convergence is indicated in the middle right plot, which shows a semilogarithmic plot of $\|r_m\|$ versus m ; it is a straight line with slope $\log_{10}(.15)$ as expected. Finally, the bottom plot plots all eight error vectors $x_m - x$. We see how they smooth out and become parallel on a semilogarithmic plot, with a constant decrease between adjacent plots of $\log_{10}(.15)$.

Figure 6.20 shows a similar example for a two-dimensional model problem.

Convergence Proof

Finally, we sketch a convergence proof that shows that the overall error in an FMG “V”-cycle is decreased by a constant less than 1, independent of grid size $N_k = 2^k - 1$. This means that the number of FMG V-cycles needed to decrease the error by any factor less than 1 is independent of k , and so the total work is proportional to the cost of a single FMG V-cycle, i.e., proportional to the number of unknowns n .

We will simplify the proof by looking at one V-cycle and assuming by induction that the coarse grid problem is solved *exactly* [42]. In reality, the coarse grid problem is not solved quite exactly, but this rough analysis suffices to capture the spirit of the proof: that low-frequency error is eliminated on the coarser grid and high-frequency error is eliminated on the fine grid.

Now let us write all the formulas defining a V-cycle and combine them all to get a single formula of the form “new $e^{(i)} = M \cdot e^{(i)}$,” where $e^{(i)} = x^{(i)} - x$ is the error and M is a matrix whose eigenvalues determine the rate of convergence; our goal is to show that they are bounded away from 1, independently of i . The line numbers in the following table refer to Algorithm 6.16.

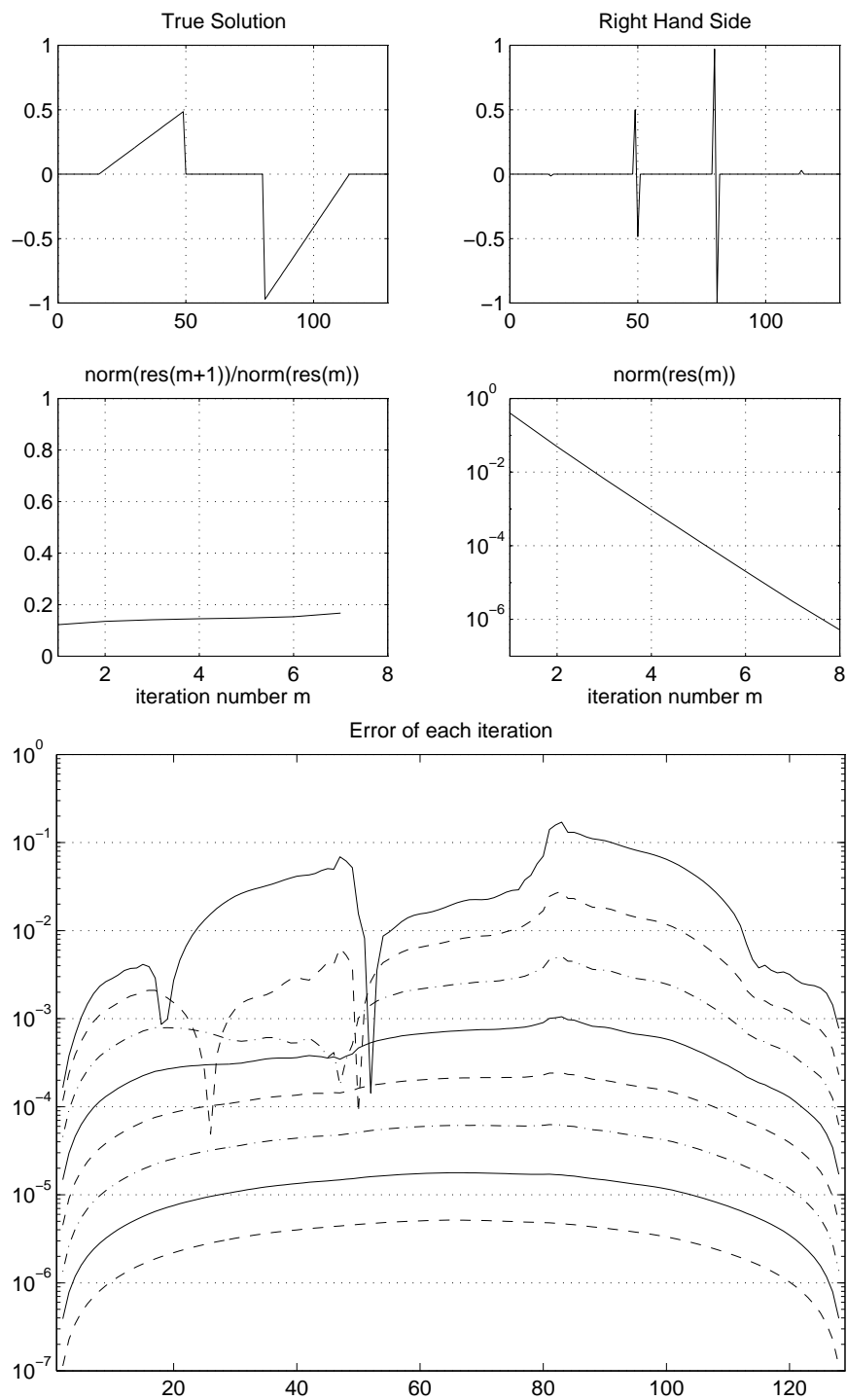


Fig. 6.19. Multigrid solution of one-dimensional model problem.

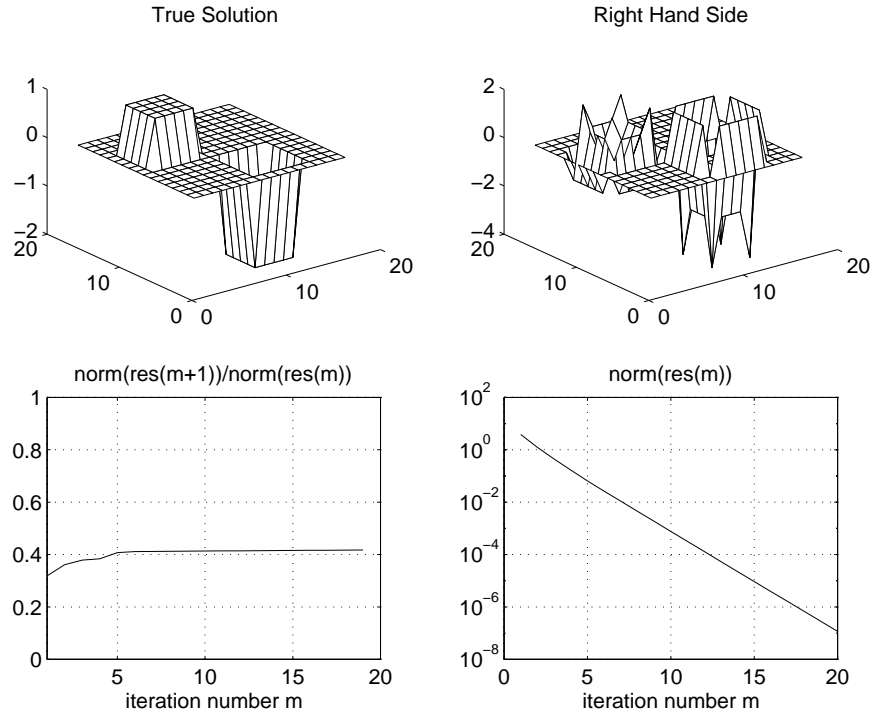


Fig. 6.20. Multigrid solution of two-dimensional model problem.

$$\begin{aligned}
 \text{(a)} \quad x^{(i)} &= S(b(i), x(i)) = R_{2/3}^{(i)} x^{(i)} + b^{(i)}/3 \\
 &\quad \text{by line 1) and equation (6.54),} \\
 \text{(b)} \quad r^{(i)} &= T^{(i)} \cdot x^{(i)} - b^{(i)} \\
 &\quad \text{by line 2),} \\
 d^{(i)} &= \text{In}(MGV(4 \cdot R(r^{(i)}), 0)) \\
 &\quad \text{by line 3)} \\
 &= \text{In}([T^{(i-1)}]^{-1} (4 \cdot R(r^{(i)}))) \\
 &\quad \text{by our assumption that the} \\
 &\quad \text{coarse grid problem is solved exactly} \\
 &= \text{In}([T^{(i-1)}]^{-1} (4 \cdot P_i^{i-1} r^{(i)})) \\
 &\quad \text{by equation (6.55)} \\
 \text{(c)} \quad &= P_{i-1}^i ([T^{(i-1)}]^{-1} (4 \cdot P_i^{i-1} r^{(i)})) \\
 &\quad \text{by equation (6.56)} \\
 \text{(d)} \quad x^{(i)} &= x^{(i)} - d^{(i)} \\
 &\quad \text{by line 4)} \\
 \text{(e)} \quad x^{(i)} &= S(b(i), x(i)) = R_{2/3}^{(i)} x^{(i)} + b^{(i)}/3 \\
 &\quad \text{by line 5).}
 \end{aligned}$$

In order to get equations updating the error $e^{(i)}$, we subtract the identity $x = R_{2/3}^{(i)} x + b^{(i)}/3$ from lines (a) and (e) above, $0 = T^{(i)} \cdot x - b^{(i)}$ from line (b),

and $x = x$ from line (d) to get

$$\begin{aligned} \text{(a)} \quad e^{(i)} &= R_{2/3}^{(i)} e^{(i)}, \\ \text{(b)} \quad r^{(i)} &= T^{(i)} \cdot e^{(i)}, \\ \text{(c)} \quad d^{(i)} &= P_{i-1}^i ([T^{(i-1)}]^{-1} (4 \cdot P_i^{i-1} r^{(i)})), \\ \text{(d)} \quad e^{(i)} &= e^{(i)} - d^{(i)}, \\ \text{(e)} \quad e^{(i)} &= R_{2/3}^{(i)} e^{(i)}. \end{aligned}$$

Substituting each of the above equations into the next yields the following formula, showing how the error is updated by a V-cycle:

$$\begin{aligned} \text{new } e^{(i)} &= R_{2/3}^{(i)} \left\{ I - P_{i-1}^i \cdot [T^{(i-1)}]^{-1} \cdot (4 \cdot P_i^{i-1} T^{(i)}) \right\} R_{2/3}^{(i)} \cdot e^{(i)} \\ &\equiv M \cdot e^{(i)}. \end{aligned} \quad (6.57)$$

Now we need to compute the eigenvalues of M . We first simplify equation (6.57), using the facts that $P_{i-1}^i = 2 \cdot (P_i^{i-1})^T$ and

$$T^{(i-1)} = 4 \cdot P_i^{i-1} T^{(i)} P_{i-1}^i = 8 \cdot P_i^{i-1} T^{(i)} (P_i^{i-1})^T \quad (6.58)$$

(see Question 6.15). Substituting these into the expression for M in equation (6.57) yields

$$M = R_{2/3}^{(i)} \left\{ I - (P_i^{i-1})^T \cdot [P_i^{i-1} T^{(i)} (P_i^{i-1})^T]^{-1} \cdot (P_i^{i-1} T^{(i)}) \right\} R_{2/3}^{(i)}$$

or, dropping indices to simplify notation,

$$M = R_{2/3} \left\{ I - P^T \cdot [PTP^T]^{-1} \cdot PT \right\} R_{2/3}. \quad (6.59)$$

We continue, using the fact that all the matrices composing M (T , $R_{2/3}$, and P) can be (nearly) diagonalized by the eigenvector matrices $Z = Z^{(i)}$ and $Z^{(i-1)}$ of $T = T^{(i)}$ and $T^{(i-1)}$, respectively: Recall that $Z = Z^T = Z^{-1}$, $T = Z\Lambda Z$, and $R_{2/3} = Z(I - \Lambda/3)Z \equiv Z\Lambda_R Z$. We leave it to the reader to confirm that $Z^{(i-1)} P Z^{(i)} = \Lambda_P$, where Λ_P is almost diagonal (see Question 6.15):

$$\lambda_{P,jk} = \begin{cases} (+1 + \cos \frac{\pi j}{2^i})/\sqrt{8} & \text{if } k = j, \\ (-1 + \cos \frac{\pi j}{2^i})/\sqrt{8} & \text{if } k = 2^i - j, \\ 0 & \text{otherwise.} \end{cases} \quad (6.60)$$

This lets us write

$$\begin{aligned} ZMZ &= (ZR_{2/3}Z) \\ &\cdot \left\{ I - (ZP^T Z^{(i-1)}) \cdot [(Z^{(i-1)} P Z)(ZT Z)(ZP^T Z^{(i-1)})]^{-1} \right. \\ &\quad \left. \cdot (Z^{(i-1)} P Z)(ZT Z) \right\} \cdot (ZR_{2/3}Z) \\ &= \Lambda_R \cdot \left\{ I - \Lambda_P^T [\Lambda_P \Lambda \Lambda_P^T]^{-1} \Lambda_P \Lambda \right\} \cdot \Lambda_R. \end{aligned}$$

The matrix ZMZ is similar to M since $Z = Z^{-1}$ and so has the same eigenvalues as M . Also, ZMZ is nearly diagonal: it has nonzeros only on its main diagonal and “perdiagonal” (the diagonal from the lower left corner to the upper right corner of the matrix). This lets us compute the eigenvalues of T explicitly.

THEOREM 6.11. *The matrix M has eigenvalues $1/9$ and 0 , independent of i . Therefore multigrid converges at a fixed rate independent of the number of unknowns.*

For a proof, see Question 6.15. For a more general analysis, see [266].

For an implementation of this algorithm, see Question 6.16. The Web site [89] contains pointers to an extensive literature, software, and so on.

6.10. Domain Decomposition

Domain decomposition for solving sparse systems of linear equations is a topic of current research. See [48, 114, 203] and especially [230] for recent surveys. We will give only simple examples.

The need for methods beyond those we have discussed arises from the irregularity and size of real problems and also from the need for algorithms for parallel computers. The fastest methods that we have discussed so far, those based on block cyclic reduction, the FFT, and multigrid, work best (or only) on particularly regular problems such as the model problem, i.e., Poisson’s equation discretized with a uniform grid on a rectangle. But the region of solution of a real problem may not be a rectangle but more irregular, representing a physical object like a wing (see Figure 2.12). Figure 2.12 also illustrates that there may be more grid points in regions where the solution is expected to be less smooth than in regions with a smooth solution. Also, we may have more complicated equations than Poisson’s equation or even different equations in different regions. Independent of whether the problem is regular, it may be too large to fit in the computer memory and may have to be solved “in pieces.” Or we may want to break the problem into pieces that can be solved in parallel on a parallel computer.

Domain decomposition addresses all these issues by showing how to systematically create “hybrid” methods from the simpler methods discussed in previous sections. These simpler methods are applied to smaller and more regular subproblems of the overall problem, after which these partial solutions are “pieced together” to get the overall solution. These subproblems can be solved one at a time if the whole problem does not fit into memory, or in parallel on a parallel computer. We give examples below. There are generally many ways to break a large problem into pieces, many ways to solve the individual pieces, and many ways to piece the solutions together. Domain decomposition theory does not provide a magic way to choose the best way to do this in all cases

but rather a set of reasonable possibilities to try. There are some cases (such as problems sufficiently like Poisson's equation) where the theory does yield "optimal methods" (costing $O(1)$ work per unknown).

We divide our discussion into two parts, *nonoverlapping methods* and *overlapping methods*.

6.10.1. Nonoverlapping Methods

This method is also called *substructuring* or a *Schur complement method* in the literature. It has been used for decades, especially in the structural analysis community, to break large problems into smaller ones that fit into computer memory.

For simplicity we will illustrate this method using the usual Poisson's equation with Dirichlet boundary conditions discretized with a 5-point stencil but on an *L-shaped region* rather than a square. This region may be decomposed into two domains: a small square and a large square of twice the side length, where the small square is connected to the bottom of the right side of a larger square. We will design a solver that can exploit our ability to solve problems quickly on squares.

In the figure below, the number of each grid point is shown for a coarse discretization (the number is above and to the left of the corresponding grid point; only grid points interior to the "L" are numbered).



Note that we have numbered first the grid points inside the two subdomains (1 to 4 and 5 to 29) and then the grid points on the boundary (30 and 31). The resulting matrix is

4 -1	-1							-1
-1 4	-1							
-1	4 -1							-1
-1	-1 4							
		4 -1	-1					-1
		-1 4 -1	-1					
		-1 4 -1	-1					
		-1 4 -1	-1					
		-1 4	-1					
		-1	4 -1	-1				-1
		-1	-1 4 -1	-1				
		-1	-1 4 -1	-1				
		-1	-1 4 -1	-1				
		-1	-1 4	-1				
			-1	4 -1	-1			
			-1	-1 4 -1	-1			
			-1	-1 4 -1	-1			
			-1	-1 4 -1	-1			
			-1	-1 4	-1			
				-1	4 -1	-1		
				-1	-1 4 -1	-1		
				-1	-1 4 -1	-1		
				-1	-1 4 -1	-1		
				-1	-1 4	-1		
					-1	4 -1	-1	
					-1	-1 4 -1	-1	
					-1	-1 4 -1	-1	
					-1	-1 4	-1	
-1	-1	-1	-1					4 -1
								-1 4

$$\equiv A \equiv \begin{bmatrix} A_{11} & 0 & A_{13} \\ 0 & A_{22} & A_{23} \\ A_{13}^T & A_{23}^T & A_{33} \end{bmatrix}.$$

Here, $A_{11} = T_{2 \times 2}$, $A_{22} = T_{5 \times 5}$, and $A_{33} = T_{2 \times 1} \equiv T_2 + 2I_2$, where T_N is defined in equation (6.3) and $T_{N \times N}$ is defined in equation (6.14). One of the most important properties of this matrix is that $A_{12} = 0$, since there is no direct coupling between the interior grid points of the two subdomains. The only coupling is through the boundary, which is numbered last (grid points 30 and 31). Thus A_{13} contains the coupling between the small square and the boundary, and A_{23} contains the coupling between the large square and the boundary.

To see how to take advantage of the special structure of A to solve $Ax = b$, write the block LU decomposition of A as follows:

$$A = \begin{bmatrix} I & 0 & 0 \\ 0 & I & 0 \\ A_{13}^T A_{11}^{-1} & A_{23}^T A_{22}^{-1} & I \end{bmatrix} \cdot \begin{bmatrix} I & 0 & 0 \\ 0 & I & 0 \\ 0 & 0 & S \end{bmatrix} \cdot \begin{bmatrix} A_{11} & 0 & A_{13} \\ 0 & A_{22} & A_{23} \\ 0 & 0 & I \end{bmatrix},$$

where

$$S = A_{33} - A_{13}^T A_{11}^{-1} A_{13} - A_{23}^T A_{22}^{-1} A_{23} \quad (6.61)$$

is called the *Schur complement* of the leading principal submatrix containing A_{11} and A_{22} . Therefore, we may write $A^{-1} =$

$$\begin{bmatrix} A_{11}^{-1} & 0 & -A_{11}^{-1}A_{13} \\ 0 & A_{22}^{-1} & -A_{22}^{-1}A_{23} \\ 0 & 0 & I \end{bmatrix} \cdot \begin{bmatrix} I & 0 & 0 \\ 0 & I & 0 \\ 0 & 0 & S^{-1} \end{bmatrix} \cdot \begin{bmatrix} I & 0 & 0 \\ 0 & I & 0 \\ -A_{13}^T A_{11}^{-1} & -A_{23}^T A_{22}^{-1} & I \end{bmatrix}.$$

Therefore, to multiply a vector by A^{-1} we need to multiply by the blocks in the entries of this factored form of A^{-1} , namely, A_{13} and A_{23} (and their transposes), A_{11}^{-1} and A_{22}^{-1} , and S^{-1} . Multiplying by A_{13} and A_{23} is cheap because they are very sparse. Multiplying by A_{11}^{-1} and A_{22}^{-1} is also cheap because we chose these subdomains to be solvable by FFT, block cyclic reduction, multi-grid, or some other fast method discussed so far. It remains to explain how to multiply by S^{-1} .

Since there are many fewer grid points on the boundary than in the subdomains, A_{33} and S have a much smaller dimension than A_{11} and A_{22} ; this effect grows for finer grid spacings. S is symmetric positive definite, as is A , and (in this case) dense. To compute it explicitly one would need to solve with each subdomain once per boundary grid point (from the $A_{11}^{-1}A_{13}$ and $A_{22}^{-1}A_{23}$ terms in (6.61)). This can certainly be done, after which one could factor S using dense Cholesky and proceed to solve the system. But this is expensive, much more so than just multiplying a vector by S , which requires just one solve per subdomain using equation (6.61). This makes a Krylov subspace-based iterative method such as CG look attractive (section 6.6), since these methods require only multiplying a vector by S . The number of matrix-vector multiplications CG requires depends on the condition number of S . What makes domain decomposition so attractive is that S turns out to be much better conditioned than the original matrix A (a condition number that grows like $O(N)$ instead of $O(N^2)$), and so convergence is fast [114, 203].

More generally, one has $k > 2$ subdomains, separated by boundaries (see Figure 6.21, where the heavy lines separate subdomains). If we number the nodes in each subdomain consecutively, followed by the boundary nodes, we get the matrix

$$A = \left[\begin{array}{ccc|c} A_{1,1} & & 0 & A_{1,k+1} \\ & \ddots & & \vdots \\ 0 & & A_{k,k} & A_{k,k+1} \\ \hline A_{1,k+1}^T & \cdots & A_{k,k+1}^T & A_{k+1,k+1} \end{array} \right], \quad (6.62)$$

where again we can factor it by factoring each $A_{i,i}$ independently and forming the Schur complement $S = A_{k+1,k+1} - \sum_{i=1}^k A_{i,k+1}^T A_{i,i}^{-1} A_{i,k+1}$.

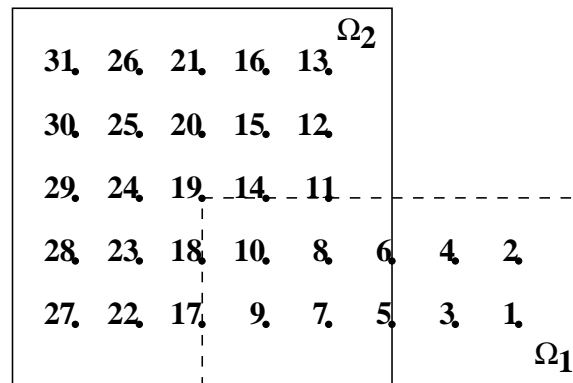
In this case, when there is more than one boundary segment, S has further structure that can be exploited to precondition it. For example, by numbering the grid points in the interior of each boundary segment before the grid points

at the intersection of boundary segments, one gets a block structure as in A . The diagonal blocks of S are complicated but may be approximated by $T_N^{1/2}$, which may be inverted efficiently using the FFT [35, 36, 37, 38, 39]. To summarize the state of the art, by choosing the preconditioner for S appropriately, one can make the number of steps of conjugate gradient independent of the number of boundary grid points N [229].

6.10.2. Overlapping Methods

The methods in the last section were called *nonoverlapping* because the domains corresponding to the nodes in $A_{i,i}$ were disjoint, leading to the block diagonal structure in equation (6.62). In this section we permit overlapping domains, as shown in the figure below. As we will see, this overlap permits us to design an algorithm comparable in speed with multigrid but applicable to a wider set of problems.

The rectangle with a dashed boundary in the figure is domain Ω_1 , and the square with a solid boundary is domain Ω_2 . We have renumbered the nodes so that the nodes in Ω_1 are numbered first and the nodes in Ω_2 are numbered last, with the nodes in the overlap $\Omega_1 \cap \Omega_2$ in the middle.



These domains are shown in the matrix A below, which is the same matrix as in section 6.10.1 but with its rows and columns ordered as shown above:

[illegible]
$$A = \left[\frac{A_{\Omega_1, \Omega_1}}{A_{\Omega \setminus \Omega_1, \Omega_1}} \mid \frac{A_{\Omega_1, \Omega \setminus \Omega_1}}{A_{\Omega \setminus \Omega_1, \Omega \setminus \Omega_1}} \right] = \left[\frac{A_{\Omega \setminus \Omega_2, \Omega \setminus \Omega_2}}{A_{\Omega_2, \Omega \setminus \Omega_2}} \parallel \frac{A_{\Omega \setminus \Omega_2, \Omega_2}}{A_{\Omega_2, \Omega_2}} \right].$$
$$\begin{aligned} x &= \left[\frac{x_{\Omega_1}}{x_{\Omega \setminus \Omega_1}} \right] = \left[\frac{x(1:10)}{x(11:31)} \right] \\ &= \left[\frac{x_{\Omega \setminus \Omega_2}}{x_{\Omega_2}} \right] = \left[\frac{x(1:6)}{x(7:31)} \right]. \end{aligned}$$

Now we have enough notation to state two basic overlapping domain decomposition algorithms. The simplest one is called the *additive Schwarz method* for historical reasons but could as well be called *overlapping block Jacobi iteration* because of its similarity to (block) Jacobi iteration from sections 6.5 and 6.6.5.

ALGORITHM 6.18. *Additive Schwarz method for updating an approximate solution x_i of $Ax = b$ to get a better solution x_{i+1} :*

$$\begin{aligned}
 r &= b - Ax_i && /* \text{compute the residual} */ \\
 x_{i+1} &= 0 \\
 x_{i+1, \Omega_1} &= x_{i, \Omega_1} + A_{\Omega_1, \Omega_1}^{-1} \cdot r_{\Omega_1} && /* \text{update the solution on } \Omega_1 */ \\
 x_{i+1, \Omega_2} &= x_{i+1, \Omega_2} + A_{\Omega_2, \Omega_2}^{-1} \cdot r_{\Omega_2} && /* \text{update the solution on } \Omega_2 */
 \end{aligned}$$

This algorithm also be written in one line as

$$x_{i+1} = x_i + \left[\frac{A_{\Omega_1, \Omega_1}^{-1} \cdot r_{\Omega_1}}{0} \right] + \left[\frac{0}{A_{\Omega_2, \Omega_2}^{-1} \cdot r_{\Omega_2}} \right].$$

In words, the algorithm works as follows: The update $A_{\Omega_1, \Omega_1}^{-1} r_{\Omega_1}$ corresponds to solving Poisson's equation just on Ω_1 , using boundary conditions at nodes 11, 14, 17, 18, and 19, which depend on the previous approximate solution x_i . The update $A_{\Omega_2, \Omega_2}^{-1} r_{\Omega_2}$ is analogous, using boundary conditions at nodes 5 and 6 depending on x_i .

In our case the Ω_i are rectangles, so any one of our earlier fast methods, such as multigrid, could be used to solve $A_{\Omega_i, \Omega_i}^{-1} r_{\Omega_i}$. Since the additive Schwarz method is iterative, it is not necessary to solve the problems on Ω_i exactly.

Indeed, the additive Schwarz method is typically used as a preconditioner for a Krylov subspace method like conjugate gradients (see section 6.6.5). In the notation of section 6.6.5, the preconditioner M is given by

$$M^{-1} = \left[\frac{A_{\Omega_1, \Omega_1}^{-1} \mid 0}{0 \mid 0} \right] + \left[\frac{0 \parallel 0}{0 \parallel A_{\Omega_2, \Omega_2}^{-1}} \right].$$

If Ω_1 and Ω_2 did not overlap, then M^{-1} would simplify to

$$\begin{bmatrix} A_{\Omega_1, \Omega_1}^{-1} & 0 \\ 0 & A_{\Omega_2, \Omega_2}^{-1} \end{bmatrix}$$

and we would be doing block Jacobi iteration. But we know that Jacobi's method does not converge particularly quickly, because "information" about the solution from one domain can only move slowly to the other domain across the boundary between them (see the discussion at the beginning of section 6.9). But as long as the overlap is a large enough fraction of the two domains, information will travel quickly enough to guarantee fast convergence. Of course we do not want too large an overlap, because this increases the work significantly. The goal in designing a good domain decomposition method is to choose the domains and the overlaps so as to have fast convergence while doing as little work as possible; we say more on how convergence depends on overlap below.

From the discussion in section 6.5, we know that the Gauss–Seidel method is likely to be more effective than Jacobi’s method. This is the case here as well, with the *overlapping block Gauss–Seidel method* (more commonly called the *multiplicative Schwarz method*) often being twice as fast as additive block Jacobi iteration (the additive Schwarz method).

ALGORITHM 6.19. *Multiplicative Schwarz method for updating an approximate solution x_i of $Ax = b$:*

- (1) $r_{\Omega_1} = (b - Ax_i)_{\Omega_1}$ /* compute residual of x_i on Ω_1 */
- (2) $x_{i+\frac{1}{2}, \Omega_1} = x_{i, \Omega_1} + A_{\Omega_1, \Omega_1}^{-1} \cdot r_{\Omega_1}$ /* update solution on Ω_1 */
- (2') $x_{i+\frac{1}{2}, \Omega \setminus \Omega_1} = x_{i, \Omega \setminus \Omega_1}$
- (3) $r_{\Omega_2} = (b - Ax_{i+\frac{1}{2}})_{\Omega_2}$ /* compute residual of $x_{i+\frac{1}{2}}$ on Ω_2 */
- (4) $x_{i+1, \Omega_2} = x_{i+\frac{1}{2}, \Omega_2} + A_{\Omega_2, \Omega_2}^{-1} \cdot r_{\Omega_2}$ /* update solution on Ω_2 */
- (4') $x_{i+1, \Omega \setminus \Omega_2} = x_{i+\frac{1}{2}, \Omega \setminus \Omega_2}$

Note that lines (2') and (4') do not require any data movement, provided that $x_{i+\frac{1}{2}}$ and x_{i+1} overwrite x_i .

This algorithm first solves Poisson’s equation on Ω_1 using boundary data from x_i , just like Algorithm 6.18. It then solves Poisson’s equation on Ω_2 , but using boundary data that has just been updated. It may also be used as a preconditioner for a Krylov subspace method.

In practice more domains than just two (Ω_1 and Ω_2) are used. This is done if the domain of solution is more complicated or if there are many independent parallel processors available to solve independent problems $A_{\Omega_i, \Omega_i}^{-1} r_{\Omega_i}$ or just to keep the subproblems $A_{\Omega_i, \Omega_i}^{-1} r_{\Omega_i}$ small and inexpensive to solve.

Here is a summary of the theoretical convergence analysis of these methods for the model problem and similar elliptic partial differential equations. Let h be the mesh spacing. The theory predicts how many iterations are necessary to converge as a function of h as h decreases to 0. With two domains, as long as the overlap region $\Omega_1 \cap \Omega_2$ is a nonzero fraction of the total domain $\Omega_1 \cup \Omega_2$, the number of iterations required for convergence is independent of h as h goes to zero. This is an attractive property and is reminiscent of multigrid, which also converged at a rate independent of mesh size h . But the cost of an iteration includes solving subproblems on Ω_1 and Ω_2 *exactly*, which may be comparable in expense to the original problem. So unless the solutions on Ω_1 and Ω_2 are very cheap (as with the L-shaped region above), the cost is still high.

Now suppose we have many domains Ω_i , each of size $H \gg h$. In other words, think of the Ω_i as the regions bounded by a coarse mesh with spacing H , plus some cells beyond the boundary, as shown by the dashed line in Figure 6.21.

Let $\delta < H$ be the amount by which adjacent domains overlap. Now let H , δ , and h all go to zero such that the overlap fraction δ/H remains constant,

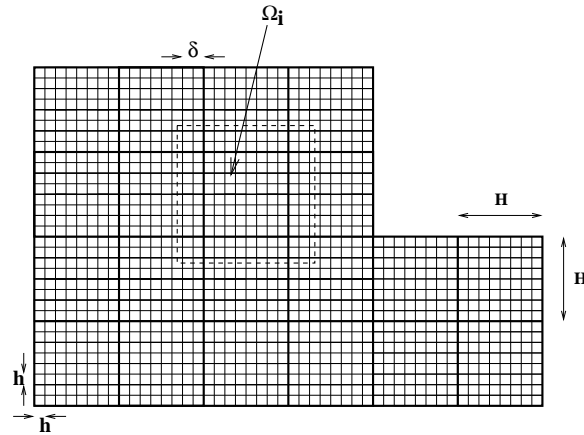


Fig. 6.21. Coarse and fine discretizations of an L-shaped region.

and $H \gg h$. Then the number of iterations required for convergence grows like $1/H$, i.e., *independently* of the fine mesh spacing h . This is close to, but still not as good as, multigrid, which does a constant number of iterations and $O(1)$ work per unknown.

Attaining the performance of multigrid requires one more idea, which, perhaps not surprisingly, is similar to multigrid. We use an approximation A_H of the problem on the coarse grid with spacing H to get a *coarse grid preconditioner* in addition to the fine grid preconditioners $A_{\Omega_i, \Omega_i}^{-1}$. We need three matrices to describe the algorithm. First, let A_H be the matrix for the model problem discretized with coarse mesh spacing H . Second, we need a *restriction operator* R to take a residual on the fine mesh and restrict it to values on the coarse mesh; this is essentially the same as in multigrid (see section 6.9.2). Finally, we need an *interpolation operator* to take values on the coarse mesh and interpolate them to the fine mesh; as in multigrid this also turns out to be R^T .

ALGORITHM 6.20. *Two-level additive Schwarz method for updating an approximate solution x_i of $Ax = b$ to get a better solution x_{i+1} :*

```

 $x_{i+1} = x_i$ 
for  $i = 1$  to the number of domains  $\Omega_i$ 
     $r_{\Omega_i} = (b - Ax_i)_{\Omega_i}$ 
     $x_{i+1, \Omega_i} = x_{i+1, \Omega_i} + A_{\Omega_i, \Omega_i}^{-1} \cdot r_{\Omega_i}$ 
endfor
 $x_{i+1} = x_{i+1} + R^T A_C^{-1} R r$ 

```

As with Algorithm 6.18, this method is typically used as a preconditioner for a Krylov subspace method.

Convergence theory for this algorithm, which is applicable to more general problems than Poisson's equation, says that as H , δ , and h shrink to 0 with

δ/H staying fixed, the number of iterations required to converge is independent of H , h or δ . This means that as long as the work to solve the subproblems $A_{\Omega_i, \Omega_i}^{-1}$ and A_H^{-1} is proportional to the number of unknowns, the complexity is as good as multigrid.

It is probably evident to the reader that implementing these methods in a real world problem can be complicated. There is software available on-line that implements many of the building blocks described here and also runs on parallel machines. It is called PETSc, for Portable Extensible Toolkit for Scientific computing. PETSc is available at <http://www.mcs.anl.gov/petsc/petsc.html> and is described briefly in [230].

6.11. References and Other Topics for Chapter 6

Up-to-date surveys of modern iterative methods are given in [15, 105, 134, 212], and their parallel implementations are also surveyed in [75]. Classical methods such as Jacobi's, Gauss-Seidel, and SOR methods are discussed in detail in [247, 135]. Multigrid methods are discussed in [42, 183, 184, 258, 266] and the references therein; [89] is a Web site with pointers to an extensive bibliography, software, and so on. Domain decomposition are discussed in [48, 114, 203, 230]. Chebyshev and other polynomials are discussed in [238]. The FFT is discussed in any good textbook on computer science algorithms, such as [3] and [246]. A stabilized version of block cyclic reduction is found in [46, 45].

6.12. Questions for Chapter 6

QUESTION 6.1. (*Easy*) Prove Lemma 6.1.

QUESTION 6.2. (*Easy*) Prove the following formulas for triangular factorizations of T_N .

1. The Cholesky factorization $T_N = B_N^T B_N$ has a upper bidiagonal Cholesky factor B_N with

$$B_N(i, i) = \sqrt{\frac{i+1}{i}} \quad \text{and} \quad B_N(i, i+1) = \sqrt{\frac{i}{i+1}}.$$

2. The result of Gaussian elimination with partial pivoting on T_N is $T_N = L_N U_N$, where the triangular factors are bidiagonal:

$$L_N(i, i) = 1 \quad \text{and} \quad L_N(i+1, i) = -\frac{i}{i+1},$$

$$U_N(i, i) = \frac{i+1}{i} \quad \text{and} \quad U_N(i, i+1) = -1.$$

3. $T_N = D_N D_N^T$, where D_N is the N -by- $(N+1)$ upper bidiagonal matrix with 1 on the main diagonal and -1 on the superdiagonal.

QUESTION 6.3. (*Easy*) Confirm equation (6.13).

QUESTION 6.4. (*Easy*)

1. Prove Lemma 6.2.
2. Prove Lemma 6.3.
3. Prove that the Sylvester equation $AX - XB = C$ is equivalent to $(I_n \otimes A - B^T \otimes I_m) \text{vec}(X) = \text{vec}(C)$.
4. Prove that $\text{vec}(AXB) = (B^T \otimes A) \cdot \text{vec}(X)$.

QUESTION 6.5. (*Medium*) Suppose that $A^{n \times n}$ is diagonalizable, so A has n independent eigenvectors: $Ax_i = \alpha_i x_i$, or $AX = X\Lambda_A$, where $X = [x_1, \dots, x_n]$ and $\Lambda_A = \text{diag}(\alpha_i)$. Similarly, suppose that $B^{m \times m}$ is diagonalizable, so b has m independent eigenvectors: $By_i = \beta_i y_i$, or $BY = Y\Lambda_B$, where $Y = [y_1, \dots, y_m]$ and $\Lambda_B = \text{diag}(\beta_j)$. Prove the following results.

1. The mn eigenvalues of $I_m \otimes A + B \otimes I_n$ are $\lambda_{ij} = \alpha_i + \beta_j$, i.e., all possible sums of pairs of eigenvalues of A and B . The corresponding eigenvectors are z_{ij} , where $z_{ij} = x_i \otimes y_j$, whose $(km+l)$ th entry is $x_i(k)y_j(l)$. Written another way,

$$(I_m \otimes A + B \otimes I_n)(Y \otimes X) = (Y \otimes X) \cdot (I_m \otimes \Lambda_A + \Lambda_B \otimes I_n). \quad (6.63)$$

2. The Sylvester equation $AX + XB^T = C$ is nonsingular (solvable for X , given any C) if and only if the sum $\alpha_i + \beta_j = 0$ for all eigenvalues α_i of A and β_j of B . The same is true for the slightly different Sylvester equation $AX + XB = C$ (see also Question 4.6).
3. The mn eigenvalues of $A \otimes B$ are $\lambda_{ij} = \alpha_i \beta_j$, i.e., all possible products of pairs of eigenvalues of A and B . The corresponding eigenvectors are z_{ij} , where $z_{ij} = x_i \otimes y_j$, whose $(km+l)$ th entry is $x_i(k)y_j(l)$. Written another way,

$$(B \otimes A)(Y \otimes X) = (Y \otimes X) \cdot (\Lambda_B \otimes \Lambda_A). \quad (6.64)$$

QUESTION 6.6. (*Easy; Programming*) Write a one-line Matlab program to implement Algorithm 6.2: one step of Jacobi's algorithm for Poisson's equation. Test it by confirming that it converges as fast as predicted in section 6.5.4.

QUESTION 6.7. (*Hard*) Prove Lemma 6.7.

QUESTION 6.8. (*Medium; Programming*) Write a Matlab program to solve the discrete model problem on a square using FFTs. The inputs should be the dimension N and a square N -by- N matrix of values of f_{ij} . The outputs should be an N -by- N matrix of solution v_{ij} and the residual $\|T_{N \times N}v - h^2 f\|_2 / (\|T_{N \times N}\|_2 \cdot \|v\|)$. You should also produce three-dimensional plots of f and v . Use the `fft` built in to Matlab. Your program should not have to be more than a few lines long if you use all the features of Matlab that you can. Solve it for several problems whose solutions you know and several you do not:

1. $f_{jk} = \sin(j\pi/(N+1)) \cdot \sin(k\pi/(N+1))$.
2. $f_{jk} = \sin(j\pi/(N+1)) \cdot \sin(k\pi/(N+1)) + \sin(3j\pi/(N+1)) \cdot \sin(5k\pi/(N+1))$.
3. f has a few sharp spikes (both positive and negative) and is 0 elsewhere. This approximates the electrostatic potential of charged particles located at the spikes and with charges proportional to the heights (positive or negative) of the spikes. If the spikes are all positive, this is also the gravitational potential.

QUESTION 6.9. (*Medium*) Confirm that evaluating the formula in (6.47) by performing the matrix-vector multiplications from right to left is mathematically the same as Algorithm 6.13.

QUESTION 6.10. (*Medium; Hard*)

1. (*Hard*) Let A and H be real symmetric n -by- n matrices that *commute*, i.e., $AH = HA$. Show that there is an orthogonal matrix Q such that $QAQ^T = \text{diag}(\alpha_1, \dots, \alpha_n)$ and $QHQ^T = \text{diag}(\theta_1, \dots, \theta_n)$ are both diagonal. In other words, A and H have the same eigenvectors. Hint: First assume A has distinct eigenvalues, and then remove this assumption.
2. (*Medium*) Let

$$\hat{T} = \begin{bmatrix} \alpha & \theta & & \\ \theta & \ddots & \ddots & \\ & \ddots & \ddots & \theta \\ & & \theta & \alpha \end{bmatrix}$$

be a symmetric tridiagonal Toeplitz matrix, i.e., a symmetric tridiagonal matrix with constant α along the diagonal and θ along the offdiagonals. Write down *simple* formulas for the eigenvalues and eigenvectors of \hat{T} . Hint: Use Lemma 6.1.

3. (*Hard*) Let

$$T = \begin{bmatrix} A & H & & \\ H & \ddots & \ddots & \\ & \ddots & \ddots & H \\ & & H & A \end{bmatrix}$$

be an n^2 -by- n^2 block tridiagonal matrix, with n copies of A along the diagonal. Let $QAQ^T = \text{diag}(\alpha_1, \dots, \alpha_n)$ be the eigendecomposition of A , and let $QHQ^T = \text{diag}(\theta_1, \dots, \theta_n)$ be the eigendecomposition of H as above. Write down *simple* formulas for the n^2 eigenvalues and eigenvectors of T in terms of the α_i , θ_i , and Q . Hint: Use Kronecker products.

4. (*Medium*) Show how to solve $Tx = b$ in $O(n^3)$ time. In contrast, how much bigger are the running times of dense LU factorization and band LU factorization?
5. (*Medium*) Suppose that A and H are (possibly different) symmetric tridiagonal Toeplitz matrices, as defined above. Show how to use the FFT to solve $Tx = b$ in just $O(n^2 \log n)$ time.

QUESTION 6.11. (*Easy*) Suppose that R is upper triangular and nonsingular and that C is upper Hessenberg. Confirm that RCR^{-1} is upper Hessenberg.

QUESTION 6.12. (*Medium*) Confirm that the Krylov subspace $\mathcal{K}_k(A, y_1)$ has dimension k if and only if the Arnoldi algorithm (Algorithm 6.9) or the Lanczos algorithm (Algorithm 6.10) can compute q_k without quitting first.

QUESTION 6.13. (*Medium*) Confirm that when $A^{n \times n}$ is symmetric positive definite and $Q^{n \times k}$ has full column rank, then $T = Q^T A Q$ is also symmetric positive definite. (For this question, Q need not be orthogonal.)

QUESTION 6.14. (*Medium*) Prove Theorem 6.9.

QUESTION 6.15. (*Medium; Hard*)

1. (*Medium*) Confirm equation (6.58).
2. (*Medium*) Confirm equation (6.60).
3. (*Hard*) Prove Theorem 6.11.

QUESTION 6.16. (*Medium; Programming*) A Matlab program implementing multigrid to solve the discrete model problem on a square is available on the class homepage at HOMEPAGE/Matlab/MG_README.html. Start by running the demonstration (type “makemgdemo” and then “testfmvg”). Then, try running testfmvg for different right-hand sides (input array b), different numbers of weighted Jacobi convergence steps before and after each recursive call to the multigrid solver (inputs jac1 and jac2), and different numbers of iterations (input iter). The software will plot the convergence rate (ratio of consecutive residuals); does this depend on the size of b ? the frequencies in b ? the values of jac1 and jac2 ? For which values of jac1 and jac2 is the solution most efficient?

QUESTION 6.17. (*Medium; Programming*) Using a fast model problem solver from either Question 6.8 or Question 6.16, use domain decomposition to build a fast solver for Poisson's equation on an L-shaped region, as described in section 6.10. The large square should be 1-by-1 and the small square should be .5-by-.5, attached at the bottom right of the large square. Compute the residual in order to show that your answer is correct.

QUESTION 6.18. (*Hard*) Fill in the entries of a table like Table 6.1, but for solving Poisson's equation in three dimensions instead of two. Assume that the grid of unknowns is $N \times N \times N$, with $n = N^3$. Try to fill in as many entries of columns 2 and 3 as you can.